Quantum Phases in Optical Lattices

Quantum Phases in Optical Lattices

Quantum Fasen in Optische Roosters

(met een samenvatting in het Nederlands)

Proefschrift

ter verkrijging van de graad van doctor aan de Universiteit Utrecht op gezag van de Rector Magnificus, Prof. dr. W. H. Gispen, ingevolge het besluit van het College voor Promoties in het openbaar te verdedigen op maandag 6 februari 2006 des middags te 12.45 uur

door

Dennis Brian Martin Dickerscheid

geboren op 3 augustus 1978, te 's-Gravenhage

promotor:

    Prof. dr. ir. H. T. C. Stoof

    Instituut voor Theoretische Fysica
    Departement Natuur- en Sterrenkunde
    Faculteit Bètawetenschappen
    Universiteit Utrecht

copromotor:

    Dr. P. J. H. Denteneer

    Instituut-Lorentz voor Theoretische Natuurkunde
    Leids Instituut voor Onderzoek in de Natuurkunde
    Universiteit Leiden

Contents

Chapter 1

Introduction

ABSTRACT

By making use of lasers and magnetic fields it is possible to trap ultracold atomic gases and very accurately control their collisional properties. In this chapter we introduce the various gases of ultracold atoms in optical lattices that we consider in this thesis. A common feature of these gases is that they all undergo, at zero temperature, a phase transition, a so-called quantum phase transition, that is driven by the competition of two distinct quantum states of matter.

1.1 Overview

Since the creation in 1995 of the first Bose-Einstein condensate in a trapped dilute gas of alkali atoms [1, 2, 3], the field of ultracold atomic gases represents one of the most exciting and active fields of physics research. The experimental realization of this novel state of matter has been made possible by trapping the atoms in a magnetic field minimum and lowering the temperature into the nanokelvin regime. It led in 2001 to the Nobel Prize in Physics for E. Cornell, C. Wieman, and W. Ketterle. Because of the technological progress made in the trapping and cooling of cold atomic gases we now have quantum degenerate Bose and Fermi [4] gases at our disposal. In particular, the motion of the trapped atoms can be controlled in magnetic and optical traps allowing, for example, the realization of quantum gases with different dimensionalities [5, 6, 7]. In addition, it is possible to trap the ultracold gases in a periodic potential formed by standing waves of laser light, a so-called optical lattice [8]. It is well known that for bosons in an optical lattice there is a quantum phase transition between a superfluid and an insulating state as a function of the lattice depth [9]. In a landmark experiment

this transition has been observed by Greiner *et al.* [10]. Atomic gases in an optical lattice are very manipulable, because different lattice geometries can be realized and many different species and isotopes are available. Because the properties of the trapped gases are very well understood, optical lattices act as general quantum simulators of lattice models and they allow for new insights into, for instance, the physics of high-temperature superconductors. Besides of being interesting to the condensed-matter physics community there are also direct applications in the fields of quantum optics and quantum-information processing [11]. For example, by creating optical lattices that depend on the internal state of the atom a coherent spin-dependent transport of neutral atoms in optical lattices has been realized [12]. With such spin-dependent lattices one can possibly bring atoms on different sites of the lattice into contact in a controlled way to realize fundamental quantum gates [13] and large-scale entanglement [14, 15].

Another new experimental technique which has caused much excitement in recent years, is the use of so-called Feshbach resonances to tune the interatomic interactions [16, 17]. In a Feshbach-resonant atomic collision two atoms collide and virtually form a long-lived molecule with a different spin configuration than the incoming two atoms, which ultimately decays again into two atoms. The scattering properties of the colliding atoms depend on the energy difference of the molecular state with respect to the threshold of the two-atom continuum. This energy difference is known as the detuning and can be changed with a magnetic field. After the first observation of Feshbach resonances in a dilute Bose-Einstein condensate of ^{23}Na atoms [18], a multitude of applications have been realized, including, the collapse of a Bose-Einstein condensate with attractive interactions [19, 20, 21], the observation of bright soliton trains in a Bose-Einstein condensate [22], coherent atom-molecule oscillations [23], and the creation of ultracold molecules from bosonic atoms [24, 25, 26] and a molecular Bose-Einstein condensate from a Fermi gas [27, 28, 29, 30, 31, 32]. Combining the optical lattice and Feshbach resonances is very exciting because it gives us even more control over the system parameters. It is also very timely to study such systems because the first experimental investigations have just been carried out [33].

1.2   Quantum phase transitions

Classical phase transitions, such as the freezing of water as one lowers the temperature, are driven by thermal fluctuations. On the contrary a quantum phase transition is a transition that occurs strictly at zero temperature between two different states of matter and is therefore solely driven by quantum fluctuations. The archetypal example from the field of condensed-matter physics is the quantum phase transition from an Ising ferromagnet to a paramagnet that occurs as a function of the external magnetic field that is transverse to the easy axis of the ferromagnet [34]. In the following we introduce the different systems from the field

of ultracold atoms that we have studied in this thesis and illustrate the important ideas and concepts that we need later on.

1.2.1 Ideal Bose gas

As a first example of a quantum phase transition we consider the ideal Bose gas in three dimensions. To clarify this point we consider the ideal Bose gas with a total number of particles N given by

$$N = \sum_{\mathbf{k}} N(\epsilon_{\mathbf{k}}) \equiv \sum_{\mathbf{k}} \frac{1}{e^{\beta(\epsilon_{\mathbf{k}} - \mu)} - 1}, \tag{1.1}$$

where $N(\epsilon_{\mathbf{k}})$ gives the average number of particles in the single-particle state $|\mathbf{k}\rangle$ with momentum $\mathbf{k}$ and energy $\epsilon_{\mathbf{k}} = \hbar^2 \mathbf{k}^2 / 2m$, μ is the chemical potential, and $\beta = 1/k_B T$ is the inverse thermal energy. Positive values of the chemical potential are forbidden because that would lead to an infinite number of particles and as a result that part of the phase diagram is excluded. In Fig. 1.1 we show the phase diagram of the ideal Bose gas as a function of temperature and chemical potential. If we cool the ideal Bose gas, keeping the number of particles fixed, the chemical potential increases. The chemical potential increases until it reaches zero at the critical temperature T_c. If we cool the gas even further, the chemical potential remains zero but more and more atoms will occupy the lowest-energy state, according to $N_0 = N \left(1 - (T/T_c)^{3/2} \right)$. At zero temperature the gas is exactly in the quantum critical point. Note that when the chemical potential and the temperature satisfy $\beta|\mu| \gg 1$ we can approximate the Bose-Einstein distribution function with a Maxwell-Boltzmann distribution function. In the case of the Maxwell-Boltzmann distribution function the chemical potential satisfies $\mu = k_B T \log(n\lambda_T^3)$, where $n = N/V$ is the density, V is the volume, and $\lambda_T = (2\pi\hbar^2/mk_B T)^{1/2}$ is the thermal de Broglie wavelength. For completeness we have also added the case of fermionic atoms for which the chemical potential increases until it reaches the Fermi energy $\epsilon_F = (\hbar^2/2m)(6\pi^2 n)^{2/3}$ at zero temperature.

In reality, the atoms interact with each other. To find the phase diagram for the weakly-interacting Bose gas at the low temperatures of interest we consider the second-quantized Hamiltonian

$$H = \int d\mathbf{x} \, \psi_{\mathrm{a}}^{\dagger}(\mathbf{x}) \left(-\frac{\hbar^2 \nabla^2}{2m} - \mu \right) \psi_{\mathrm{a}}(\mathbf{x}) \; + \frac{V_0}{2} \int d\mathbf{x} \, \psi_{\mathrm{a}}^{\dagger}(\mathbf{x}) \psi_{\mathrm{a}}^{\dagger}(\mathbf{x}) \psi_{\mathrm{a}}(\mathbf{x}) \psi_{\mathrm{a}}(\mathbf{x}) \; . \tag{1.2}$$

Here the field operators $\psi_{\mathrm{a}}^{\dagger}(\mathbf{x})$ and $\psi_{\mathrm{a}}(\mathbf{x})$ create and annihilate an atom at position $\mathbf{x}$, respectively. Moreover, $V_0 > 0$ is the strength of the atom-atom interaction that is assumed to be repulsive. The phase transition from the normal phase to a Bose-Einstein condensed phase is described by the order parameter $\langle \psi_{\mathrm{a}}(\mathbf{x}) \rangle$, where the brackets $\langle \ldots \rangle$ are a shorthand notation for the averaging of the observable of interest using the grand-canonical ensemble. It is impossible to exactly solve this

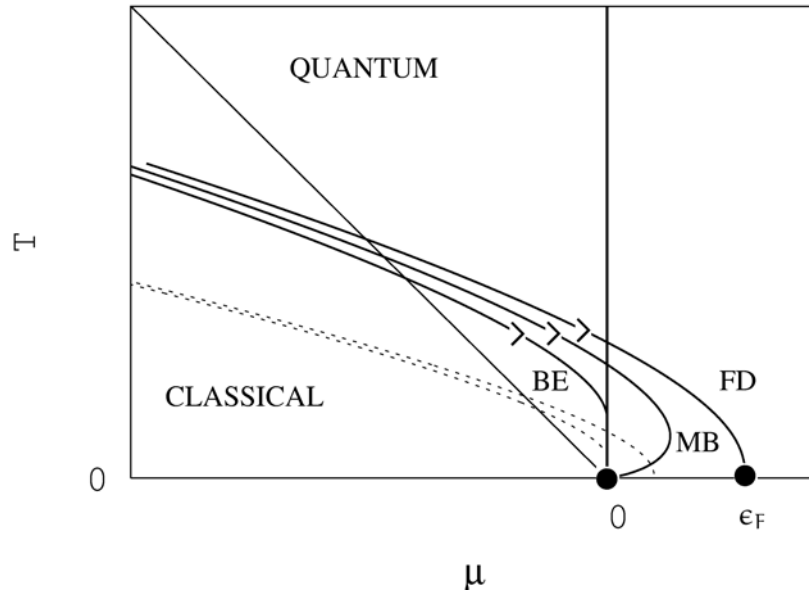Figure 1.1: Illustration of the quantum phase transition in the ideal Bose gas. The solid lines show the behaviour of the chemical potential for a fixed particle number of a gas that satisfies Bose-Einstein (BE), Fermi-Dirac (FD), or Maxwell-Boltzmann (MB) statistics. The dashed line shows the same but for a smaller number of particles. The diagonal line shows the location of the crossover between the classical and quantum regimes.
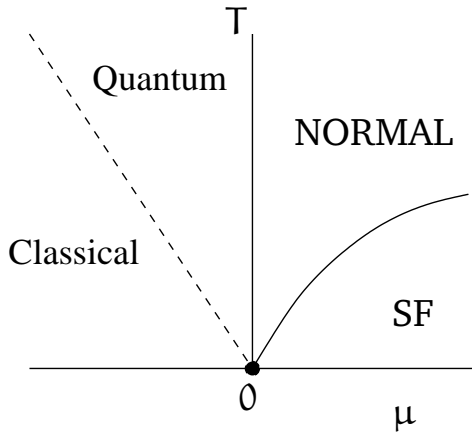
Figure 1.2: Illustration of the quantum phase transition in the weakly-interacting Bose gas. The solid line for positive values of the chemical potential distinguishes between the normal state and the superfluid state. The dashed diagonal line for negative chemical potential shows the crossover between the classical and the quantum regimes.

problem and we have to resort to an approximate theory. The usual way to proceed is to write the annihilation operator for the atoms as $\psi_a(\mathbf{x}) = \sqrt{n_0} + \delta\psi_a(\mathbf{x})$ [35], with $n_0 = N_0/V$ the condensate density, and neglect the terms that are third and fourth order in the fluctuations $\delta\psi_a(\mathbf{x})$. The expression for the chemical potential that follows from the one-loop Popov theory [36, 37] for partially Bose-Einstein condensed gases is given by

$$\mu = n_0 V_0 + \frac{V_0}{V} \sum_{\mathbf{k}} \left[\frac{2\epsilon_{\mathbf{k}} + n_0 V_0 - 2\hbar\omega_{\mathbf{k}}}{2\hbar\omega_{\mathbf{k}}} + \frac{2\epsilon_{\mathbf{k}} + n_0 V_0}{\hbar\omega_{\mathbf{k}}} N(\hbar\omega_{\mathbf{k}}) \right]. \qquad (1.3)$$

Here $\hbar\omega_{\mathbf{k}} = (\epsilon_{\mathbf{k}}^2 + 2n_0 V_0 \epsilon_{\mathbf{k}})^{1/2}$ is the Bogoliubov dispersion relation, and $N(x) = 1/(e^{\beta x} - 1)$ is the Bose-Einstein distribution function. The first term on the right-hand side of Eq. (1.3) physically expresses the fact that to add an atom to the condensate we first of all have to add the average interaction energy that the atom has with all the other Bose-Einstein condensed atoms. The other two terms express the fact that the condensate is depleted by quantum and thermal fluctuations, respectively, and the atom has also a twice as large average interaction with this part of the gas.

If we increase the temperature, starting from a fully Bose-Einstein condensed state we find a phase transition to the normal state when $n_0(T_c) = 0$ and consequently $\mu \approx 2(V_0/V)\sum_{\mathbf{k}} N(\epsilon_{\mathbf{k}}) = 2V_0 n$. In Fig. 1.2 we show the phase diagram for the weakly-interacting Bose gas. Taking the limit of $V_0 \downarrow 0$, we then also recover
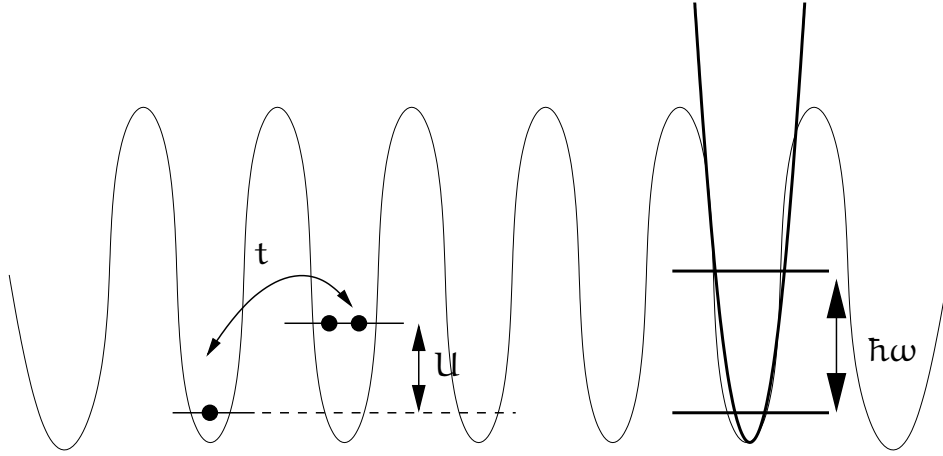
Figure 1.3: Illustration of the superfluid - Mott-insulator quantum phase transition of ultracold bosons in an optical lattice.

the somewhat pathological phase diagram of the ideal Bose gas shown already in Fig. 1.1. In that case the superfluid area of the phase diagram collapses into the single line $\mu = 0$.

1.2.2 Superfluid - Mott insulator transition

A second example of a quantum phase transition is the so-called superfluid-Mott insulator transition of bosons in an optical lattice. The two competing ground states in this case are a superfluid phase with a well-defined macroscopic phase and a Mott insulator where each lattice site has the same integer occupation number. To understand this qualitatively we show in Fig. 1.3 a one-dimensional optical lattice. Consider an atom localized on a lattice site. In order to minimize its kinetic energy the atom wants to become delocalized. It can do so by tunneling to a neighbouring site and gain a hopping energy t. The energy penalty for tunneling to an occupied site, however, is the interaction energy U, which we assume to be positive.

For a sufficiently deep optical lattice the hopping and interaction energies for atoms in the lowest band are to a very good approximation calculated by making a harmonic potential approximation of the optical lattice potential. This introduces the energy $\hbar\omega$, which is the level splitting of the harmonic potential, and we show in the following chapter how the optical lattice potential determines $\hbar\omega$. We then also show that the hopping energy and the interaction energy in this so-called

tight-binding limit are given by [78]

$$t = \frac{\hbar\omega}{2}\left[1 - \left(\frac{2}{\pi}\right)^2\right]\left(\frac{\lambda}{4l}\right)^2 e^{-(\lambda/4l)^2}, \qquad (1.4)$$

and

$$U = \frac{2\hbar\omega}{\sqrt{2\pi}}\left(\frac{a}{l}\right). \qquad (1.5)$$

Here λ is the wavelength of the light used to create the optical lattice, a is the s-wave scattering length and $l = \sqrt{\hbar/m\omega}$ is the harmonic oscillator length. From this we see that both the hopping strength and the interaction energy depend on the depth of the optical lattice potential.

If the optical lattice is switched on adiabatically the ratio U/t is small and the ground state remains in first instance a superfluid. This implies that the wave function of the system exhibits long-range phase coherence, i.e., the atoms are completely delocalized. On the other hand, if the interaction energy U is large compared to the hopping energy t, the total energy is minimized by having an equal number of particles on each site and the fluctuations in the atom number on each site are strongly reduced. The ground state thus formed is the Mott insulator and it is fundamentally different from the superfluid phase. The reduction of the fluctuations in the atom number on each site leads to an increase in the fluctuations of the phase of the atoms.

This distinction in phase coherence between the two phases has been observed in the experiment by Greiner *et al.* [10]. In that experiment a Bose-Einstein condensate of ^{87}Rb atoms was loaded into an optical lattice for various lattice depths. The phase coherence of the system after applying the optical lattice was demonstrated by removing the optical lattice and allowing the atoms to expand freely and interfere with each other. The absorption images taken after the expansion show a dramatic change in the interference pattern as the lattice depth is increased. Theoretically, the above-mentioned system is described by the Hamiltonian we presented in Eq. (1.2) with an additional external potential $V_0(\mathbf{x}) = \sum_j V_{j0}\cos^2(2\pi x_j/\lambda)$, that represents the optical lattice where V_{j0} is the lattice depth along the j axis and λ is the wavelength of the laser. For the low temperatures of interest, and if the lattice is sufficiently deep, we show later that the Hamiltonian takes the form of the Bose-Hubbard Hamiltonian that describes bosons hopping on a lattice with an on-site interaction term. Although strictly speaking the Mott-insulator state only exists at zero temperature, in reality the experiments are always performed at a nonzero temperature. Therefore we want to know what the nature is of the phase diagram near the quantum-critical point as a function of temperature and interaction strength. This is the topic of Chapter 3.

1.2.3 Ising transition

Our third example of a quantum phase transition involves a so-called Ising transition. This transition takes place in an atomic Bose gas near a Feshbach resonance at zero temperature [73, 74]. We leave the details of the physics of the Feshbach resonance for a later chapter. For now it suffices to say that the relevant physics near resonance is described by atoms that are coupled to molecules via an interaction energy that is proportional to $\int d\mathbf{x} \left[\psi_{\mathrm{m}}^{\dagger}(\mathbf{x})\psi_{\mathrm{a}}(\mathbf{x})\psi_{\mathrm{a}}(\mathbf{x}) + \psi_{\mathrm{a}}^{\dagger}(\mathbf{x})\psi_{\mathrm{a}}^{\dagger}(\mathbf{x})\psi_{\mathrm{m}}(\mathbf{x}) \right]$, where $\psi_{\mathrm{a}}(\mathbf{x})$ and $\psi_{\mathrm{m}}(\mathbf{x})$ annihilate an atom and a molecule at position $\mathbf{x}$, respectively. This coupling term implies that if the atoms are Bose-Einstein condensed, we necessarily also have a molecular Bose-Einstein condensate. However, if we have a molecular Bose-Einstein condensate then there does not need to be an atomic condensate. The reason for this is that the symmetry of the phase with only a molecular condensate is different from the phase with both an atomic and a molecular condensate. To see how this comes about we note that without the interaction the gas is invariant under the phase transformations $\psi_{\mathrm{a}}(\mathbf{x}) \rightarrow e^{i\theta}\psi_{\mathrm{a}}(\mathbf{x})$ and $\psi_{\mathrm{m}}(\mathbf{x}) \rightarrow e^{i\theta'}\psi_{\mathrm{m}}(\mathbf{x})$. The interaction energy requires however that $\theta' = 2\theta$ and physically the additional factor of two expresses the fact that the molecule consists of two atoms. If the gas only consists of a molecular condensate there is still an Ising-like residual symmetry left, i.e., if we let $\psi_{\mathrm{a}}(\mathbf{x}) \rightarrow -\psi_{\mathrm{a}}(\mathbf{x})$ the system remains unchanged. We have illustrated this in Fig. 1.4, where we represent the coupled phases of the atom-molecule system by two sprockets and a chain.

Another and more technical way to see this is to consider the microscopic atom-molecule theory given by the following Hamiltonian,

$$
\begin{aligned}
H \;=\; & \int d\mathbf{x} \; \psi_{\mathrm{a}}^{\dagger}(\mathbf{x}) \left\{ -\frac{\hbar^2 \nabla^2}{2m} - \mu \right\} \psi_{\mathrm{a}}(\mathbf{x}) \\
& + \int d\mathbf{x} \; \psi_{\mathrm{m}}^{\dagger}(\mathbf{x}) \left\{ -\frac{\hbar^2 \nabla^2}{4m} + \delta - 2\mu \right\} \psi_{\mathrm{m}}(\mathbf{x}) \\
& + g \int d\mathbf{x} \left[\psi_{\mathrm{m}}^{\dagger}(\mathbf{x})\psi_{\mathrm{a}}(\mathbf{x})\psi_{\mathrm{a}}(\mathbf{x}) + \psi_{\mathrm{a}}^{\dagger}(\mathbf{x})\psi_{\mathrm{a}}^{\dagger}(\mathbf{x})\psi_{\mathrm{m}}(\mathbf{x}) \right] .
\end{aligned}
\tag{1.6}
$$

Here the field operators $\psi_a^{\dagger}(\mathbf{x})$ and $\psi_a(\mathbf{x})$ create and annihilate an atom at position $\mathbf{x}$, respectively. The field operators $\psi_m^{\dagger}(\mathbf{x})$ and $\psi_m(\mathbf{x})$ create and annihilate a molecule at position $\mathbf{x}$, respectively. The strength of the atom-molecule coupling is determined by g. As we will explain in a later chapter the atoms and molecules have different spin configurations and the energy difference between the closed-channel molecules and the two-atom open channel is known as the detuning δ. As a side remark we note that after integrating out the molecules in the above Hamiltonian, we obtain the Hamiltonian of Eq. (1.2) with for long wavelengths the effective interaction $V_0 = -2g^2/\delta$ between the atoms. We now make an important observation: Suppose that we have Bose-Einstein condensation of the atoms and correspondingly $\langle \psi_{\mathrm{a}}(\mathbf{x}) \rangle = \sqrt{n_{\mathrm{a}}} \neq 0$. Substituting this into the Hamiltonian in
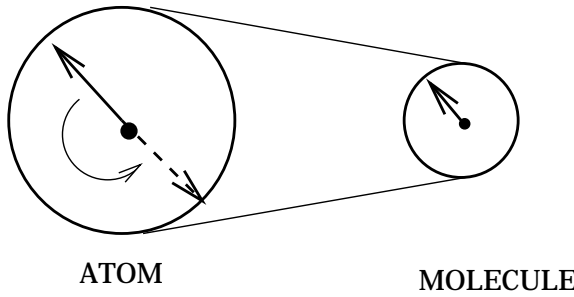
ATOM   **MOLECULE**

Figure 1.4: Illustration of the quantum Ising transition in a Bose gas near a Feshbach resonance. Fixing the phase of the molecules fixes the phase of the individual atoms only up to a sign. There is therefore a residual Z_2 symmetry that can spontaneously be broken.

Eq. (1.6) leads to the following energy for the molecules,

$$H_{\mathrm{m}} = \int d\mathbf{x}\ \psi_{\mathrm{m}}^{\dagger}(\mathbf{x}) \left\{ -\frac{\hbar^2 \nabla^2}{4m} - 2\mu \right\} \psi_{\mathrm{m}}(\mathbf{x}) \ + g\ n_{\mathrm{a}} \int d\mathbf{x} \left[\psi_{\mathrm{m}}^{\dagger}(\mathbf{x}) + \psi_{\mathrm{m}}(\mathbf{x}) \right]. \quad (1.7)$$

Minimizing this energy with respect to the molecular field $\psi_{\mathrm{m}}(\mathbf{x})$ shows that the expectation value of the molecular condensate is also nonzero because of the presence of the linear terms. On the other hand, assume that the order parameter $\langle \psi_m(\mathbf{x}) \rangle$ has a nonzero expectation value. Substituting explicitly this expectation value into the original Hamiltonian results to second order in the fluctuations in a quadratic action for the atoms. As a result this implies that a Bose-Einstein condensate of molecules does not necessarily imply a Bose-Einstein condensate of atoms.

1.2.4   Bose-Fermi mixture

Until now we have only mentioned bosonic systems. If we also allow for a fermionic species to be present, a novel kind of quantum phase transition can be shown to exist. To show this we consider a mixture of bosonic and fermionic atoms with equal densities and suppose the system is near an interspecies Feshbach resonance between the bosonic and fermionic atoms. Recently, such interspecies Feshbach resonances have indeed been observed [38, 39]. The molecule in this case consists of a boson and a fermion and is effectively a fermion. If the bound-state energy lies far below the two-atom energy, i.e., for large negative detunings, then the ground state is a filled Fermi sea of molecules. For large positive detuning the ground state is a filled Fermi sea of atoms and a Bose-Einstein condensate of atoms with a broken $U(1)$ symmetry. The quantum phase transition is therefore of the XY kind in this case and the phase diagram is very similar to Fig. 1.2

11

if we replace the chemical potential μ by the detuning δ. An interesting aspect of this resonantly-interacting mixture is that it is possible to reversibly destroy a Bose-Einstein condensate of atoms by associating the bosonic atoms into fermionic molecules. Moreover, in the Bose-Einstein condensed phase there is a macroscopic quantum coherence between the fermionic atoms and molecules.

1.3 Outlook

The outline of the thesis is as follows. In Chapter 2 we show how the potential energy of an atom changes in a light field. If this potential energy, which depends on the intensity of the light field, changes as a function of position, the atoms experience a force. This force can be used to trap atoms and it is also possible to provide them with a periodic potential. In this way perfect solid-state crystals can be realized. The theoretical description of these systems is given by the Bose-Hubbard model. In Chapter 3 we analyse the physical properties of the Bose-Hubbard model by means of the so-called slave-boson method. In detail we quantify the phase diagram of the Bose-Hubbard model at nonzero temperatures. Chapters 4 and 5 are the introductory chapters for the remaining part of the thesis. In Chapter 4 we introduce the physics of Feshbach resonances that are presently used to tune the interatomic interactions. In Chapter 5 we derive from first principles the effective Hamiltonian for a dilute atomic gas in an optical lattice near a Feshbach resonance. As an application we apply the theory in Chapter 6 to the Bose gas near a Feshbach resonance. In the following Chapter we consider a Bose-Fermi mixture at low filling fractions of the optical lattice and near a Feshbach resonance. Finally, in Chapter 8 we consider Feshbach molecules in a one-dimensional Fermi gas.

Chapter 2

Optical Lattices

─────── ABSTRACT

In this chapter we give details of the atomic physics that underlies the Bose-Hubbard model used to describe ultracold atoms in optical lattices. We show how the AC-Stark effect is responsible for the presence of the optical lattice [43, 44, 40] and discuss briefly how various crystal structures can be realized. As mentioned, the Bose-Hubbard model describes ultracold atoms in optical lattices and we end the chapter with a derivation of this model.

2.1 Polarization

Before we discuss the coupling between atoms and light in the next section, we first consider the interference pattern of crossed beams of laser light. For a single plane wave traveling in the positive z-direction, the electric field is given by,

$$\mathbf{E}(\mathbf{x}, t) = E_0 \hat{\boldsymbol{\epsilon}} \cos\left(kz - \omega t\right), \tag{2.1}$$

where $\hat{\boldsymbol{\epsilon}}$ is the unit polarization vector perpendicular to the z-axis, E_0 is the amplitude of the light field, $k = 2\pi/\lambda$, and $\omega = ck$ with c the speed of light. In the following section we show how the coupling between the light field and the dipole moment of the atoms leads to a potential for the atoms. By using standing waves created by two counter-propagating laser beams we obtain a periodic potential for the atoms which is known as an optical lattice. The simplest example of such an optical lattice is a single standing wave of linear polarized light directed perpendicular to the z axis with a magnitude described by

$$E(z, t) = E_0 \cos\left(kz\right)\left(e^{-i\omega t} + e^{+i\omega t}\right). \tag{2.2}$$

Using the above we can create a three-dimensional optical lattice potential by superimposing three pairs of counter-propagating running-wave laser beams.

The situation becomes more complicated when the polarization of the laser beams are different. In this case the polarization has a gradient, and multilevel atoms in different ground states couple differently to the light. In particular, the orientation of the dipole moment of the atoms with respect to the polarization of the light determines the coupling and for atoms in different ground states this is in general different. Making use of this it is possible to create state-dependent optical lattices

2.2 Interaction of atoms with electromagnetic radiation

When an atom is placed into two counterpropagating laser beams, the time-dependent electric field $\mathbf{E}(\mathbf{x}, t) = \hat{\boldsymbol{\epsilon}} \, E(\mathbf{x}) \cos(\omega t)$ with polarization vector $\hat{\boldsymbol{\epsilon}}$ and driving frequency ω induces an atomic dipole moment $\mathbf{p}$. The amplitude of the dipole moment p is related to the amplitude of the electric field by $p = \alpha E$, where the constant of proportionality α is called the polarizability. The electric-field induced dipole interacts with the electric field and as a result the atomic energy levels are shifted. It is this effect that is used to trap atoms. The dipole moment $\mathbf{p}$ is the quantum-mechanical expectation value of the electric dipole-moment operator $\mathbf{d}$, where

$$\mathbf{d} = -e \sum_j \mathbf{r}_j \tag{2.3}$$

and the $\mathbf{r}_j$ are the position operators for the electrons relative to the atomic nucleus. The interaction between the atom and the electric field is given by

$$H' = -\mathbf{d} \cdot \mathbf{E}. \tag{2.4}$$

For the alkali atoms only the valence electron matters and the dipole operator simplifies to a single term. The most interesting cases for the polarization of the light field are the linearly polarized light and circularly polarized light. For these polarizations it is convenient to rewrite the interaction H' by introducing the spherical unit vectors $\hat{\boldsymbol{\epsilon}}_m$ where,

$$\begin{aligned} \hat{\boldsymbol{\epsilon}}_0 &= \hat{\boldsymbol{\epsilon}}_z, \\ \hat{\boldsymbol{\epsilon}}_{\pm 1} &= \mp (\hat{\boldsymbol{\epsilon}}_x \pm i\hat{\boldsymbol{\epsilon}}_y)/\sqrt{2}. \end{aligned} \tag{2.5}$$

Here $\hat{\boldsymbol{\epsilon}}_0$ corresponds to linearly polarized light and $\hat{\boldsymbol{\epsilon}}_{\pm 1}$ corresponds to circularly polarized light. Similarly, we can represent the position operators for the electrons

in Eq. (2.3) in terms of the spherical components $\mathbf{r}_{\pm 1,0}$ [44], with

$$
\begin{aligned}
\mathbf{r}_0 &= r\left(\frac{4\pi}{3}\right)^{1/2} Y_{1,0}(\theta, \phi), \\
\mathbf{r}_{\pm 1} &= r\left(\frac{4\pi}{3}\right)^{1/2} Y_{1,\pm 1}(\theta, \phi).
\end{aligned}
\tag{2.6}
$$

Here the $Y_{l,m}(\theta, \phi)$ are the well-known spherical harmonic functions, and θ and ϕ are the axial and azimuthal angles of the vector $\mathbf{r}$. With these spherical unit vectors we can write the interaction H' for a particular polarization $m = \pm 1, 0$ as

$$
H' = -e\, E(\mathbf{x}) \cos(\omega t) r \sqrt{\frac{4\pi}{3}} Y_{1,m}^*(\theta, \phi) \hat{\boldsymbol{\epsilon}}_m.
\tag{2.7}
$$

Because the ground state $|g\rangle$ of the alkali atoms has no permanent dipole moment, it follows that the first-order correction to the ground-state energy is zero. Another way to see this is to consider the matrix elecment

$$
E_g^{(1)} = \langle g|H'|g\rangle.
\tag{2.8}
$$

Because the ground-state wave function has a definite parity and the dipole operator has odd parity this contribution must vanish. Therefore, the first nonzero contribution to the energy is of second order and it is given by

$$
E_g^{(2)}(\mathbf{x}) = \frac{1}{4}\sum_{e\neq g}|\langle e|\mathbf{d}\cdot\hat{\boldsymbol{\epsilon}}|g\rangle|^2\left(\frac{1}{E_e - E_g - \hbar\omega} + \frac{1}{E_e - E_g + \hbar\omega}\right)(E(\mathbf{x}))^2,
\tag{2.9}
$$

where $|g\rangle$ denotes the ground state and the sum is over all excited states $|e\rangle$. The first term between brackets corresponds to stimulated absorbtion of a photon, whereas the second term describes the stimulated emision of a photon from the excited state. Throughout we have assumed that the excited states have an infinitely long lifetime. This assumption is not correct since the excited states can decay by the sponteneous emmision of photons. If the lifetime of the excited state is $1/\Gamma_e$ we have to add $-i\hbar\Gamma_e/2$ to the energy E_e of the excited state. The resulting energy corrections are then complex valued. The real part of the energy determines the shift of the atomic levels in the light field and the imaginary part determines the effective lifetime of the ground state. Traditionally the difference between the laser frequency and the frequency of the atomic transition is called the detuning $\delta = \omega - (E_e - E_g)/\hbar$ and the so-called Rabi frequency Ω is defined by $\hbar\Omega(\mathbf{x}) = E(\mathbf{x})\langle e|\mathbf{d}\cdot\hat{\boldsymbol{\epsilon}}|g\rangle$.

For the simplest case of a two-level system the light shift V_g including the

15

lifetime $-i\hbar\Gamma_e/2$ of the excited state is given by,

$$
\begin{aligned}
V_g(\mathbf{x}) &= \operatorname{Re}\left[\frac{|\langle e|\mathbf{d}\cdot\hat{\boldsymbol{\epsilon}}|g\rangle|^2}{4}\left(\frac{1}{E_e - i\hbar\Gamma_e/2 - E_g - \hbar\omega}\right.\right. \\
&\qquad\qquad\qquad\qquad\left.\left.+\frac{1}{E_e - i\hbar\Gamma_e/2 - E_g + \hbar\omega}\right)(E(\mathbf{x}))^2\right] \\
&= \frac{|\hbar\Omega(\mathbf{x})|^2}{4}\operatorname{Re}\left[\left(\frac{1}{E_e - i\hbar\Gamma_e/2 - E_g - \hbar\omega}+\frac{1}{E_e - i\hbar\Gamma_e/2 - E_g + \hbar\omega}\right)\right] \\
&= \frac{|\hbar\Omega(\mathbf{x})|^2\cdot\hbar\delta}{4(\hbar\delta)^2 + \hbar^2\Gamma_e^2} + \frac{|\hbar\Omega(\mathbf{x})|^2\left(E_e - E_g + \hbar\omega\right)}{4\left(E_e - E_g + \hbar\omega\right)^2 + \hbar^2\Gamma_e^2}.
\end{aligned}
\tag{2.10}
$$

If the detuning is relatively small the second term on the right-hand side of the above equation can be neglected, because then $\hbar\omega$ is by far the largest energy scale in the problem and the light shift takes the simple form

$$
V_g(\mathbf{x}) = \left(\frac{|\Omega(\mathbf{x})|}{\Gamma_e}\right)^2\frac{\hbar\delta}{1 + 4\left(\delta/\Gamma_e\right)^2}.
$$

This corresponds to the so-called rotating-wave approximation. It is straightforward to generalize the above and take into account the contributions of other atomic transitions. From Eq. (2.10) we see that if the detuning is negative, i.e., if the light is red detuned with respect to the atomic transition, the light shift is negative and atoms are attracted to the light. Correspondingly the potential minima coincide with the intensity maxima. In the other case the light is blue detuned with respect to the atomic transition and the potential minima correspond to the minima of the intensity. Note that the excited state experiences the opposite shift. We find the effective photon absorption rate $\Gamma_{\text{eff}}(\mathbf{x})$ of the atoms in the optical lattice by calculating the imaginary part of the term between brackets in Eq. (2.10), i.e.,

$$
\begin{aligned}
\Gamma_{\text{eff}}(\mathbf{x}) &= \frac{\hbar|\Omega(\mathbf{x})|^2}{4}\operatorname{Im}\left[\left(\frac{1}{E_e - i\hbar\Gamma_e/2 - E_g - \hbar\omega}+\frac{1}{E_e - i\hbar\Gamma_e/2 - E_g + \hbar\omega}\right)\right] \\
&= \frac{1}{2}\left[\frac{\hbar|\Omega(\mathbf{x})|^2\hbar\Gamma_e}{4(\hbar\delta)^2 + \hbar^2\Gamma_e^2} + \frac{\hbar|\Omega(\mathbf{x})|^2\hbar\Gamma_e}{4\left(E_e - E_g + \hbar\omega\right)^2 + \hbar^2\Gamma_e^2}\right].
\end{aligned}
\tag{2.11}
$$

For detunings that are large with respect to the natural linewidth Γ_e, but small compared to $\hbar\omega$ of course, the effective absorption rate is given by $\Gamma_{\text{eff}}(\mathbf{x}) = \Gamma_e\left(|\Omega(\mathbf{x})|^2/8\delta^2\right)$.

As a second and more complicated example we calculate now the optical potential experienced by a ^{87}Rb atom in the limit where the detuning of the laser light is such that the hyperfine structure splitting is unresolved but the fine structure is resolved. As a brief reminder, we recall that the ground states of the alkali atoms

have a closed shell with one valence electron. All electrons occupy closed shells except the valence electron, which is in an *s*-orbital. The state of the atom is determined by its orbital angular momentum and its spin angular momentum and is denoted by $|^{2S+1}L_J\rangle$, where S is the total spin angular momentum, L the total orbital angular momentum and J the total angular momentum for all electrons. The spin-orbit coupling $\propto \mathbf{L} \cdot \mathbf{S}$ of the orbital angular momentum and the spin angular momentum leads to a splitting of the states, i.e., the so-called fine structure splitting of the atom. A further splitting of the states occurs when we include the interaction $\propto \mathbf{I} \cdot \mathbf{J}$ of the nuclear spin with the total angular momentum. The angular momenta of the nucleus and electrons couple to form the total angular momentum $\mathbf{F} = \mathbf{I} + \mathbf{J}$. The resulting level splitting is known as the hyperfine structure.

If we neglect the small coupling to the nuclear spin and take only into account the much larger spin-orbit coupling of the electrons. The laser field couples the ground-state configuration with total electronic angular momentum $J = 1/2$ to the two excited $L = 1$ states, which have $J = 1/2$ and $J = 3/2$ respectively. The relevant states can be written in the basis spanned by the vectors $|\alpha J M_J\rangle$, where J is the total electronic angular momentum, M_J is the projection and α labels all other quantum numbers. The transition matrix elements $\langle e|\mathbf{d} \cdot \hat{\boldsymbol{\epsilon}}|g\rangle$ consist of a radial contribution, which is the same for all states, and an angular part which determines the relative strengths of atomic transitions. For the above-mentioned transitions associated with the so-called D_1 and D_2 lines we therefore have to calculate the following matrix elements $\langle J'M_{J'}|z|JM_J\rangle$. Here $J' = 1/2$ for the D_1 line and $J' = 3/2$ for the D_2 line. As we have seen in Eq. (2.7) the light couples to the angular momentum component $\mathbf{L}$ and not to the spin. Therefore, we first perform a change of basis and expand the states in terms of angular momentum and spin wave functions explicitly as

$$|JM_J\rangle = \sum_{LM_LSM_S} \langle LM_LSM_S|JM_J\rangle|LM_L\rangle \otimes |SM_S\rangle. \qquad (2.12)$$

Here the $\langle LM_LSM_S|JM_J\rangle$ are the Clebsch-Gordan coefficients. Next we explicitly give the Clebsch-Gordan coefficients for the case of $M_J = 1/2$. For the ground state we have,

$$|1/2, 1/2\rangle = |0, 0\rangle \otimes |1/2, 1/2\rangle, \qquad (2.13)$$

and for the excited states we have,

$$|1/2, 1/2\rangle = \frac{1}{\sqrt{3}}|1, 0\rangle \otimes |1/2, 1/2\rangle - \sqrt{\frac{2}{3}}|1, 1\rangle \otimes |1/2, -1/2\rangle,$$

$$|3/2, 1/2\rangle = \sqrt{\frac{2}{3}}|1, 0\rangle \otimes |1/2, 1/2\rangle + \frac{1}{\sqrt{3}}|1, 1\rangle \otimes |1/2, -1/2\rangle. \qquad (2.14)$$

17

From this we see that the contribution to the light shift coming from the D_2 line is twice as strong as that of the D_1 line. Summarizing the above, we find that the shift of the ground-state is given by,

$$V_g(\mathbf{x}) = \frac{(\hbar|\Omega(\mathbf{x})|)^2}{12} \ \operatorname{Re}\left[\frac{2}{-\hbar\delta_{D_2} - i\hbar\Gamma_{D_2}/2} + \frac{2}{E_{D_2} - E_g + \hbar\omega - i\hbar\Gamma_{D_2}/2}\right.$$
$$\left. + \frac{1}{-\hbar\delta_{D_1} - i\Gamma_{D_1}/2} + \frac{1}{E_{D_1} - E_g + \hbar\omega + i\hbar\Gamma_{D_1}/2}\right].$$
$$(2.15)$$

Here $\delta_{D_{1,2}} = \omega - (E_{D_{1,2}} - E_g)/\hbar$ are the detunings of the D_1 and D_2 lines, respectively. For large enough detunings we cannot resolve the fine structure anymore and the two lines add up and we recover Eq. (2.10). In general the atom undergoes cycles of absorption and sponteneous emision and the force on the atom is an average of the force in the ground state and in the excited state. In the interesting case of low saturation or low laser intensity the atom is mostly in the ground state and the light-shifted ground state is the relevant potential for the atoms. With a spatially inhomogeneous intensity one can create a periodic potential for the atoms. Such a periodic potential is known as an optical lattice. For a deep optical lattice we can make a harmonic approximation at the potential minimum. This defines the on-site trapping frequency ω of the atoms through $V_g(\mathbf{x}) = m\omega^2 x^2/2$. Note that this ω should not be confused with the one in Eq. (2.9) that appears in the definition of the detuning and represents the laser frequency.

2.3 Band structure

The wave function of a free atom is a plane wave $e^{i\mathbf{k}\cdot\mathbf{x}}$ and has an energy dispersion relation $\epsilon_{\mathbf{k}} = \hbar^2\mathbf{k}^2/2m$. Neutral atoms in a periodic optical-lattice potential are described by Bloch wave functions, just like electrons in a solid-state crystal. The wave function in this case can be written as a product of a plane wave and a function $u_{\mathbf{n},\mathbf{k}}(\mathbf{x})$ that is periodic with the lattice period, i.e., $\psi_{\mathbf{n},\mathbf{k}}(\mathbf{x}) = e^{i\mathbf{k}\cdot\mathbf{x}}u_{\mathbf{n},\mathbf{k}}(\mathbf{x})$. This result is the well-known Bloch theorem [45, 46]. Accordingly, the dispersion relation is no longer quadratic with the lattice momentum but develops gaps at specific locations determined by the lattice structure. Equivalently, the energy of an atom can be specified by a band index $\mathbf{n}$ and a momentum that takes on values within the first Brillouin zone. As a concrete example, for the one-dimensional lattice with lattice constant $\lambda/2$ the dispersion looks like the free-particle dispersion for small momenta. When the momentum approaches the boundary of the first Brillouin zone at $\mathbf{k} = \pm 2\pi/\lambda$, with λ the wavelength of the laser light, the dispersion starts to deviate from the quadratic result. If the momentum is increased past the boundary of the first Brillouin zone the dispersion has a discontinuity and the jump in energy is the band gap.

Consider now an atom in a deep optical lattice centered at a lattice site x_i. In the tight-binding limit we approximate the Hamiltonian near a lattice site with an on-site Hamiltonian and use the associated wave functions $\phi_{\mathbf{n}}(\mathbf{x} - \mathbf{x}_i)$ of single atoms located at the lattice site. These wave functions can be used to create a new function $\psi_{\mathbf{n},\mathbf{k}}(\mathbf{x})$ that satisfies Bloch's theorem,

$$\psi_{\mathbf{n},\mathbf{k}}(\mathbf{x}) = \sum_i e^{i\mathbf{k}\cdot\mathbf{x}_i} \phi_{\mathbf{n}}(\mathbf{x} - \mathbf{x}_i). \qquad (2.16)$$

Even though the above function satisfies Bloch's theorem it is not the exact solution to the Schrödinger equation. However, it can be shown that there exist so-called Wannier functions $w_{\mathbf{n}}(\mathbf{x} - \mathbf{x}_i)$ for each band such that the wave function of Eq. (2.16), with $\phi_{\mathbf{n}}$ replaced by $w_{\mathbf{n}}$, gives the exact Bloch wave function for each band [45, 46]. The Wannier functions are orthogonal for different bands $\mathbf{n}$ as well as for different sites i. For sufficiently deep optical lattices the Wannier functions are of course well approximated by the tight-binding orbitals. This approximation is used throughout this thesis.

2.4   The Bose-Hubbard model

By using standing waves of laser light we can thus create a periodic potential for atoms. A system of bosonic atoms in such a potential can be modeled by the following Hamiltonian.

$$
\begin{aligned}
H \;=\; & \int d^3 x \; \psi_{\mathrm{a}}^{\dagger}(\mathbf{x}) \left(-\frac{\hbar^2 \nabla^2}{2m} + V_0(\mathbf{x}) \right) \psi_{\mathrm{a}}(\mathbf{x}) \\
& + \frac{1}{2} \int d^3\mathbf{x} \; d^3\mathbf{x}' \; \psi_{\mathrm{a}}^{\dagger}(\mathbf{x}) \psi_{\mathrm{a}}^{\dagger}(\mathbf{x}') V(\mathbf{x} - \mathbf{x}') \psi_{\mathrm{a}}(\mathbf{x}') \psi_{\mathrm{a}}(\mathbf{x}) \;,
\end{aligned}
$$
$$(2.17)$$

where the field operators $\psi_{\mathrm{a}}^{\dagger}(\mathbf{x})$ and $\psi_{\mathrm{a}}(\mathbf{x})$ create and annihilate an atom at position $\mathbf{x}$, respectively. The interaction potential between the atoms is given by $V(\mathbf{x} - \mathbf{x}')$ and the periodic potential is given by $V_0(\mathbf{x}) = \sum_j V_{j0} \cos^2(2\pi x_j / \lambda)$, where λ is the wavelength of the laser light. Using the Wannier functions introduced above we have that

$$\psi_a^{\dagger}(\mathbf{x}) = \sum_{\mathbf{n},i} a_{\mathbf{n},i}^{\dagger} w_{\mathbf{n}}^{*}(\mathbf{x} - \mathbf{x}_i), \text{ and } \psi_{\mathrm{a}}(\mathbf{x}) = \sum_{\mathbf{n},i} a_{\mathbf{n},i} w_{\mathbf{n}}(\mathbf{x} - \mathbf{x}_i). \qquad (2.18)$$

Here the operators $a_{\mathbf{n},i}^{\dagger}$ and $a_{\mathbf{n},i}$ create and annihilate an atom in the n-th trap state of site i, respectively. Note that the quantum number $\mathbf{n}$ in general denotes a vector, for example in the tight-binding limit the Wannier functions of the optical lattice are replaced by harmonic oscillator states on each site that, in cartesian

19

coordinates, depend on the three quantum numbers n_x, n_y and n_z. At sufficiently low temperatures and if the interaction energy is sufficiently small, the atoms will be in the lowest $\mathbf{n} = \mathbf{0}$ state of the lattice. Taking only this contribution into account gives the following lattice Hamiltonian,

$$
\begin{aligned}
H &= \sum_{ij} a_i^\dagger a_j \int d\mathbf{x}\ w_{\mathbf{0}}^*(\mathbf{x} - \mathbf{x}_i) \left(-\frac{\hbar^2 \nabla^2}{2m} + V_0(\mathbf{x}) - \mu \right) w_{\mathbf{0}}(\mathbf{x} - \mathbf{x}_j) \\
&\quad + \frac{1}{2} \sum_{iji'j'} a_i^\dagger a_{i'}^\dagger a_j a_{j'} \\
&\quad \times \int d\mathbf{x} d\mathbf{x}'\ w_{\mathbf{0}}^*(\mathbf{x} - \mathbf{x}_i) w_{\mathbf{0}}^*(\mathbf{x}' - \mathbf{x}_{i'}) V(\mathbf{x} - \mathbf{x}') w_{\mathbf{0}}(\mathbf{x}' - \mathbf{x}_j) w_{\mathbf{0}}(\mathbf{x} - \mathbf{x}_{j'}),
\end{aligned}
$$

$$(2.19)$$

where we have suppressed the band index $\mathbf{0}$ in the creation and annihilation operators. We can now write the above Hamiltonian in the form of the Bose-Hubbard model

$$
H = -t \sum_{\langle i,j \rangle} a_i^\dagger a_j + \sum_i (\epsilon_i - \mu) \hat{N}_i + \frac{1}{2} U \sum_i \hat{N}_i (\hat{N}_i - 1). \tag{2.20}
$$

Here $\hat{N}_i = a_i^\dagger a_i$ is the number operator and we have introduced the on-site energy,

$$
\epsilon_i = \int d\mathbf{x}\ w_{\mathbf{0}}^*(\mathbf{x} - \mathbf{x}_i) \left\{ -\frac{\hbar^2 \nabla^2}{2m} + V_0(\mathbf{x}) \right\} w_{\mathbf{0}}(\mathbf{x} - \mathbf{x}_i), \tag{2.21}
$$

and the tunneling amplitude,

$$
t_{ij} = -\int d\mathbf{x}\ w_{\mathbf{0}}^*(\mathbf{x} - \mathbf{x}_i) \left\{ -\frac{\hbar^2 \nabla^2}{2m} + V_0(\mathbf{x}) \right\} w_{\mathbf{0}}(\mathbf{x} - \mathbf{x}_j) \tag{2.22}
$$

for the nearest-neighbouring sites $\langle i, j \rangle$. In the tight-binding limit the Wannier function of the lowest band in the above equation is given by a Gaussian wave function. Explicitly substituting this into the above expression leads to the expression for the hopping-strength that we gave in Eq. (1.4). If we make the usual pseudo-potential approximation and replace the interatomic potential by a point interaction with the appropriate strength, i.e.,

$$
V(\mathbf{x} - \mathbf{x}') = \frac{4\pi a \hbar^2}{m} \delta(\mathbf{x} - \mathbf{x}'), \tag{2.23}
$$

we find for the interaction term

$$
\begin{aligned}
H_{\text{int}} &= \frac{1}{2} \sum_{iji'j'} a_i^\dagger a_{i'}^\dagger a_j a_{j'} \\
&\quad \times \int d\mathbf{x} d\mathbf{x}' \; w_\mathbf{0}^*(\mathbf{x} - \mathbf{x}_i) w_\mathbf{0}^*(\mathbf{x}' - \mathbf{x}_{i'}) V(\mathbf{x} - \mathbf{x}') w_\mathbf{0}(\mathbf{x}' - \mathbf{x}_i) w_\mathbf{0}(\mathbf{x} - \mathbf{x}_{j'}) \\
&\approx \frac{1}{2} \sum_i a_i^\dagger a_i^\dagger a_i a_i \frac{4\pi a \hbar^2}{m} \int d\mathbf{x} \; |w_\mathbf{0}(\mathbf{x} - \mathbf{x}_i)|^4 \\
&\equiv \frac{U}{2} \sum_i a_i^\dagger a_i^\dagger a_i a_i .
\end{aligned}
\tag{2.24}
$$

As before, in the tight-binding limit the Wannier function is replaced by a Gaussian wave function and the interaction energy U is given by Eq. (1.5). It should be noted that in the above derivation of the interaction energy, we have made the approximation that the atoms are in the lowest band. It is, however, possible to exactly solve the problem of two atoms in a harmonic potential with a point interaction [47, 48]. We then find that for the realistic values of the background interaction strenghts a that we consider in this thesis the above expression coincides in a very good approximation with the exact solution [48].

Chapter 3

Ultracold atoms in optical lattices

ABSTRACT

Bosonic atoms trapped in an optical lattice at very low temperatures, can be modeled by the Bose-Hubbard model. In this paper, we propose a slave-boson approach for dealing with the Bose-Hubbard model, which enables us to analytically describe the physics of this model at nonzero temperatures. With our approach the phase diagram for this model at nonzero temperatures can be quantified.

3.1   Introduction

The physics of the Bose-Hubbard model was the subject of intensive study for some years after the seminal paper by Fisher *et al.*, which focused on the behavior of bosons in a disordered environment [9]. More recently it has been realized that the Bose-Hubbard model can also be applied to bosons trapped in so-called optical lattices [81], and mean-field theories [49, 78, 50] and exact diagonalization [51] have been succesfully applied to these systems in one, two and three dimensional systems. The experiments performed by Greiner *et al.* [10] have confirmed the theoretically predicted quantum phase transition, i.e., a phase transition induced by quantum fluctuations, between a superfluid and a Mott-insulating phase. A review of the work carried out in this field has been given by Zwerger [52]. Strictly
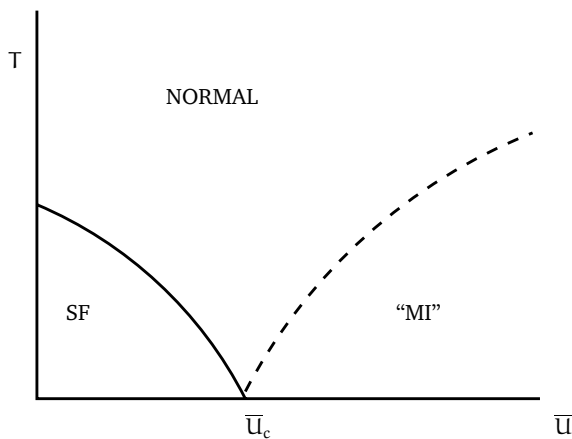
Figure 3.1: Qualitative phase diagram for a fixed and integer filling fraction in terms of the temperature T and the dimensionless coupling constant $\overline{U} = U/zt$, with superfluid (SF), normal and Mott insulating phases (MI). Only at $T = 0$ a true Mott insulator exists.

speaking the above mentioned quantum phase transition occurs only at zero temperature [34]. At nonzero temperatures there is a 'classical' phase transition, i.e., a phase transition induced by thermal fluctuations, between a superfluid phase and a normal phase and there is only a crossover between the normal phase and a Mott insulator. It is important to mention here that a Mott insulator is by definition incompressible. In principle there exists, therefore, no Mott insulator for any nonzero temperature where we always have a nonvanishing compressibillity. Nevertheless, there is a region in the phase diagram where the compressibillity is very close to zero and it is therefore justified to call this region for all practical purposes a Mott insulator [50]. Qualitatively this phase diagram is sketched in Fig. 3.1 for a fixed density. This figure shows how at a sufficiently small but nonzero temperature we start with a superfluid for small positive on-site interaction U, we encounter a phase transition to a normal phase as the interaction strength increases, and ultimately crossover to a Mott insulator for even higher values of the interaction strength. We can also incorporate this nonzero temperature behaviour into the phase diagram in Fig. 3.2. This figure shows how at zero temperature we only have a superfluid and a Mott insulator phase, but as the temperature is increased a normal phase appears in between these two phases.

The aim of this paper is to extend the mean-field approach for the Bose-Hubbard model to include nonzero temperature effects and make the qualitative phase diagrams in Figs. 3.1 and 3.2 more quantitative. To do that we make use of auxiliary particles that are known as slave bosons [53]. The idea behind this is
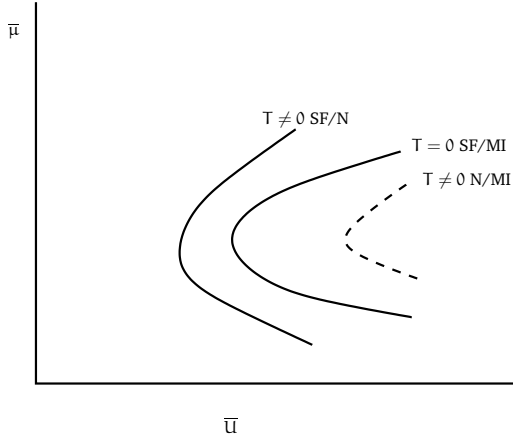
$\overline{\mu}$

Figure 3.2: Qualitative phase diagram in terms of the chemical potential $\overline{\mu} = \mu/zt$ and the dimensionless coupling constant $\overline{U} = U/zt$. The solid lines indicate real phase transitions between superfluid, normal and Mott insulating phases. The dashed line corresponds to a crossover between a normal and a Mott insulating phase.

that if we consider a single lattice site, the occupation number on that site can be any integer. With each different occupation number we identify a new particle. Although this means that we introduce a lot of different new particles, the advantage of this procedure is that it allows us to transform the on-site repulsion into an energy contribution that is quadratic in terms of the new particles. Because we want to be able to uniquely label each different state of the system, the new particles cannot independently be present at each lattice site. That is why we have to introduce a constraint. Using this we derive within a functional-integral formalism an effective action for the superfluid order parameter which depends on the temperature. The equivalence with previous work at zero temperature is demonstrated.

The outline of the paper is as follows. In Sec. 3.2 we introduce the slave-boson formalism and derive an effective action for the superfluid order parameter. In Sec. 3.3 we present the zero- and nonzero-temperature mean-field results. The remainder of the paper is devoted to the effect that the creation of quasiparticle-quasihole pairs have on the system.

3.2 Slave-boson theory for the Bose-Hubbard model

In this section we formalize the above introduced idea of the slave bosons. We rewrite the Bose-Hubbard model in terms of these slave bosons within a path-integral formulation and derive an effective action for the superfluid order parameter, which then describes all the physics of our Bose gas in the optical lattice.

The slave-boson technique was introduced by Kotliar and Ruckenstein [53], who used it to deal with the fermionic Hubbard model. A functional integral approach to the problem of hard-core bosons hopping on a lattice has been previously put forward by Ziegler [54] and Frésard [55]. Let us first shed some light on this slave-boson formalism. We consider a single site of our lattice. If the creation and anihilation operators for the bosons are denoted by $\hat{a}_i^\dagger$ and $\hat{a}_i$ respectively, we can form the number operator $\hat{N}_i = \hat{a}_i^\dagger \hat{a}_i$, which counts the number of bosons at the site i. In the slave-boson formalism, for any occupation number a pair of bosonic creation and annihilation operators is introduced that create and annihilate the state with precisely that given integer number of particles. The original occupation number states $|n_i\rangle$ are now decomposed as $|n_i^0, n_i^1, \ldots\rangle$, where n_i^α is the eigenvalue of the number operator $\hat{n}_i^\alpha \equiv (\hat{a}_i^\alpha)^\dagger \hat{a}_i^\alpha$ formed by the pair of creation $(\hat{a}_i^\alpha)^\dagger$ and annihilation $\hat{a}_i^\alpha$ operators that create and annihilate bosons of type α at the site i. As it stands, this decomposition is certainly not unique. For example, the original state $|2\rangle$ could be written as $|0,0,1,0,\ldots\rangle$ or as $|0,2,0,\ldots\rangle$. Our Hilbert space thus greatly increases. To make sure that every occupation occurs only once we have to introduce an additional constraint, namely

$$\sum_\alpha \hat{n}_j^\alpha = 1 \tag{3.1}$$

for every site j. This constraint thus makes sure that there is always just one slave boson per site. Because in the positive U Bose-Hubbard model bosons on the same site repel each other, high on-site occupation numbers are disfavored. It is therefore conceivable that a good approximation of the physics of the Bose-Hubbard model is obtained by allowing a relatively small maximum number, e.g. two or three or four, of bosons per site.

As is well known, the Hamiltonian of the Bose-Hubbard model reads,

$$\hat{H} = -\sum_{\langle i,j\rangle} \hat{a}_i^\dagger t_{ij} \hat{a}_j - \mu \sum_i \hat{a}_i^\dagger \hat{a}_i + \frac{U}{2}\sum_i \hat{a}_i^\dagger \hat{a}_i^\dagger \hat{a}_i \hat{a}_i. \tag{3.2}$$

Here $\langle i,j\rangle$ denotes the sum over nearest neighbours, t_{ij} are the hopping parameters, and μ is the chemical potential. Using our slave-boson operators we now rewrite

Eq. (3.2) into the form

$$\hat{H} = \ - \ \sum_{\langle i,j \rangle} \sum_{\alpha,\beta} \sqrt{\alpha+1}\sqrt{\beta+1}(\hat{a}_i^{\alpha+1})^\dagger \hat{a}_i^\alpha t_{ij} \hat{a}_j^{\beta+1}(\hat{a}_j^\beta)^\dagger - \mu \sum_i \sum_\alpha \alpha \hat{n}_i^\alpha$$
$$+ \ \frac{U}{2} \sum_i \sum_\alpha \alpha(\alpha-1)\hat{n}_i^\alpha, \qquad (3.3)$$

with the additional constraint given in Eq. (3.1). We see that the quartic term in the original Bose-Hubbard Hamiltonian has been replaced by one that is quadratic in the slave-boson creation and annihilation operators, which is the most important motivation for the introduction of slave bosons.

Now that we have introduced the slave-boson method and derived its representation of the Bose-Hubbard model, we want to turn the Hamiltonian into an action for the imaginary time evolution. Using the standard recipe [56, 57] we find

$$
\begin{aligned}
S[(a^\alpha)^*, a^\alpha, \lambda] \ = \ & \int_0^{\hbar\beta} d\tau \left\{ \sum_i \sum_{\alpha\beta} (a_i^\alpha)^* M^{\alpha\beta} a_i^\beta - i \sum_i \lambda_i(\tau) \left(\sum_\alpha n_i^\alpha - 1 \right) \right. \\
& \left. - \sum_{\langle i,j \rangle} \sum_{\alpha,\beta} \sqrt{\alpha+1}\sqrt{\beta+1}(a_i^{\alpha+1})^* a_i^\alpha t_{ij} a_j^{\beta+1}(a_j^\beta)^* \right\}, \qquad (3.4)
\end{aligned}
$$

where M is a diagonal matrix that has as the αth diagonal entry the term $\hbar\partial/\partial\tau - \alpha\mu + \alpha(\alpha-1)U/2$, and $\beta = 1/k_B T$ is the inverse thermal energy. The real-valued constraint field λ enters the action through,

$$\prod_i \delta(\sum_\alpha n_i^\alpha - 1) = \int d[\lambda] \exp\left[\frac{i}{\hbar} \int_0^{\hbar\beta} \sum_i \lambda_i(\tau) \left(\sum_\alpha n_i^\alpha - 1 \right) d\tau \right]. \qquad (3.5)$$

Although we have simplified the interaction term, the hopping term has become more complicated. By performing a Hubbard-Stratonovich transformation on the above action we can, however, decouple the hopping term in a similar manner as in Ref. [78]. This introduces a field Φ into the action which, as we will see, may be identified with the superfluid order parameter. The Hubbard-Stratonovich transformation basically consists of adding a complete square to the action, i.e., adding

$$\int_0^{\hbar\beta} d\tau \sum_{i,j} \left(\Phi_i^* - \sum_\alpha \sqrt{\alpha+1}(a_i^{\alpha+1})^* a_i^\alpha \right) t_{ij} \left(\Phi_j - \sum_\alpha \sqrt{\alpha+1} a_j^{\alpha+1}(a_j^\alpha)^* \right).$$

Since a complete square can be added to the action without changing the physics we see that this procedure allows us to decouple the hopping term. We also perform a Fourier transform on all fields by means of

27

$a_i^\alpha(\tau) = (1/\sqrt{N_s\hbar\beta}) \sum_{\mathbf{k},n} a_{\mathbf{k},n}^\alpha e^{i(\mathbf{k}\cdot\mathbf{x}_i - \omega_n\tau)}$. If we also carry out the remaining integrals and sums we find

$$
\begin{aligned}
S[\Phi^*, \Phi, (a^\alpha)^*, a^\alpha, \lambda] = &\sum_{\mathbf{k},n} \epsilon_\mathbf{k} |\Phi_{\mathbf{k},n}|^2 + \sum_{\mathbf{k},n} (a_{\mathbf{k},n}^\alpha)^* M^{\alpha\beta}(i\omega_n) a_{\mathbf{k},n}^\beta \\
&-i\frac{1}{\sqrt{N_s\hbar\beta}} \sum_{\mathbf{k},\mathbf{q}} \sum_{n,n'} \lambda_{\mathbf{q},n'} (a_{\mathbf{k},n}^\alpha)^* a_{\mathbf{k}+\mathbf{q},n+n'}^\alpha + iN_s\hbar\beta\lambda \\
&- \sum_{\mathbf{k},\mathbf{k}',n,n'} \frac{\epsilon_{\mathbf{k}'}}{\sqrt{N_s\hbar\beta}} \left\{ \left(\sum_\alpha \sqrt{\alpha+1}(a_{\mathbf{k}+\mathbf{k}',n+n'}^{\alpha+1})^* a_{\mathbf{k},n}^\alpha \right) \Phi_{\mathbf{k}',n'} \right. \\
&\left. + \Phi_{\mathbf{k}',n'}^* \left(\sum_\alpha \sqrt{\alpha+1}a_{\mathbf{k}+\mathbf{k}',n+n'}^{\alpha+1}(a_{\mathbf{k},n}^\alpha)^* \right) \right\},
\end{aligned}
$$
(3.6)

where the matrix $M(i\omega_n)$ is related to the matrix M in Eq. (3.4) through a Fourier transform. Furthermore, $\lambda = (\lambda_{\mathbf{0},0}/\sqrt{N_s\hbar\beta})$, $\epsilon_\mathbf{k} = 2t \sum_{j=1}^d \cos(k_j a)$, where a is the lattice constant of the square lattice with N_s lattice sites. For completeness we point out that the integration measure has become

$$
\int d[(a^\alpha)^*] d[a^\alpha] = \int \prod_{\mathbf{k},n} d[(a_{\mathbf{k},n}^\alpha)^*] d[a_{\mathbf{k},n}^\alpha] \frac{1}{\hbar\beta}.
$$
(3.7)

In principle Eq. (3.6) is still an exact rewriting of the Bose-Hubbard model. As a first approximation we soften the constraint by replacing the general constraint field $\lambda_i(\tau)$ with a time and position independent field λ. By neglecting the position dependence we enforce the constraint only on the sum of all lattice sites. Doing this we are only left with the $\lambda_{\mathbf{0},0}$ contribution in Eq. (3.6), which can then be added to the matrix M. The path-integral over the constraint field reduces to an ordinary integral. So we have,

$$
S[\Phi^*, \Phi, (a^\alpha)^*, a^\alpha, \lambda] = S_0 + S_I
$$
(3.8a)

where,

$$
\begin{aligned}
S_0 &= iN_s\hbar\beta\lambda + \sum_{\alpha,\beta} \sum_{\mathbf{k},n} \left\{ \epsilon_\mathbf{k} |\Phi_{\mathbf{k},n}|^2 + (a_{\mathbf{k},n}^\alpha)^* M^{\alpha\beta}(i\omega_n) a_{\mathbf{k},n}^\beta \right\} \\
&\equiv S_0^{SB} + \sum_{\mathbf{k},n} \epsilon_\mathbf{k} |\Phi_{\mathbf{k},n}|^2,
\end{aligned}
$$
(3.8b)

28

The matrix $M^{\alpha\beta}(i\omega_n) = \delta_{\alpha\beta}(-i\hbar\omega_n - i\lambda - \alpha\mu + \alpha(\alpha-1)U/2)$, and

$$
S_I = \quad -\sum_{\mathbf{k},\mathbf{k}',n,n'} \frac{\epsilon_{\mathbf{k}'}}{\sqrt{N_s\hbar\beta}} \left\{ \left(\sum_\alpha \sqrt{\alpha+1}(a^{\alpha+1}_{\mathbf{k}+\mathbf{k}',n+n'})^* a^\alpha_{\mathbf{k},n} \right) \Phi_{\mathbf{k}',n'} \right.
$$
$$
\left. + \Phi^*_{\mathbf{k}',n'} \left(\sum_\alpha \sqrt{\alpha+1} a^{\alpha+1}_{\mathbf{k}+\mathbf{k}',n+n'}(a^\alpha_{\mathbf{k},n})^* \right) \right\}.
$$
$$(3.8c)$$

The crucial idea of Landau theory is that near a critical point the quantity of most interest is the order parameter. In our theory the superfluid field Φ plays the role of the order parameter. Only $\Phi_{\mathbf{0},0}$ can have a nonvanishing expectation value in our case and, therefore, we can write the free energy as an expansion in powers of $\Phi_{\mathbf{0},0}$,

$$
F(\Phi_{\mathbf{0},0}) = a_0(\alpha, U, \mu) + a_2(\alpha, U, \mu)|\Phi_{\mathbf{0},0}|^2 + \mathcal{O}(|\Phi_{\mathbf{0},0}|^4), \qquad (3.9)
$$

and minimize it as a function of the superfluid order parameter $\Phi_{\mathbf{0},0}$. We thus find that $\langle\Phi_{\mathbf{0},0}\rangle = 0$ when $a_2(\alpha, U, \mu) > 0$ and that $\langle\Phi_{\mathbf{0},0}\rangle \neq 0$ when $a_2(\alpha, U, \mu) < 0$. This means that $a_2(\alpha, U, \mu) = 0$ signals the boundary between the superfluid and the insulator phases at zero temperature and the boundary between the superfluid and the normal phases at nonzero temperature. Therefore we are going to calculate the effective action of our theory up to second order in Φ. The zeroth-order term in the expansion of the action in powers of the order parameter gives us the zeroth-order contribution Ω_0 to the thermodynamic potential Ω. We have,

$$
e^{-\beta\Omega_0} \equiv \int \prod_\alpha \left(\prod_{\mathbf{k},n} d[(a^\alpha_{\mathbf{k},n})^*]d[a^\alpha_{\mathbf{k},n}]\frac{1}{\hbar\beta} \right) e^{-S_0^{SB}/\hbar}. \qquad (3.10)
$$

From this it follows that,

$$
-\beta\Omega_0 = -iN_s\beta\lambda + N_s \sum_\alpha \log\left(1 - e^{-\beta M^{\alpha\alpha}(0)}\right), \qquad (3.11)
$$

and $M^{\alpha\alpha}(0) = (-i\lambda - \alpha\mu + \alpha(\alpha-1)U/2)$. Next we must calculate $\langle S_I^2\rangle$ where $\langle\cdots\rangle$ denotes averaging with respect to S_0, i.e.,

$$
\langle A\rangle = \frac{1}{e^{-\beta\Omega_0}} \int \prod_\alpha \left(\prod_{\mathbf{k},n} d[(a^\alpha_{\mathbf{k},n})^*]d[a^\alpha_{\mathbf{k},n}]\frac{1}{\hbar\beta} \right) A[(a^\alpha)^*, a^\alpha]e^{-S_0^{SB}/\hbar}. \qquad (3.12)
$$

Once we have this contribution, we automatically also find the dispersion relations for the quasiparticles in our system as we will see shortly. For small Φ we are

29

allowed to expand the exponent in the integrand of the functional integral for the partition function as

$$e^{-S/\hbar} = e^{-(S_0+S_I)/\hbar} \approx e^{-S_0/\hbar}(1 - S_I/\hbar + \frac{1}{2}(S_I/\hbar)^2). \qquad (3.13)$$

It can be shown that the expectation value of S_I vanishes. The second order contribution is found to be,

$$\langle S_I^2 \rangle = 2 \sum_{\mathbf{k},\mathbf{k}',n,n'} \epsilon_{\mathbf{k}}^2 \frac{|\Phi_{\mathbf{k}}|^2}{N_s \hbar \beta} \sum_\alpha (\alpha+1)\langle (a_{\mathbf{k}+\mathbf{k}',n+n'}^{\alpha+1})^* a_{\mathbf{k}+\mathbf{k}',n+n'}^{\alpha+1} \rangle \langle (a_{\mathbf{k},n}^{\alpha})^* a_{\mathbf{k},n}^{\alpha} \rangle. \qquad (3.14)$$

One of the sums over the Matsubara frequencies ω_n can be performed and the sum over $\mathbf{k}'$ produces an overal factor N_s. We thus find

$$\langle S_I^2 \rangle = \sum_{\mathbf{k},n} \epsilon_{\mathbf{k}}^2 \frac{|\Phi_{\mathbf{k}}|^2}{\hbar \beta} \sum_\alpha (\alpha+1)\frac{n^\alpha - n^{\alpha+1}}{-i\hbar\omega_n - \mu + \alpha U}, \qquad (3.15)$$

where we have defined the occupation numbers $n^\alpha \equiv \langle (a_i^\alpha)^* a_i^\alpha \rangle$ that equal

$$n^\alpha = \frac{1}{\exp\left\{\beta\left(-i\lambda - \alpha\mu + \frac{1}{2}\alpha(\alpha-1)U\right)\right\} - 1}. \qquad (3.16)$$

Having performed the integrals over the slave-boson fields to second order, we can exponentiate the result to obtain the effective action for the order parameter

$$S^{\text{eff}}[\Phi^*, \Phi] \quad = \quad \left(\hbar\beta\Omega_0 - \hbar \sum_{\mathbf{k},n} \Phi_{\mathbf{k},n}^* G^{-1}(\mathbf{k}, i\omega_n)\Phi_{\mathbf{k},n}\right), \qquad (3.17)$$

where we have defined the Green's function

$$-\hbar G^{-1}(\mathbf{k}, i\omega_n) = \left(\epsilon_{\mathbf{k}} - \epsilon_{\mathbf{k}}^2 \sum_\alpha (\alpha+1)\frac{n^\alpha - n^{\alpha+1}}{-i\hbar\omega_n - \mu + \alpha U}\right). \qquad (3.18)$$

This result is one of the key results of this paper, which is correct in the limit of small $\Phi_{\mathbf{k},n}$. If we want to make the connection with the Landau theory again, we can identify the $a_2(\alpha, U, \mu)$ in Eq. (3.9) with $G^{-1}(\mathbf{0}, 0)/\beta$. In Sec. 3.3 we analyse this further.

3.2.1   Mott insulator

In the Mott insulator where $n_0 \equiv |\langle \Phi_{\mathbf{0},0}\rangle|^2 = 0$, the thermodynamic potential is now easily calculated by integrating out the superfluid field. In detail

$$
\begin{aligned}
Z \equiv e^{-\beta\Omega} &= \int d\lambda d[\Phi^*] d[\Phi] e^{-S^{\text{eff}}/\hbar} \\
&= \int d\lambda \exp\Big\{ -\beta\Omega_0 \\
&\quad - \sum_{\mathbf{k},n} \log\left[\beta\left(\epsilon_{\mathbf{k}} - \epsilon_{\mathbf{k}}^2 \sum_{\alpha}(\alpha+1)\frac{n^\alpha - n^{\alpha+1}}{-i\hbar\omega_n - \mu + \alpha U} \right) \right] \Big\}.
\end{aligned}
$$
$$(3.19)$$

At this point we perform a saddle point approximation for the constraint field λ. This implies that we only take into account that value of λ that maximizes the canonical partition function. If we now thus minimize the free energy with respect to the chemical potential and the constraint field, we get two equations that need to be solved. The first is $\partial\Omega/\partial\lambda = 0$ and reads,

$$
N_s\left(1 - \sum_{\alpha} n^\alpha\right) - \frac{i}{\beta}\sum_{\mathbf{k},n} G(\mathbf{k}, i\omega_n)\frac{\partial G^{-1}(\mathbf{k}, i\omega_n)}{\partial\lambda} = 0.
$$
$$(3.20a)$$

In a mean-field approximation the last term is neglected, and this equation tells us that the sum of the average slave-boson occupation numbers must be equal to one. This reflects the constraint of one slave boson per site. The second equation follows from $-\partial\Omega/\partial\mu = N$ and gives

$$
N_s\sum_{\alpha}\alpha n^\alpha + \frac{1}{\beta}\sum_{\mathbf{k},n} G(\mathbf{k}, i\omega_n)\frac{\partial G^{-1}(\mathbf{k}, i\omega_n)}{\partial\mu} = N.
$$
$$(3.20b)$$

This equation shows how the particle density can be seen as the sum of terms αn^α and a correction coming from the propagator of the superfluid order parameter. The latter is again neglected in the mean-field approximation.

3.2.2   Superfluid phase

In the superfluid phase the order parameter $|\Phi_{\mathbf{0},0}|^2$ has a nonzero expectation value. We find this expectation value by calculating the minimum of the classical part of the action, i.e., $-\hbar G^{-1}(\mathbf{0},0)|\Phi_{\mathbf{0},0}|^2 + a_4|\Phi_{\mathbf{0},0}|^4$. This minimum becomes nonzero when $-\hbar G^{-1}(\mathbf{0},0)$ becomes negative, and is then equal to

$$
|\langle \Phi_{\mathbf{0},0}\rangle|^2 = \frac{\hbar G^{-1}(\mathbf{0},0)}{2a_4} \equiv n_0
$$
$$(3.21)$$

31

In appendix 3.6 we calculate the coefficient a_4 of the fourth order term $|\Phi_{\mathbf{0},0}|^4$. We approximate the prefactor to the fourth order term, which in general depends on momenta and Matsubara frequencies, with the zero-momentum and zero-frequency value of a_4 so that the approximate action to fourth order becomes,

$$
\begin{aligned}
S \;=\; & \hbar\beta\Omega_0 - \hbar\sum_{\mathbf{k},n}\Phi^*_{\mathbf{k},n}G^{-1}(\mathbf{k},i\omega_n)\Phi_{\mathbf{k},n} \\
& +a_4\sum_{\mathbf{k},\mathbf{k}',\mathbf{k}''}\sum_{n,n',n''}\Phi^*_{\mathbf{k},n}\Phi^*_{\mathbf{k}',n'}\Phi_{\mathbf{k}'',n''}\Phi_{\mathbf{k}+\mathbf{k}'-\mathbf{k}'',n+n'-n''} \quad (3.22)
\end{aligned}
$$

We now write the order parameter as the sum of its expectation value plus fluctuations, i.e., $\Phi_{\mathbf{0},0} \rightarrow \sqrt{n_0}\cdot\sqrt{N_s\hbar\beta} + \Phi_{\mathbf{0},0}$ and a similar expression for $\Phi^*_{\mathbf{0},0}$. If we put this into the action and only keep the terms up to second order, the contribution of the fourth-order term is given by

$$
a_4 n_0 \sum_{\mathbf{k},n}\left(\Phi_{\mathbf{k},n}\Phi_{-\mathbf{k},-n} + 4\Phi^*_{\mathbf{k},n}\Phi_{\mathbf{k},n} + \Phi^*_{\mathbf{k},n}\Phi^*_{-\mathbf{k},-n}\right).
$$

There is also a contribution $-\hbar G^{-1}(\mathbf{0},0)n_0$ from the second-order term. To summarize, in the superfluid phase we can write the action Eq. (3.22) to second order as

$$
\begin{aligned}
S^{\mathrm{SF}} = & \hbar\beta\Omega_0 - \hbar G^{-1}(\mathbf{0},0)n_0 \\
& -\frac{\hbar}{2}\sum_{\mathbf{k},n}\begin{pmatrix}\Phi^*_{\mathbf{k},n} & \Phi_{-\mathbf{k},-n}\end{pmatrix}\mathbf{G}^{-1}(\mathbf{k},i\omega_n)\begin{pmatrix}\Phi_{\mathbf{k},n}\\ \Phi^*_{-\mathbf{k},-n}\end{pmatrix}
\end{aligned} \quad (3.23)
$$

with

$$
-\mathbf{G}^{-1}(\mathbf{k},i\omega_n) = \begin{pmatrix} -G^{-1}(\mathbf{k},i\omega_n) + 4\hbar a_4 n_0 & 2\hbar a_4 n_0 \\ 2\hbar a_4 n_0 & -G^{-1}(-\mathbf{k},-i\omega_n) + 4\hbar a_4 n_0 \end{pmatrix}.
$$

$$(3.24)$$

Integrating out the field $\Phi_{\mathbf{k},n}$ we find the Bogoliubov expression for the thermodynamic potential in the superfluid phase,

$$
\begin{aligned}
Z \equiv e^{-\beta\Omega} \;=\; & \int d\lambda d[\Phi^*]d[\Phi]e^{-S^{\mathrm{SF}}/\hbar} \\
=\; & \int d\lambda \exp\left\{-\beta\Omega_0 + n_0 G^{-1}(\mathbf{0},0) - \mathrm{Tr}\left[\log\left(-\hbar\beta\mathbf{G}^{-1}\right)\right]\right\}
\end{aligned}
$$

$$(3.25)$$

3.3 Mean-field theory

In this section, we apply the theory we have developed in the previous section. First, using the Landau procedure, we reproduce the mean-field zero-temperature

phase diagram. We then study the phase diagram at nonzero temperatures. To do so we calculate the compressibillity of our system as a function of temperature, showing how for fixed on-site repulsion U the Mott insulating region gets smaller. By also looking at the condensate density as a function of temperature, we get a quantitative picture of what happens at fixed on-site repulsion U. The nice feature is that all our expressions are analytic. Next, we consider our system at zero temperature again and we study at the mean-field level the behaviour of the compressibillity as we go from the superfluid phase to the Mott insulating phase. What we find is consistent with the general idea that the quantum phase transition between the Mott insulator and the superfluid phases belongs to different universality classes depending on how you walk through the phase diagram (cf. Ref. [34]). We then obtain an analytic expression for the critical temperature of the superfluid-normal phase transition in the approximation of three slave bosons, i.e., up to doubly-occupied sites. Numerically we extend this study to include a fourth slave boson and find only slight changes to T_c. From the propagator of the superfluid field we extract the dispersion relations of the quasiparticle-quasihole pairs and their temperature dependence.

3.3.1 Zero-temperature phase-diagram

From the zeros of $G^{-1}(\mathbf{0}, 0)$ in Eq. (3.18), we obtain the mean-field phase diagram in the (μ, U) plane. For a Mott insulating state with integer filling factor α' we have $n^{\alpha} = \delta_{\alpha, \alpha'}$. When this is substituted into the equation $G^{-1}(\mathbf{0}, 0) = 0$ we can find the $U(\mu)$ curve that solves that equation and thus determines the size of this Mott insulating state. For given filling factor α' we also define U_c as the minimal U that solves the equation. Within the Mott insulating phase we have a zero compressibility $\kappa \equiv \partial n / \partial \mu$, where $n = n(\mu, U)$ is the total density as determined from the thermodynamic potential. Straightforward calculation gives that we are in a Mott insulating phase whenever $\bar{\mu}$ lies between $\bar{\mu}_-^{\alpha'}$ and $\bar{\mu}_+^{\alpha'}$ where,

$$\bar{\mu}_\pm^{\alpha'} = \frac{1}{2}\left(\bar{U}(2\alpha' - 1) - 1\right) \pm \frac{1}{2}\sqrt{\bar{U}^2 - 2\bar{U}(2\alpha' + 1) + 1}. \qquad (3.26)$$

Here we have introduced the dimensionless chemical potential $\bar{\mu} \equiv \mu/zt$ and on-site repulsion strength $\bar{U} \equiv U/zt$. When $\bar{\mu}$ does not lie between any $\bar{\mu}_-^{\alpha'}$ and $\bar{\mu}_+^{\alpha'}$ the 'superfluid' density $|\langle \Phi_{\mathbf{0},0}\rangle|^2$ will no longer be zero and the Mott insulating phase has disappeared. We have drawn the zero temperature phase diagram in Fig. 3.3. Our slave-boson approach reproduces here the results of previous mean-field studies [9, 49, 78]. For nonzero temperatures the equation $G^{-1}(\mathbf{0}, 0) = 0$ no longer describes a quantum phase transition between a superfluid and a Mott insulator but it describes a thermal phase transition between a superfluid and a normal phase. We will look into this in more detail in Sec. 3.3.6.
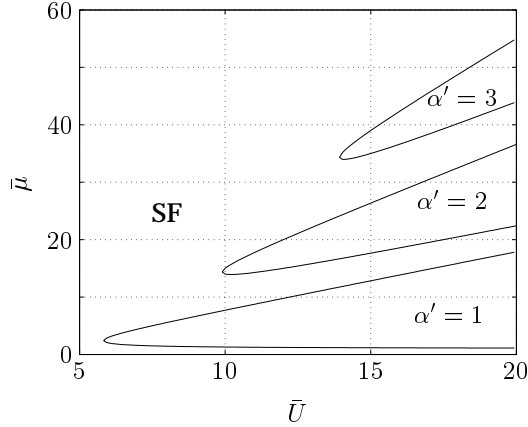
Figure 3.3: Phase diagram of the Bose-Hubbard Hamiltonian as obtained from the mean-field zero-temperature limit in the slave-boson formalism. It shows the superfluid (SF) phase and the Mott insulator regions with different integer filling factors here denoted by α'. The vertical axis shows the dimensionless chemical potential $\bar{\mu} = \mu/zt$ and the horizontal axis shows the dimensionless interaction strength $\bar{U} = U/zt$.

3.3.2 Compressibillity

To see what happens to the Mott insulator as we move away from zero temperature we must look at the compressibillity as a function of temperature. Numerically we have solved Eq. (3.20), which gives us the occupation numbers of the slave bosons as depicted in Fig. 3.4. With that we can determine the total density in the phase where the order parameter is zero. It is clear that within a mean-field approximation the compressibillity at zero temperature is exactly zero. In Fig. 3.4 we have plotted the total density as a function of temperature. As the temperature is raised we find that the compressibillity, which is the slope of the curve, for a given value of $\bar{U}$ becomes nonzero for all values of $\bar{\mu}$. Although the slope can be exponentially small, this shows that there is no longer a Mott insulator present. Because we are dealing with a crossover there is not a unique way to define the transition from a normal to a Mott insulator phase. There are various ways to determine the crossover line. For instance we can define it by requiring that $\Delta(T)/k_B T$ is of order one, where $\Delta(T)$ is defined as the difference of the quasiparticle and quasihole dispersions at $\mathbf{k} = 0$. Another possibility is to define it by requiring that the incommensurability is equal to a certain small value.
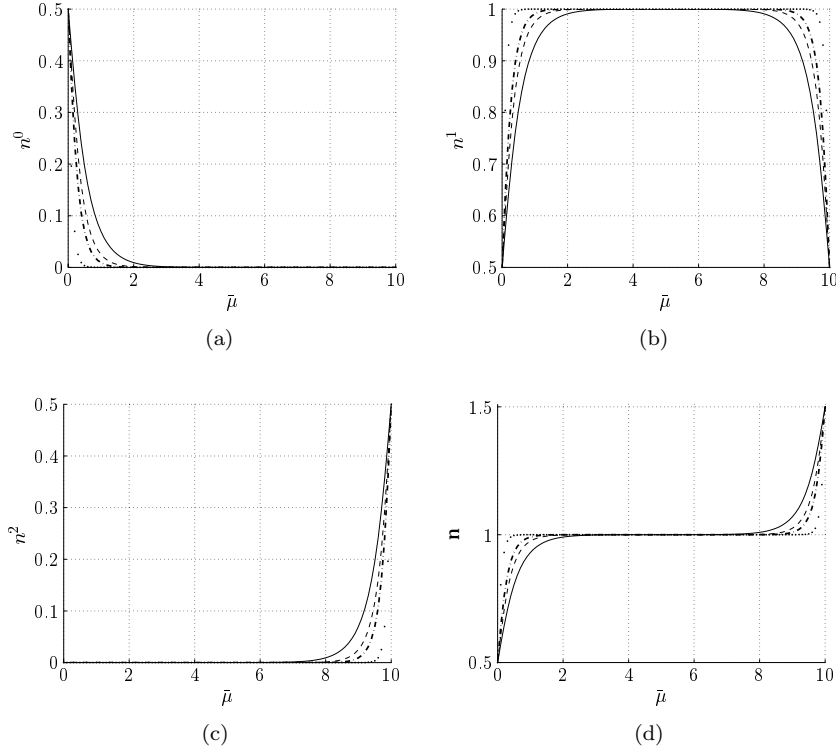
Figure 3.4: Numerical solution of the slave-boson occupation numbers n^0, n^1 and n^2 is shown in Figs. (a)-(c) as a function of $\bar{\mu}$ for various temperatures and for fixed $U/zt = 10$. Figure (d) shows the total density n. As a function of temperature the compressibillity increases. In the figures the solid line corresponds to $zt\beta = 2$, the dashed line corresponds to $zt\beta = 3$, the dashed-dotted line corresponds to $zt\beta = 4$ and the dotted line corresponds to $zt\beta = 10$.

Figure 3.5: Superfluid density $|\Phi_{\mathbf{0},0}|^2$ as a function of $\bar{\mu}$ for various temperatures and for $U/zt = 10$. The superfluid density as well as the region of superflu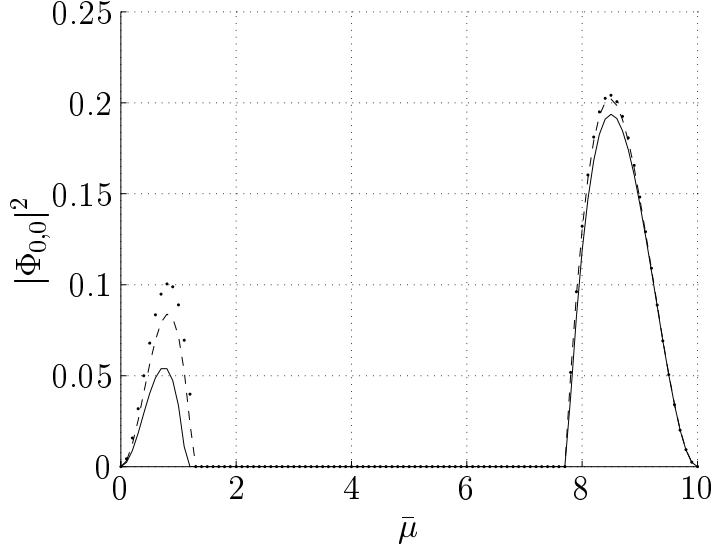id phase diminish as a function of increasing temperature. The vanishing of $|\Phi_{\mathbf{0},0}|^2$ at $\bar{\mu} = 0$ and $\bar{\mu} = 10$ is an artefact of our approximation (see text). In the figure the dotted line corresponds to $zt\beta = 10$, the dashed line corresponds to $zt\beta = 3$ and the solid line corresponds to $zt\beta = 2$.

3.3.3 Superfluid density

In a mean-field approximation the superfluid density is extracted from the action by finding the $|\langle\Phi_{\mathbf{0},0}\rangle|^2$ that minimizes the fourth-order action in Eq. (3.22),

$$|\langle\Phi_{\mathbf{0},0}\rangle|^2 = \frac{\hbar G^{-1}(\mathbf{0},0)}{2a_4}, \tag{3.27}$$

whenever μ is not between $\mu_-^{\alpha'}$ and $\mu_+^{\alpha'}$, and zero otherwise. We have plotted this expectation value in Fig. 3.5 for $\alpha' = 1$. In this figure we see how the superfluid density grows as a function of μ moving away from the Mott insulator phase. Our expansion of the Landau free energy is only valid around the edge of the Mott lobes and therefore breaks down when we go too far away from the Mott insulator. This can be seen in the figure as the decrease of the superfluid density when μ approaches 0 and/or U. It can also be seen from the propagator of the superfluid field, which has poles when $\mu = \alpha U$. For μ not too far away from the insulating phase the figure quantitatively agrees with the ones calculated by other authors

[78].

3.3.4   Bogoliubov dispersion relation

We now demonstrate that the dispersion $\hbar\omega_{\mathbf{k}}$ is linear in $\mathbf{k}$ in the superfluid phase and that the spectrum is gapless. In the superfluid phase we can expand around the expectation value $n_0 = \hbar G^{-1}(\mathbf{0},0)/2a_4$ of the order parameter. Up to quadratic-order this gives,

$$
\begin{aligned}
S &= \hbar\beta\Omega_0 - \hbar \sum_{\mathbf{k},n} \Phi_{\mathbf{k},n}^* G^{-1}(\mathbf{k},i\omega_n)\Phi_{\mathbf{k},n} \\
&\quad + a_4 n_0 \sum_{\mathbf{k},n} \left(\Phi_{\mathbf{k},n}\Phi_{-\mathbf{k},-n} + 4\Phi_{\mathbf{k},n}^*\Phi_{\mathbf{k},n} + \Phi_{\mathbf{k},n}^*\Phi_{-\mathbf{k},-n}^* \right).
\end{aligned}
\tag{3.28}
$$

From this we find the dispersion-relation $\hbar\omega_{\mathbf{k}}$ in the superfluid in the usual way. We perform an analytic continuation $G^{-1}(\mathbf{k},i\omega_n) \to G^{-1}(\mathbf{k},\omega_k)$ and find

$$
\hbar\omega_{\mathbf{k}} = \hbar\sqrt{\left(G^{-1}(\mathbf{k},\omega_{\mathbf{k}})/2 - G^{-1}(\mathbf{0},0)\right)^2 - \left(G^{-1}(\mathbf{0},0)/2\right)^2}.
\tag{3.29}
$$

Note that $(\mathbf{k},\omega_{\mathbf{k}}) = (\mathbf{0},0)$ is a solution. Expanding around this solution in $\mathbf{k}$ now gives,

$$
\hbar\omega_{\mathbf{k}} = a\frac{\hbar G^{-1}(\mathbf{0},0)}{\sqrt{2}}|\mathbf{k}|,
\tag{3.30}
$$

where a is again the lattice constant.

3.3.5   Near the edges of the Mott lobe

If we substitute the vacuum expectation value of the order parameter back into our effective action, we see that the zeroth-order contribution to the thermodynamic potential in the superfluid phase in mean-field approximation is given by,

$$
\hbar\beta\Omega = \hbar\beta\Omega_0 - \frac{\left(\hbar G^{-1}(\mathbf{0},0)\right)^2}{2a_4}.
\tag{3.31}
$$

From this the particle density can be obtained by making use of the thermodynamic identity $N = -\partial\Omega/\partial\mu$. We can calculate this at $T = 0$ and take the limit $\mu \to \mu_{\pm}^{\alpha'}$ to show that the derivative of the density with respect to μ, i.e, $\partial n/\partial\mu$ shows a kink for all $U \neq U_c$. This means that only if we walk through the tip of the Mott lobes there is not a kink in the compressibility. In fact it's not hard to see why this is true. At zero temperature the roots of $-\hbar G^{-1}(\mathbf{0},0)$ are by definition $\mu_{\pm}^{\alpha'}$. This means that we can write $-\hbar G^{-1}(\mathbf{0},0) = C(\mu - \mu_-^{\alpha'})(\mu - \mu_+^{\alpha'})$. The proportionality constant can be shown to be equal to $C = \epsilon_{\mathbf{0}}/((\alpha'U - \mu)((\alpha'-1)U - \mu))$.

This then shows that the thermodynamic potential is,

$$\hbar\beta\Omega = \hbar\beta\Omega_0 + \frac{C^2}{4}\frac{\left(\mu - \mu_-^{\alpha'}\right)^2 \left(\mu - \mu_+^{\alpha'}\right)^2}{a_4}.$$

(3.32)

Remembering that the density is the derivative of the thermodynamic potential we see that the second derivative of the thermodynamic potential with respect to μ can show a nonzero value upon approaching the Mott lobe. Since in the Mott isolator the density is constant and equal to α' we have shown the existence of a kink in the slope of the density for all paths not going through the tip of the Mott lobe. This causes the difference in the universality class of the quantum phase transition.

3.3.6   The superfluid-normal phase transition

In this subsection, we show that it is possible to obtain an analytical expression for the critical temperature T_c of the transition between superfluid and normal phases as a function of U, for values of U below the critical U of the zero-temperature superfluid-Mott insulator transition. The analytical result is obtained if we include occupations up to two per site, i.e., three slave bosons or occupation numbers n^0, n^1, n^2. Along similar lines T_c can be found numerically if more slave bosons are included. We have carried out this procedure for the case of adding a fourth boson (triple occupancy) and find only modest quantitative changes.

   If we restrict the system to occupancies 0, 1 and 2, and fix the total density $n \equiv N/N_s$ at 1, the occupation numbers n^0, n^1 and n^2 should obey the following relations if we neglect fluctuation corrections (cf. Eq. (3.20)):

$$n^0 + n^1 + n^2 = 1,$$

(3.33)

and

$$n^1 + 2n^2 = 1.$$

(3.34)

The n^α are furthermore given by Eq. (3.16), enabling us to eliminate λ and express n^0 and n^2 in terms of n^1. We obtain

$$n^0 = \frac{n^1}{(n^1 + 1)\exp(\beta\mu) - n^1},$$

(3.35)

and

$$n^2 = \frac{n^1}{(n^1 + 1)\exp(\beta(U - \mu)) - n^1}.$$

(3.36)

The constraints in Eqs. (3.33) and (3.34) immediately lead to $n^0 = n^2$, so that, according to Eqs. (3.35) and (3.36), we must have $\mu = U/2$. We notice that at this level of approximation, we obtain a slight discrepancy with the result from

Sec. 3.3.1 that at zero temperature the critical value of $\bar{U}$ of the superfluid-Mott insulator transition, which is the limiting $\bar{U}$ for the superfluid-normal transition that is addressed here, is according to Eq. (3.26) with $\alpha' = 1$ determined by $\bar{\mu} = (\bar{U} - 1)/2$ [58].

As argued above the criticality condition for the superfluid-normal transition is obtained by putting $G^{-1}(\mathbf{0}, 0) = 0$. Restricting the sum in the right-hand side of Eq. (3.18) to $\alpha = 0$ and $\alpha = 1$, we obtain [59]

$$1 = \frac{2}{\bar{\mu} - \bar{U}} \left(n^2 - n^1 \right) + \frac{1}{\bar{\mu}} \left(n^1 - n^0 \right). \tag{3.37}$$

Since the relation between μ and U is fixed by Eqs. (3.33) and (3.34), and n^0 and n^2 can be expressed in n^1 as $n^0 = n^2 = (1 - n^1)/2$, the criticality condition Eq. (3.37) results in a remarkably simple relation between n^1 and $\bar{U}$ at T_c, namely $n^1 = (\bar{U} + 3)/9$. Using this in Eq. (3.35) leads to the following analytic formula for $\bar{T}_c \equiv T_c/zt$ for the superfluid-normal transition:

$$k_B \bar{T}_c = \frac{\bar{U}}{2} \ln^{-1} \left[\frac{(\bar{U} - 24)(\bar{U} + 3)}{(\bar{U} - 6)(\bar{U} + 12)} \right]. \tag{3.38}$$

It is straightforward to generalize this procedure to arbitrary integer density α' while allowing occupation numbers $n^{\alpha'-1}, n^{\alpha'}, n^{\alpha'+1}$ only. The result is

$$k_B \bar{T}_c^{\alpha'} = \frac{\bar{U}}{2} \ln^{-1} \left[\frac{(\bar{U} - 8(2\alpha' + 1))(\bar{U} + (2\alpha' + 1))}{(\bar{U} - 2(2\alpha' + 1))(\bar{U} + 4(2\alpha' + 1))} \right]. \tag{3.39}$$

The critical temperature T_c for integer filling factor $n \equiv N/N_s = 1$, i.e., Eq. (3.38), is plotted in Fig. 3.6. The overall qualitative behavior is as one would expect (cf. Fig. 3.1). A few finer details appear to be less satisfactory. For instance, T_c vanishes for $\bar{U} = 6$, whereas we would expect this to coincide with the mean-field result for $\bar{U}_c$ for the superfluid-Mott insulator transition for the first Mott lobe, i.e., $\bar{U}_c = 5.83$ obtained from Eq. (3.26) with $\alpha' = 1$. We note that the discrepancy is not large and is even smaller for the higher Mott lobes. Indeed $\bar{U}(T_c \to 0) = 2(2\alpha' + 1)$ versus $\bar{U}_c = (2\alpha' + 1) + \sqrt{(2\alpha' + 1)^2 - 1}$. Another feature is the maximum in the $\bar{T}_c(U)$ curve (cf. Fig. 3.1 and [49]). Both features mentioned are caused by the fact that the two conditions Eqs. (3.33) and (3.34) are strictly enforced, whereas they become less appropriate for small U. The exact solution [60] for four slave bosons on a four site lattice for small $\bar{U}$ shows that a better result may be obtained if a fourth boson occupation number n^3 is included in our approach. The set of equations to be solved then becomes, again for $n = 1$,

$$n^0 + n^1 + n^2 + n^3 = 1 \tag{3.40}$$

$$n^1 + 2n^2 + 3n^3 = 1 \tag{3.41}$$

$$\frac{3}{\bar{\mu} - 2\bar{U}} \left(n^3 - n^2 \right) + \frac{2}{\bar{\mu} - \bar{U}} \left(n^2 - n^1 \right) + \frac{1}{\bar{\mu}} \left(n^1 - n^0 \right) = 1. \tag{3.42}$$
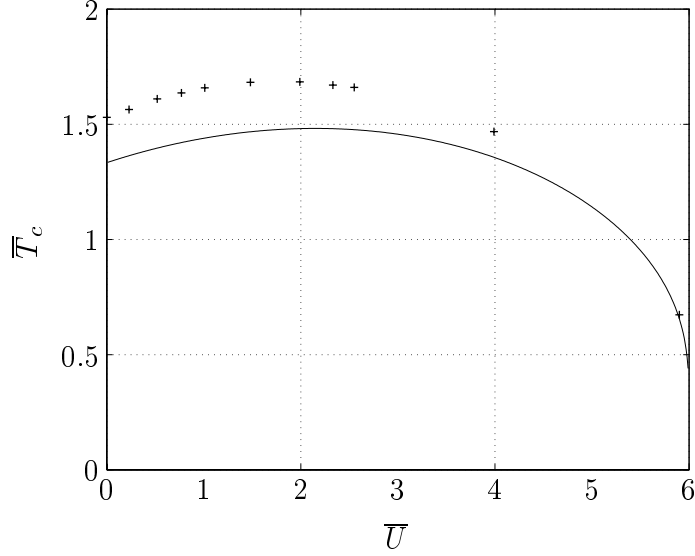
Figure 3.6: Critical temperature T_c of the superfluid-normal phase transition as a function of the interaction strength $\overline{U} = U/zt$. The solid line is an analytic expression obtained in the approximation where we only take into account three slave bosons. The plusses correspond to a numerical solution for the case of four slave bosons.

Again n^0, n^2, and n^3 can easily be expressed in terms of n^1, but no exact solution appears to be possible in this case. However, we have managed to find solutions numerically. The results for T_c are depicted in Fig. 3.6 and show fairly little quantitative change compared to the analytical result Eq. (3.38). In particular, $\bar{T}_c$ still vanishes for $\bar{U} \approx 6$, and the maximum is still there, although shifted to a lower $\bar{U} \approx 1.8$ compared to $\bar{U} = 2.15$ for Eq. (3.38). It is satisfactory to find that for the higher values of $\bar{U}$, n^1 starts to increase rapidly towards 1, signalling the approach of the Mott-insulator phase, whereas n^3 is almost negligible ($< 1\%$) already for $\bar{U} \approx 3$, supporting a description in terms of 3 slave bosons only [61].

3.3.7 Quasiparticle-quasihole dispersion relations

Consider now the propagator $G^{-1}(\mathbf{k}, \omega)$, given by

$$-\hbar G^{-1}(\mathbf{k}, \omega) = \left(\epsilon_{\mathbf{k}} - \epsilon_{\mathbf{k}}^2 \sum_{\alpha} (\alpha + 1) \frac{n^{\alpha} - n^{\alpha+1}}{-\hbar \omega - \mu + \alpha U} \right). \tag{3.43}$$
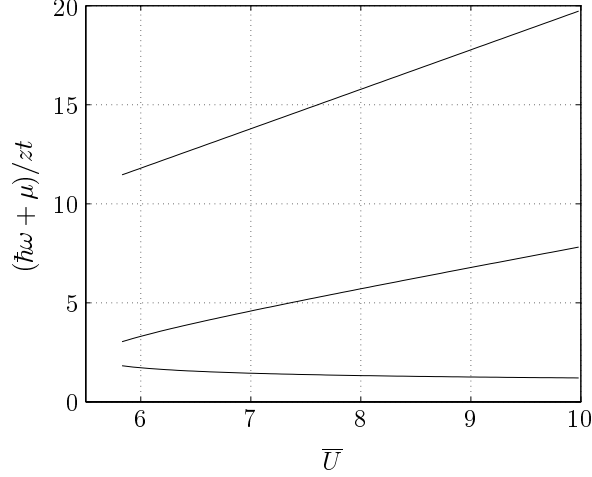
40

Figure 3.7: The dispersion relations for $\mathbf{k} = 0$ in the case where we take into account higher filling factors at nonzero temperature. On the vertical axis is $(\hbar\omega + \mu)/zt$ and on the horizontal axis is $\bar{U}$. Here we have taken into account all the terms with $\alpha = 0, 1, 2$ at a temperature of $zt\beta = 10$.

At zero temperature and for a given integer filling factor α', we have in a mean-field approximation that $n^{\alpha} = \delta_{\alpha,\alpha'}$ and we retrieve the previously found result for the quasiparticle-quasihole dispersions [78]. In this case the real solutions of $\hbar\omega$ follow from a quadratic equation $G^{-1}(\mathbf{k}, \omega_n) = 0$. At nonzero temperature the occupation numbers in general are all nonzero and there will be more than just two solutions for $\hbar\omega$. In the set of solutions there are still two solutions that correspond to the original single quasiparticle and quasihole dispersions. The physical interpretation of the other solutions is that they correspond to the excitation of a higher number of quasiparticles and quasiholes. In Fig. 3.7. we show the three low-lying excitation energies for $\mathbf{k} = 0$ at a temperature of $zt\beta = 10$. To obtain an analytic expression for the single quasiparticle-quasihole dispersion we only take into account the two terms in the sum in Eq.(3.18) which have numerators $n^{\alpha'-1} - n^{\alpha'}$ and $n^{\alpha'} - n^{\alpha'+1}$. These correspond to processes where the occupation of a site changes between $\alpha' - 1, \alpha'$ and $\alpha' + 1$. We find
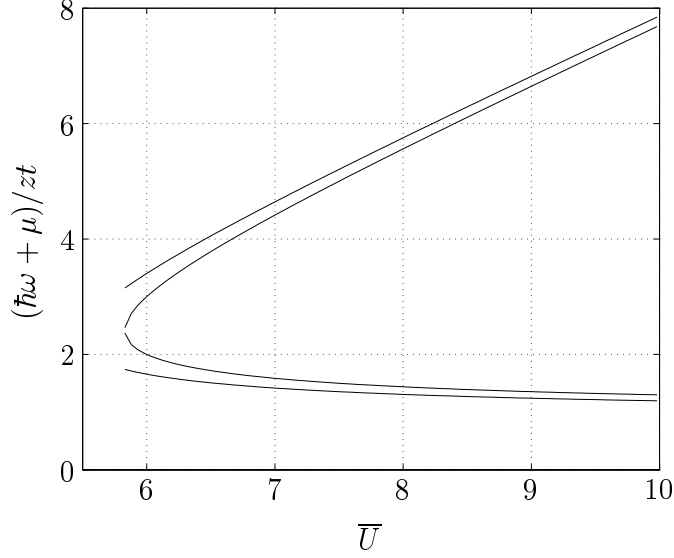
41

Figure 3.8: Dispersion relations $\hbar\omega + \mu$ as a function of U/zt for $\mathbf{k} = \mathbf{0}$ for zero and nonzero temperatures. The inner lobe corresponds to zero temperature. The outer lobe correponds to a temperature of $zt\beta = 3$. Here we have only taken into account the first three terms in the right-hand side of Eq. (3.18), i.e., in the sum we only include the terms with $\alpha = 0$ and $\alpha = 1$.

$$
\begin{aligned}
\hbar\omega_{\mathbf{k}}^{qp,qh} = &-\mu + \frac{U}{2} + \frac{1}{2}\epsilon_{\mathbf{k}}(\alpha' n^{\alpha'-1} - n^{\alpha'} + (\alpha'+1)n^{\alpha'+1}) \\
&\pm \frac{1}{2}\left(U^2 + 2(\alpha' n^{\alpha'-1} - (1+2\alpha')n^{\alpha'} + (1+\alpha')n^{\alpha'+1})U\epsilon_{\mathbf{k}}\right. \\
&\left. + (\alpha n^{\alpha'-1} + n^{\alpha'} - (1+\alpha')n^{\alpha'+1})^2 \epsilon_{\mathbf{k}}^2.\right)^{1/2}
\end{aligned}
$$

$$(3.44)$$

In Fig. 3.8 we have plotted these dispersions at $\mathbf{k} = 0$ as a function of U. Comparison with Fig. 3.7 shows that Eq. (3.44) gives an appropriate description of the single quasiparticle-quasihole dispersions. As can be seen from Fig. 3.8 the tip of the lobe moves to smaller U as a function of increasing temperature. This can be understood because that point now describes the superfluid-normal phase transition (cf. Figs. 3.1, 3.6). In Fig. 3.9 we show how the superfluid-normal boundary in the $\bar{\mu} - \bar{U}$ plane evolves for nonzero temperatures. If we define the
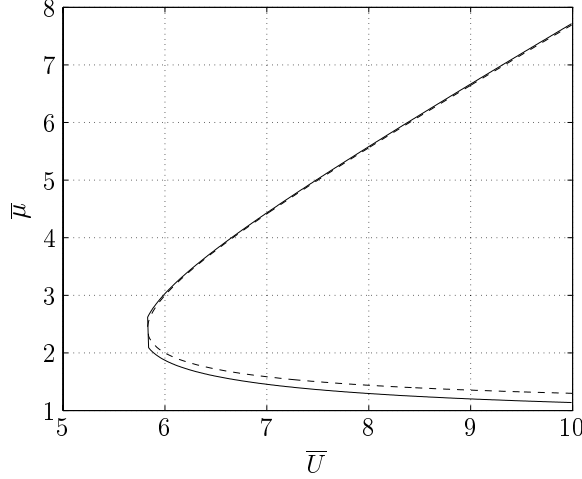
Figure 3.9: The $\bar{\mu}$-$\bar{U}$ phase diagram for zero and nonzero temperatures. The inner lobe corresponds to the zero-temperature case. The outer lobe corresponds to a temperature of $zt\beta = 2$

gap as the difference between the two solutions at $\mathbf{k} = 0$, we find that the gap grows bigger as the temperature increases. As we have seen in Sec. 3.3.2 it is incorrect, however, to conclude from this that the region of the Mott insulating phase in the μ-U phase diagram grows as temperature increases. As mentioned previously, strictly speaking there is no Mott insulator away from zero temperature and at nonzero temperatures there is only a crossover between a phase which has a very small compressibillity and the normal phase.

3.4 Fluctuations

In this section we make a first step towards the study of fluctuation effects and derive an identity between the atomic Green's function and the superfluid Green's function in Eq. (3.18). This we then use to calculate the atomic particle density. In appendix 3.7 we show that the easiest way to calculate the density is by making use of currents that couple to the atomic fields. We start with the action of the Bose-Hubbard model

$$S[a^*, a] = \int_0^{\hbar\beta} d\tau \left[\sum_i a_i^* \left(\hbar \frac{\partial}{\partial\tau} - \mu \right) a_i - \sum_{ij} t_{ij} a_i^* a_j + \frac{U}{2} \sum_i a_i^* a_i^* a_i a_i \right].$$

$$(3.45)$$

43

We are interested in calculating the $\langle a_i^* a_i \rangle$ correlation function. Therefore we add currents J^*, J that couple to the a^* and a fields as

$$
Z[J^*, J] = \int d[a^*]d[a] \exp\left\{ -S_0/\hbar + \frac{1}{\hbar} \int_0^{\hbar\beta} d\tau \sum_{ij} a_i^* t_{ij} a_j \right.
$$

$$
\left. + \int_0^{\hbar\beta} d\tau \sum_i [J_i^* a_i + a_i^* J_i] \right\}. \tag{3.46}
$$

Here $S_0 = S_0[a^*, a]$ denotes the action for $t_{ij} = 0$. The most important step in the remainder of the calculation is to a perform again a Hubbard-Stratonovich transformation by adding a complete square to the action. The latter can be written as,

$$
\int d\tau \sum_{i,j} \left(a_i^* - \Phi_i^* + \hbar t_{ij'}^{-1} J_{j'}^* \right) t_{ij} \left(a_j - \Phi_j + \hbar t_{jj''}^{-1} J_{j''} \right), \tag{3.47}
$$

where the sums over j' and j'' are left implicit for simplicity. Straightforward algebra yields

$$
Z[J^*, J] = \int d[\Phi^*]d[\Phi] \exp\left\{ \sum_{\mathbf{k},n} \left(-\hbar \Phi_{\mathbf{k},n}^* G^{-1}(\mathbf{k}, i\omega_n) \Phi_{\mathbf{k},n} \right. \right.
$$

$$
\left. \left. + J_{\mathbf{k},n}^* \Phi_{\mathbf{k},n} + J_{\mathbf{k},n} \Phi_{\mathbf{k},n}^* - \frac{\hbar}{\epsilon_{\mathbf{k}}} J_{\mathbf{k},n}^* J_{\mathbf{k},n} \right) \right\}. \tag{3.48}
$$

Differentiating twice with respect to the currents gives then the relation

$$
\frac{1}{Z[0,0]} \frac{\delta^2}{\delta J_{\mathbf{k},n}^* \delta J_{\mathbf{k},n}} Z[J^*, J] \bigg|_{J^*, J=0} = \langle a_{\mathbf{k},n}^* a_{\mathbf{k},n} \rangle = \langle \Phi_{\mathbf{k},n}^* \Phi_{\mathbf{k},n} \rangle - \frac{\hbar}{\epsilon_{\mathbf{k}}}. \tag{3.49}
$$

This is very useful indeed since the correlator $\langle \Phi_{\mathbf{k},n}^* \Phi_{\mathbf{k},n} \rangle = -G(\mathbf{k}, i\omega_n)$. At zero temperature the retarded Green's function can be written as

$$
-\frac{1}{\hbar} G(\mathbf{k}, \omega) = \frac{Z_{\mathbf{k}}}{-\hbar\omega + \epsilon_{\mathbf{k}}^{qp}} + \frac{1 - Z_{\mathbf{k}}}{-\hbar\omega + \epsilon_{\mathbf{k}}^{qh}} + \frac{1}{\epsilon_{\mathbf{k}}}, \tag{3.50a}
$$

where the wavefunction renormalization factor is

$$
Z_{\mathbf{k}} = \frac{U(1 + 2\alpha') - \epsilon_{\mathbf{k}} + \sqrt{U^2 - 2U\epsilon_{\mathbf{k}}(1 + 2\alpha') + \epsilon_{\mathbf{k}}^2}}{2\sqrt{U^2 - 2U\epsilon_{\mathbf{k}}(1 + 2\alpha') + \epsilon_{\mathbf{k}}^2}}, \tag{3.50b}
$$

and

$$
\epsilon_{\mathbf{k}}^{qp,qh} = -\mu + \frac{U}{2}(2\alpha' - 1) - \frac{\epsilon_{\mathbf{k}}}{2} \pm \frac{1}{2} \sqrt{\epsilon_{\mathbf{k}}^2 - (4\alpha' + 2)U\epsilon_{\mathbf{k}} + U^2}. \tag{3.50c}
$$

Note that $Z_{\mathbf{k}}$ is always positive and in the limit where $U \to \infty$ we have that $Z_{\mathbf{k}} \to (1 + \alpha')$. The quasiparticle dispersion $\epsilon_{\mathbf{k}}^{qp}$ is always greater than or equal to zero and $\epsilon_{\mathbf{k}}^{qh}$ is always smaller than or equal to zero. Because of this only the quasiholes give a contribution to the total density at zero temperature. The density can be calculated from,

$$
\begin{aligned}
n &= \frac{1}{N_s \hbar \beta} \sum_{\mathbf{k},n} \langle a_{\mathbf{k},n}^* a_{\mathbf{k},n} \rangle = \frac{1}{N_s \hbar \beta} \sum_{\mathbf{k},n} \left\{ -G(\mathbf{k}, \omega_n) - \frac{\hbar}{\epsilon_{\mathbf{k}}} \right\} \\
&\stackrel{\beta \to \infty}{=} \frac{1}{N_s} \sum_{\mathbf{k}} (Z_{\mathbf{k}} - 1) \stackrel{U \to \infty}{=} \alpha'.
\end{aligned}
\tag{3.51}
$$

If we expand the square-root denominator of Z for small $\mathbf{k}$ we see that it behaves as $1/\mathbf{k}$, therefore in two and three dimensions we expect the integration over $\mathbf{k}$ to converge. In Fig. 3.10 we have plotted the density for $\alpha' = 1$ as given by the equation above. We see that the density quickly converges to one, but near the tip
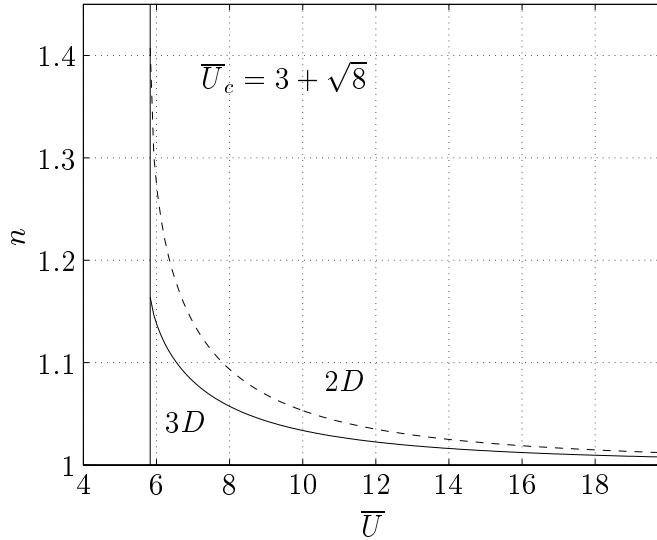
Figure 3.10: Total density n at $T = 0$ as a function of interaction strength $\overline{U} = U/zt$ for the first Mott lobe in two (dashed line) and three dimensions (solid line) when including fluctuations. The density approaches a finite value different from one, when approaching U_c.

of the Mott lobe in all dimensions it deviates significantly from one. This result is somewhat unexpected [34] and may be due to the break-down of the Gaussian

approximation near the quantum phase transition. A more detailed study of the fluctuations is beyond the scope of the present paper and is therefore left to future work.

3.5   Conclusions

In summary, we have applied the slave-boson formalism to the Bose-Hubbard model, which enabled us to analytically describe the physics of this model at nonzero temperatures. We have reproduced the known zero-temperature results and we have computed the critical temperature for the superfluid-normal phase transition. The crossover from a Mott insulator to a normal phase has also been quantified. We have shown how thermal fluctuations introduce additional dispersion modes associated with paired quasiparticles-quasiholes propagating through the system. We have also considered density fluctuations induced by the creation of quasiparticle-quasihole pairs. These fluctuations do not average out to zero in the Gaussian approximation.

3.6   Higher-order terms

If we also want to calculate quantities like the superfluid density, we have to calculate the effective action up to fourth order. One way to do this is by going to higher order in the interaction part. Here we follow a slightly different strategy. Because we are only interested in the mean-field theory, it suffices to just consider $\Phi_{\mathbf{0},0}$ terms. The effective action for $\Phi_{\mathbf{0},0}$ is found from

$$Z = \int \frac{d[\Phi_{\mathbf{0},0}^*]d[\Phi_{\mathbf{0},0}]}{\hbar\beta} \int \prod_{\alpha,\mathbf{k},n} \frac{d[(a^\alpha)_{\mathbf{k},n}^*]d[a_{\mathbf{k},n}^\alpha]}{\hbar\beta} \exp\left(-\frac{1}{\hbar}S\right), \qquad (3.52)$$

where from Eq. (3.6) we have

$$S = iN_s\hbar\beta\lambda + \epsilon_{\mathbf{0}}|\Phi_{\mathbf{0},0}|^2 + \sum_{\alpha\beta}\sum_{\mathbf{k},n}(a_{\mathbf{k},n}^\alpha)^*M^{\alpha\beta}a_{\mathbf{k},n}^\beta. \qquad (3.53)$$

Note, however, that now the matrix M is only blockdiagonal and it contains off-diagonal terms proportional to $\Phi_{\mathbf{0},0}$. When we take the determinant of that matrix, you get automatically all powers in $\Phi_{\mathbf{0},0}$. This can be made more explicit by looking at the block-structure of the matrix which is

$$M = \begin{pmatrix} B_0 & & & \\ & B_2 & & \\ & & B_4 & \\ & & & \ddots \end{pmatrix}, \qquad (3.54a)$$

where

$$B_\alpha = \begin{pmatrix} \chi_\alpha & \frac{\sqrt{\alpha+1}}{\sqrt{N_s\hbar\beta}}\epsilon_{\mathbf{0}}\Phi_{\mathbf{0},0} \\ \frac{\sqrt{\alpha+1}}{\sqrt{N_s\hbar\beta}}\epsilon_{\mathbf{0}}\Phi_{\mathbf{0},0}^* & \chi_{\alpha+1} \end{pmatrix}, \tag{3.54b}$$

with $\chi_\alpha = -i\hbar\omega_n - i\lambda - \alpha\mu + \alpha(\alpha-1)U/2$. The slave bosons can be integrated out with the result

$$Z = \int \frac{d[\Phi_{\mathbf{0},0}^*]d[\Phi_{\mathbf{0},0}]}{\hbar\beta} \exp\left\{ -\frac{1}{\hbar}\left(iN_s\hbar\beta\lambda + \epsilon_{\mathbf{0}}|\Phi_{\mathbf{0},0}|^2 \right) \right\} \exp\left\{ -\sum_{\mathbf{k},n} \ln\left[\det\beta M\right] \right\}. \tag{3.55}$$

The determinant can be calculated up to fourth order in $\Phi_{\mathbf{0},0}$ as

$$\begin{aligned}
\det\beta M &= \left(\prod_\alpha \beta\chi_\alpha\right)\left(1 + \sum_\alpha \frac{\epsilon_{\mathbf{0}}^2}{N_s\hbar\beta}|\Phi_{\mathbf{0},0}|^2\frac{(\alpha+1)}{\chi_\alpha\chi_{\alpha+1}} + \right. \\
&\qquad\left. \sum_\alpha \sum_{|\alpha-\beta|\geq 2} \frac{\epsilon_{\mathbf{0}}^4}{(N_s\hbar\beta)^4}|\Phi_{\mathbf{0},0}|^4\frac{(\alpha+1)(\beta+1)}{\chi_\alpha\chi_{\alpha+1}\chi_\beta\chi_{\beta+1}} \right). \tag{3.56}
\end{aligned}$$

For small $\Phi_{\mathbf{0},0}$ we can expand the logarithm in Eq. (3.55) by using the Taylor expansion

$$\ln\left\{ 1 - \alpha x^2 + \gamma x^4 \right\} = -\alpha x^2 + \frac{1}{4}(-2\alpha^2 + 4\gamma)x^4 + \mathcal{O}(x^5).$$

Combining the latter equation with Eq. (3.55), we also recover that the second-order term in the effective action for $\Phi_{\mathbf{0},0}$ is given by

$$\begin{aligned}
\left(\epsilon_{\mathbf{0}} - \hbar\sum_{\mathbf{k},n}\sum_\alpha \frac{\epsilon_{\mathbf{0}}^2}{N_s\hbar\beta}\frac{(\alpha+1)}{\chi_\alpha\chi_{\alpha+1}} \right)|\Phi_{\mathbf{0},0}|^2 &= \left(\epsilon_{\mathbf{0}} + \epsilon_{\mathbf{0}}^2\frac{n^\alpha - n^{\alpha+1}}{-\mu+\alpha U} \right)|\Phi_{\mathbf{0},0}|^2 \\
&= -\hbar G^{-1}(\mathbf{0},0)|\Phi_{\mathbf{0},0}|^2. \tag{3.57}
\end{aligned}$$

We determine the effective action to fourth order in the case of the first four slave bosons. Using the above we can readily verify that

$$\begin{aligned}
-S^{\text{eff}}/\hbar = -\frac{1}{\hbar}\left(\epsilon_{\mathbf{0}}|\Phi_{\mathbf{0},0}|^2 + iN_s\hbar\beta\lambda - \sum_{j=0}^{3}\ln\beta\chi_j \right. \\
-\ln\left(1 - (\frac{\epsilon_{\mathbf{0}}}{N\hbar\beta})^2\left(\frac{3}{\chi_3\chi_2} + \frac{2}{\chi_2\chi_1} + \frac{1}{\chi_1\chi_0} \right)|\Phi_{\mathbf{0},0}|^2 \right. \\
\left.\left. +(\frac{\epsilon_{\mathbf{0}}}{N_s\hbar\beta})^4\frac{3}{\chi_0\chi_1\chi_2\chi_3}|\Phi_{\mathbf{0},0}|^4 \right) \right). \tag{3.58}
\end{aligned}$$

47

From this we find that a_4 in the case of four slave bosons is given by

$$a_4 = \frac{\hbar}{4}\left(\frac{\epsilon_0}{\sqrt{N_s\hbar\beta}}\right)^4 \sum_{\mathbf{k},n}\left(-2\left(\sum_{\alpha=0}^{3}\frac{(\alpha+1)}{\chi_\alpha\chi_{\alpha+1}}\right)^2 + \frac{12}{\chi_0\chi_1\chi_2\chi_3}\right), \qquad (3.59)$$

or explicitly,

$$
\begin{aligned}
a_4 =& -\left(\frac{\epsilon_0}{2N_s^2\hbar\beta}\right)\left\{\frac{9}{(2\bar{U}-\bar{\mu})^2}\left(3n^3(1-n^3)+2n^2(1-n^2)\right)\right. \\
&+\frac{18}{(2\bar{U}-\bar{\mu})^3}\left(n^3-n^2\right)+\frac{4}{(\bar{U}-\bar{\mu})^2}\left(2n^2(1-n^2)+n^1(1-n^1)\right) \\
&+\frac{8}{(\bar{U}-\bar{\mu})^3}\left(n^2-n^1\right)+\frac{1}{(\bar{\mu})^2}\left(n^0(1-n^0)+n^1(1-n^1)\right) \\
&+\frac{2}{\bar{\mu}^3}\left(n^0-n^1\right)+\frac{4}{(\bar{U}-2\bar{\mu})\bar{\mu}^2}n^0 - \frac{4}{(\bar{U}-2\bar{\mu})(\bar{U}-\bar{\mu})^2}n^2 \\
&+\frac{4}{(\bar{U}-\bar{\mu})\bar{\mu}}n^1(1-n^1)-\frac{4\bar{U}}{(\bar{U}-\bar{\mu})^2\bar{\mu}^2}n^1 - \frac{12}{(3\bar{U}-2\bar{\mu})(2\bar{U}-\bar{\mu})^2}n^3 \\
&-\frac{12}{(2\bar{U}^2-3\bar{U}\bar{\mu}+\bar{\mu}^2)}2n^2(1-n^2)-\frac{12\bar{U}}{(2\bar{U}^2-3\bar{U}\bar{\mu}+\bar{\mu}^2)^2}n^2 \\
&\left.+\frac{12}{(3\bar{U}-2\bar{\mu})(\bar{U}-\bar{\mu})^2}n^1\right\}.
\end{aligned}
$$

$$(3.60)$$

Note that in the zero-temperature limit for the first Mott lobe, when the slave-boson occupation numbers are proportional to a Kronecker delta, this result coincides exactly with the one previously derived in standard perturbation theory (cf. Ref. [78]).

3.7 Density calculations

In this section we demonstrate for the noninteracting case the equivalence of the calculation of the total particle density through the thermodynamic relation $N = -\partial\Omega/\partial\mu$ and through the use of source currents that couple to the atomic fields. We consider a system of noninteracting bosons described by creation and annihilation fields $a_i^*(\tau)$ and $a_i(\tau)$ on a lattice. First we calculate the generating

functional $Z[J^*, J]$ for this system,

$$
\begin{aligned}
Z[J^*, J] &= \int d[a^*]d[a] \exp \left\{ -\frac{1}{\hbar} S_0[a^*, a] + \frac{1}{\hbar} \int d\tau \sum_{ij} a_i^* t_{ij} a_j \right. \\
&\quad \left. + \int d\tau \sum_i \left(J_i^* a_i + a_i^* J_i \right) \right\}.
\end{aligned}
\tag{3.61}
$$

In this equation S_0 is the on-site action, which in frequency-momentum representation typically looks like

$$
S_0[a^*, a] = \sum_{\mathbf{k},n} a_{\mathbf{k},n}^* \left(-i\hbar\omega_n - \mu \right) a_{\mathbf{k},n}.
\tag{3.62}
$$

The hopping term is decoupled by means of a Hubbard-Stratonovich transformation, i.e., we add the following complete square to the action,

$$
\sum_{ij} \left(a_i^* - \Phi_i^* + \hbar \sum_{j'} t_{ij'}^{-1} J_{j'}^* \right) t_{ij} \left(a_j - \Phi_j + \hbar \sum_{j''} t_{ij''}^{-1} J_{j''} \right).
$$

The atomic fields a^*, a can now be integrated out. Going through the straightforward algebra one arrives at the following expression for the generating functional,

$$
\begin{aligned}
Z[J^*, J] &= \int d[\Phi^*]d[\Phi] \exp \left\{ \sum_{\mathbf{k},n} \Phi_{\mathbf{k},n}^* G^{-1}(\mathbf{k}, i\omega_n) \Phi_{\mathbf{k},n} \right. \\
&\quad \left. + J_{\mathbf{k},n}^* \Phi_{\mathbf{k},n} + J_{\mathbf{k},n} \Phi_{\mathbf{k},n}^* - \hbar \frac{J_{\mathbf{k},n} J_{\mathbf{k},n}^*}{\epsilon_{\mathbf{k}}} \right\},
\end{aligned}
\tag{3.63}
$$

where $-\hbar G^{-1}(\mathbf{k}, i\omega_n) = \epsilon_{\mathbf{k}} - \epsilon_{\mathbf{k}}^2 \left(-i\hbar\omega_n - \mu \right)^{-1}$. The total density may be calculated from this expression by first calculating the correlator $\langle a_{\mathbf{k},n}^* a_{\mathbf{k},n} \rangle$ through functional differentiation with respect to the source-currents J, and then to sum over all momenta and Matsubara frequencies. We have for the first step

$$
\langle a_{\mathbf{k},n}^* a_{\mathbf{k},n} \rangle = \frac{1}{Z[0,0]} \left. \frac{\delta^2}{\delta J_{\mathbf{k},n}^* \delta J_{\mathbf{k},n}} Z[J^*, J] \right|_{J^*, J=0} = \frac{\hbar}{-i\hbar\omega_n - \mu - \epsilon_{\mathbf{k}}}.
\tag{3.64}
$$

We see that there is a pole here at $i\hbar\omega_n = -\epsilon_{\mathbf{k}} - \mu$. The density now can be calculated from $n = (1/N_s \hbar\beta) \sum_{\mathbf{k},n} \langle a_{\mathbf{k},n}^* a_{\mathbf{k},n} \rangle$. This is the expected result.

On the other hand, we can also calculate the density from the thermodynamic potential Ω, by using the relation $N = -\partial\Omega/\partial\mu$ where N is the total number of

particles. Doing that for this case we use that

$$\Omega = \frac{1}{\beta} \sum_{\mathbf{k},n} \left\{ \ln\left[\beta(-i\hbar\omega_n - \mu)\right] + \ln\left[-\hbar\beta G^{-1}(\mathbf{k}, i\omega_n)\right] \right\} \tag{3.65}$$

and obtain

$$n = -\frac{1}{N_s}\frac{\partial\Omega}{\partial\mu} = \frac{1}{N_s\hbar\beta} \sum_{\mathbf{k},n} \left\{ \frac{\hbar}{-i\hbar\omega_n - \mu} + \frac{\hbar}{-i\hbar\omega_n - \mu - \epsilon_{\mathbf{k}}} \cdot \frac{\epsilon_{\mathbf{k}}}{-i\hbar\omega_n - \mu} \right\}.$$
$$\tag{3.66}$$

When doing the sum over Matsubara frequencies the pole at $i\hbar\omega_n = -\mu$ in the first term in the right-hand side is canceled by the second term and only the other pole at $i\hbar\omega_n = -\epsilon_{\mathbf{k}} - \mu$ gives a contribution. This shows the equivalence of both methods.

3.8 Density calculations revisited [1]

In the previous section we showed the equivalence in the noninteracting case of calculating the density from the thermodynamic potential and by tracing over the Green's function of the system. For the interacting case this equivalence is not obvious if the self-energy depends on the chemical potential. In that case differentiating the thermodynamic potential with respect to the chemical potential gives an additional term that is absent if we directly take the Green's function to calculate the density. The correct way to calculate the density is to use the thermodynamic potential. To calculate the thermodynamic potential we make use of the Green's function $G(\mathbf{k}, i\omega_n)$ in Eq. (3.50a). We note that the Green's function of the atoms $G_{\mathrm{a}}(\mathbf{k}, i\omega_n)$ is related to $G(\mathbf{k}, i\omega_n)$ according to Eq. (3.49) and can also be written as

$$G_{\mathrm{a}}(\mathbf{k}, i\omega_n) = \frac{-\hbar}{-i\hbar\omega_n - \epsilon_{\mathbf{k}} - \mu + \hbar\Sigma(\mathbf{k}, i\hbar\omega_n)}, \tag{3.67}$$

where the selfenergy is given by

$$\hbar\Sigma(\mathbf{k}, i\hbar\omega_n) = 2\alpha U + \frac{\alpha(\alpha + 1)U^2}{-i\hbar\omega_n - \mu - U}. \tag{3.68}$$

In more detail we have for the thermodynamic potential (cf. Eq.(3.17)),

$$\Omega = \Omega_0 + \frac{1}{\beta}\mathrm{Tr}\left[\log\left(-\hbar\beta G^{-1}\right)\right]. \tag{3.69}$$

---

[1]This section was not included in the original paper and was added during the writing of this thesis.
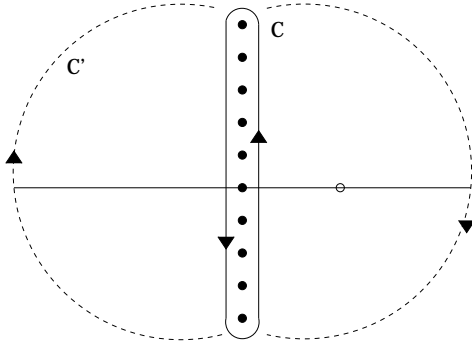
Figure 3.11: The contours used to perform the summation over the Matsubara frequencies. The black dots represent the Matsubara frequencies and the other poles of the integrant are depicted with the unfilled dot.

Note that in the above expression for the thermodynamic potential we have omited the contribution from the Hubbard-Stratonovich transformation, which is due to the fact that the path-integral over the Hubbard-Stratonovich fields that we used to obtain Eq. (3.17) is not equal to one. However, this term does not depend on the chemical potential and in this section we are interested in the density expression which follows from the thermodynamic potential by differentiating with respect to the chemical potential. Therefore, we are allowed to omit this term.

We differentiate the thermodynamic potential in Eq. (3.69) with respect to the chemical potential to find the density. Using the expression for Ω_0 from Eq. (3.10) we see that differentiating this term with respect to the chemical potential gives α, where α is the number of particles per site in the Mott lobe that we consider. Due to the contribution of the second term we obtain in total

$$
\begin{aligned}
n &= -\frac{\partial \Omega}{\partial \mu} = -\frac{\partial \Omega_0}{\partial \mu} - \frac{1}{\beta}\frac{\partial}{\partial \mu}\mathrm{Tr}\left[\log\left(-\hbar\beta G^{-1}\right)\right] \\
&= \alpha - \frac{1}{\beta}\sum_{\mathbf{k},n} G(\mathbf{k}, i\omega_n)\frac{\partial G^{-1}(\mathbf{k}, i\omega_n)}{\partial \mu}.
\end{aligned}
\tag{3.70}
$$

To calculate the sum over the Matsubara frequencies in the above trace we are going to rewrite it as a complex integral [57]. This is achieved by making use of the function $N(z) = \hbar\beta/(e^{\hbar\beta z} - 1)$, which has poles at the even Matsubara frequencies $z = i\omega_n$, where $\omega_n = 2n\pi/\hbar\beta$. The residue of the pole at $z = i\omega_n$ of the function $N(z)G(\mathbf{k}, z)/\hbar\beta$ can be shown to be equal to $G(\mathbf{k}, i\omega_n)$ and as a result the sum over Matsubara frequencies in Eq. (3.70) is equal to the complex integral along the closed contour C that encloses the imaginary axis, this is also shown in Fig. 3.11.

From Eq. (3.50a) we find that the poles of $G(z)$ are located at the quasiparticle

51

$\epsilon_{\mathbf{k}}^{qp}$ and quasihole $\epsilon_{\mathbf{k}}^{qh}$ dispersion, respectively. Using Eq. (3.43) we find that the derivative term $\partial G^{-1}(z)/\partial \mu$ has two second-order poles located at $z = (\alpha U - \mu)/\hbar$ and $z = ((\alpha - 1)U - \mu)/\hbar$, respectively. Explicitely we thus have,

$$
\begin{aligned}
\sum_n &G(\mathbf{k}, i\omega_n) \frac{\partial G^{-1}(\mathbf{k}, i\omega_n)}{\partial \mu} \\
&= \sum_n \epsilon_{\mathbf{k}}^2 \left(\frac{Z_{\mathbf{k}}}{-i\hbar\omega_n + \epsilon_{\mathbf{k}}^{qp}} + \frac{1 - Z_{\mathbf{k}}}{-i\hbar\omega_n + \epsilon_{\mathbf{k}}^{qh}} + \frac{1}{\epsilon_{\mathbf{k}}} \right) \\
&\quad \times \left(-\frac{\alpha + 1}{(-i\hbar\omega_n - \mu + \alpha U)^2} + \frac{\alpha}{(-i\hbar\omega_n - \mu + (\alpha - 1)U)^2} \right) \\
&= \frac{\epsilon_{\mathbf{k}}^2}{\hbar^2} \frac{1}{2\pi i} \oint_C dz \; N(z) \left(\frac{Z_{\mathbf{k}}}{-z + \epsilon_{\mathbf{k}}^{qp}/\hbar} + \frac{1 - Z_{\mathbf{k}}}{-z + \epsilon_{\mathbf{k}}^{qh}/\hbar} + \frac{1}{\epsilon_{\mathbf{k}}/\hbar} \right) \\
&\quad \times \left(-\frac{\alpha + 1}{(-z - (\mu - \alpha U)/\hbar)^2} + \frac{\alpha}{(-z - (\mu - (\alpha - 1)U)/\hbar)^2} \right). \quad (3.71)
\end{aligned}
$$

For the Mott-insulator state with filling fraction α we have that $\overline{\mu}$ lies between $\overline{\mu}_{\pm}^{\alpha}$, as given in Eq. (3.26). As a result this means that for the poles that come from the derivative term we have that $\mu > (\alpha - 1)U$ and $\mu < \alpha U$. Next we want to know how the quasiparticle and quasihole poles depend on the chemical potential within the Mott lobe. It is convenient to define the particle-hole gap

$$
\Delta_{\mathbf{k}} = \sqrt{U^2 - 2U\epsilon_{\mathbf{k}}(2\alpha + 1) + \epsilon_{\mathbf{k}}^2}. \tag{3.72}
$$

From this it follows that $\mu_+^{\alpha} - \mu_-^{\alpha} = \Delta_{\mathbf{0}}$. For $\mu_-^{\alpha} < \mu < \mu_+^{\alpha}$ we can write $\mu = \mu_-^{\alpha} + \delta\mu$, where $0 < \delta\mu < \Delta_{\mathbf{0}}$. We find for the quasiparticle pole that,

$$
\epsilon_{\mathbf{k}}^{qp}(\mu_-^{\alpha} + \delta\mu) = -\delta\mu + 1/2 - \epsilon_{\mathbf{k}}/2 + \frac{\Delta_{\mathbf{k}}}{2} + \frac{\Delta_{\mathbf{0}}}{2} \geq 0. \tag{3.73}
$$

A similar expression can be obtained for the quasihole pole,

$$
\epsilon_{\mathbf{k}}^{qh}(\mu_-^{\alpha} + \delta\mu) = -\delta\mu + 1/2 - \epsilon_{\mathbf{k}}/2 - \frac{\Delta_{\mathbf{k}}}{2} + \frac{\Delta_{\mathbf{0}}}{2} \leq 0. \tag{3.74}
$$

Therefore, at $T = 0$, only the quasihole pole is important and we find for the residue of that pole

$$
\frac{(1 - Z_{\mathbf{k}})\epsilon_{\mathbf{k}}^2}{\hbar^2} \left(-\frac{\alpha + 1}{(-z - (\mu - \alpha U)/\hbar)^2} + \frac{\alpha}{(-z - (\mu - (\alpha - 1)U)/\hbar)^2} \right)_{z = \epsilon_{qh}/\hbar} = +1.
$$

$$\tag{3.75}$$

The residue of the pole that is located at $z = -(\mu - \alpha U)/\hbar$ is given by,

$$\frac{-(\alpha + 1)\epsilon_{\mathbf{k}}^2}{\hbar^2} \frac{d}{dz} \left[N(z) \left(\frac{Z_{\mathbf{k}}}{-z + \epsilon_{\mathbf{k}}^{qp}/\hbar} + \frac{1 - Z_{\mathbf{k}}}{-z + \epsilon_{\mathbf{k}}^{qh}/\hbar} + \frac{1}{\epsilon_{\mathbf{k}}/\hbar} \right) \right]_{z=-(\mu-\alpha U)/\hbar} = -1.$$

(3.76)

Adding the two gives zero and as a result we have proven that the density in the Mott-insulator is, as expected, exactly given by the integer α. This resolves the problem mentioned at the end of section 3.4.

Chapter 4

Feshbach resonances

——— ABSTRACT
In this chapter we introduce the Feshbach resonances that are used to tune the interatomic interactions. Due to the low temperatures of the ultracold gases, their effective interactions are completely determined by a single parameter, the s-wave scattering length. The observed resonances in the collision of two-atoms are a result of the exchange interaction that allows the incoming atoms to form a bound state with a different spin configuration. The incoming atoms are said to be in the open channel and the bound state is said to be in the closed channel. Because of the difference in magnetic moments between the atoms in the open and closed channel their Zeeman energies change differently in a magnetic field and as a result the s-wave scattering length, and hence the magnitude and sign of the interatomic interactions, can be tuned to essentially any desired value.

4.1 Single-channel scattering

Before we treat Feshbach resonances in ultracold gases, we first describe the single-channel scattering problem for two indistinguishable colliding atoms. The motion of two atoms that interact via the potential $V(\mathbf{r})$ separates into the center-of-mass motion and the relative motion. The wave function of the relative part is determined by the time-independent Schrödinger equation

$$\left[-\frac{\hbar^2 \nabla^2}{m} + V(\mathbf{r}) \right] \psi(\mathbf{r}) = [H_0 + V(\mathbf{r})] \, \psi(\mathbf{r}) = E\psi(\mathbf{r}). \tag{4.1}$$

The positive energy solutions of the above equation describe atom-atom scattering and for elastic scattering we should have that E equals twice the kinetic energy

$\epsilon_{\mathbf{k}} = \hbar^2 \mathbf{k}^2 / 2m$ of a single atom. Formally, we can express the solutions $|\psi^{(+)}\rangle$ to the scattering problem in Eq. (4.1) in terms of the eigenstates $|\phi\rangle$ of the problem with $V = 0$ as

$$|\psi^{(+)}\rangle = |\phi\rangle + \frac{1}{E - H_0 + i\epsilon} V |\psi^{(+)}\rangle, \qquad (4.2)$$

where $\epsilon \downarrow 0$. Consider now the limit where the interatomic separation is large and the potential V has vanished, then the solutions are plane waves. In more detail, the solution to Eq. (4.1) at distances that are much larger than the range of the interaction can be written as the sum of an incoming plane wave with relative momentum $\hbar \mathbf{k}$ and and an outgoing spherical wave [65],

$$\psi^{(+)}(\mathbf{r}) = \frac{1}{(2\pi)^{3/2}} \left(\exp\left(i\mathbf{k} \cdot \mathbf{r}\right) + f(\mathbf{k}', \mathbf{k}) \frac{e^{+ikr}}{r} \right), \qquad (4.3)$$

where $\mathbf{k}' = k\hat{\mathbf{r}}$. The function $f(\mathbf{k}', \mathbf{k})$ is known as the scattering amplitude and it is given by

$$f(\mathbf{k}', \mathbf{k}) = -\frac{1}{4\pi}(2\pi)^3 \frac{m}{\hbar^2} \langle \mathbf{k}' | V | \psi^{(+)} \rangle. \qquad (4.4)$$

For spherically symmetric potentials the interatomic potential depends only on the distance between the atoms and as a result the scattering amplitude depends only on the angle θ between $\mathbf{k}'$ and $\mathbf{k}$ and the magnitude k. For scattering by spherically symmetric potentials we can decompose the scattering states into states with definite angular momentum and this leads to the method of partial waves. Specifically we have,

$$f(\mathbf{k}', \mathbf{k}) = \sum_{l=0}^{\infty} f_l(k) P_l(\cos \theta), \qquad (4.5)$$

where $P_l(x)$ are the Legendre polynomials. To see the physical meaning of the partial-wave amplitudes $f_l(k)$ we note that even if the atoms do not scatter the plane-wave solutions of the scattering problem can conveniently be written as the sum of an incoming and outgoing spherical waves as

$$e^{i\mathbf{k} \cdot \mathbf{r}} = \sum_{l} (2l + 1) P_l(\cos \theta) \left(\frac{e^{ikr} - e^{-i(kr - l\pi)}}{2ikr} \right). \qquad (4.6)$$

With the expansion in Eq. (4.5) we can show that the scattering process changes the coefficient of the outgoing wave according to $e^{ikr}/r \to (1 + 2ikf_l(k))e^{ikr}/r$. Moreover, because of flux conservation we can show that the magnitude of this coefficient has to be one [65] and we conclude that at large distances the change in the wave function due to the collision is to change in every partial wave the phase of the outgoing wave. This phase shift is called $2\delta_l$ and for ultracold atoms we usually only consider s-wave scattering with $l = 0$. For low energy and momenta

we define the *s*-wave scattering length a by

$$a = -\lim_{k \downarrow 0} \frac{\delta_0(k)}{k}. \tag{4.7}$$

It is convenient to also introduce the so-called T matrix, that satisfies $T|\phi\rangle = V|\psi^{(+)}\rangle$. In the low-energy limit we can solve for the T matrix in Eq. (4.4) and we find,

$$\lim_{k \downarrow 0} f_0(k) = -a = -\frac{1}{4\pi}(2\pi)^3 \frac{m}{\hbar^2} \langle \mathbf{0}|T|\mathbf{0}\rangle. \tag{4.8}$$

In reality ultracold atoms interact through a short-ranged potential $V(\mathbf{x} - \mathbf{x}')$. It turns out that for a system of two atoms we can account for all two-body processes by replacing the potential $V(\mathbf{q}) = \int d\mathbf{x} V(\mathbf{x}) e^{-i\mathbf{q} \cdot \mathbf{x}}$ by $(2\pi)^3$ times the T matrix and only use first-order perturbation theory to avoid double counting [66]. This means that the interactions between the atoms can be represented by the point interaction

$$V(\mathbf{x} - \mathbf{x}') = \frac{4\pi a \hbar^2}{m} \delta(\mathbf{x} - \mathbf{x}'). \tag{4.9}$$

This justifies the use of this pseudopotential in Chapter 2.

4.2   Multi-channel scattering

In the previous section we saw that the collision proces in the absence of the coupling to other channels is determined by the *s*-wave scattering length. For reasons that become clear in a moment, we denote this scattering length now by a_{bg}, which is known as the background scattering length. In this section we explain that near a Feshbach resonance there are resonant corrections to this result because of the coupling to another channel, leading to a magnetic-field dependend total scattering length $a(B)$. To understand the physical origin of this correction we have to use some concepts from atomic physics. Because most experiments are performed with alkali atoms we use these atoms to illustrate the main ideas. The ground-state electronic structure of alkali atoms is such that all electronic shells are filled and there is a single valence electron in the highest-occupied shell. The atoms have a nuclear spin $\mathbf{I}$ that couples to the electronic spin by means of the hyperfine interaction. For the alkali atoms the electrons have zero orbital angular momentum and the coupling arises solely because of the magnetic field produced by the electron spin $\mathbf{S}$. This means that there are two values for the total spin $\mathbf{F} = \mathbf{I} + \mathbf{S}$, with $F = I \pm 1/2$. In the absence of an external magnetic field the levels are split because of the hyperfine interaction $H_{\mathrm{hf}} = \alpha_{\mathrm{hf}} \mathbf{I} \cdot \mathbf{S}$ where α_{hf} is the hyperfine coupling strength and $\mathbf{I}$ and $\mathbf{S}$ are the operators for the

nuclear spin and the electronic spin, respectively. Moreover, in the presence of an external magnetic field the energies are split further because of the interaction of the magnetic moments of the electron and the nucleus with the magnetic field. If we take the magnetic field to be along the z axis this Zeeman interaction is given by $H_z = 2\mu_B B S_z - g_I(\mu_N/\hbar)BI_z$, where μ_B is the Bohr magneton, μ_N the nuclear magneton and g_I the nuclear g factor [44].

When two atoms collide the effective interaction potential is determined by the state of the valence electrons of the colliding atoms [63]. In Fig. 4.1 we schematically show the relevant physics for the description of a Feshbach resonance. Initially the atoms are far apart and their spin configuration is such that they see the interaction potential of the "open" channel. The exchange coupling flips the spins of one of the colliding atoms and in this different spin state or "closed" channel the colliding atoms see a different interaction potential [76]. Because of the different spin arrangement the continuum level of the closed channel is shifted due to the Zeeman effect by an energy $\Delta\mu B$, where B is the magnetic field and $\Delta\mu$ the difference in magnetic moments. The closed-channel potential in general has bound-states and we consider the case that there is one bound-state with energy E_m close to the open-channel continuum. The energy difference between the bound-state in the closed channel and the energy of the two-atom continuum is known as the detuning δ. On resonance, the binding energy of the molecules equals the difference of the continuum levels $\Delta\mu B$. Therefore, near resonance, we have that $\delta = \Delta\mu B - E_m \equiv \Delta\mu(B - B_0)$, where B_0 determines the position of the resonance.

In the multi-channel scattering problem the scattering state $|\psi^{(+)}\rangle$ is now a sum of contributions in the open $|\psi_{\text{open}}\rangle$ and closed $|\psi_{\text{closed}}\rangle$ channels. By introducing projection operators P_O and P_C for the open and closed subspaces, respectively, we can derive from the Schrödinger equation explicit coupled equations for the state vectors $|\psi_{\text{open}}\rangle$ and $|\psi_{\text{closed}}\rangle$ [67]. We have

$$P_O H(P_O + P_C)|\psi\rangle = EP_O|\psi\rangle$$
$$P_C H(P_O + P_C)|\psi\rangle = EP_C|\psi\rangle.$$

$$(4.10)$$

Formally, we can solve the equation for the closed channel and obtain the equation for the open-channel wave function as

$$\left[E - P_O H P_O - V_{\text{am}}\left(E - P_C H P_C + i\epsilon\right)^{-1} V_{\text{am}}\right]|\psi_{\text{open}}\rangle = 0. \qquad (4.11)$$

Here we have defined the atom-molecule coupling $V_{\text{am}} = P_O H P_C = P_C H P_O$. Without the coupling to the molecular channel, i.e., $V_{\text{am}} = 0$, the above equation reduces to Eq. (4.1). The physics of the Feshbach resonance is described by the coupling term in Eq. (4.11) and as before we can calculate the T matrix for the multi-channel problem. In general there are a lot of bound states in the subspace
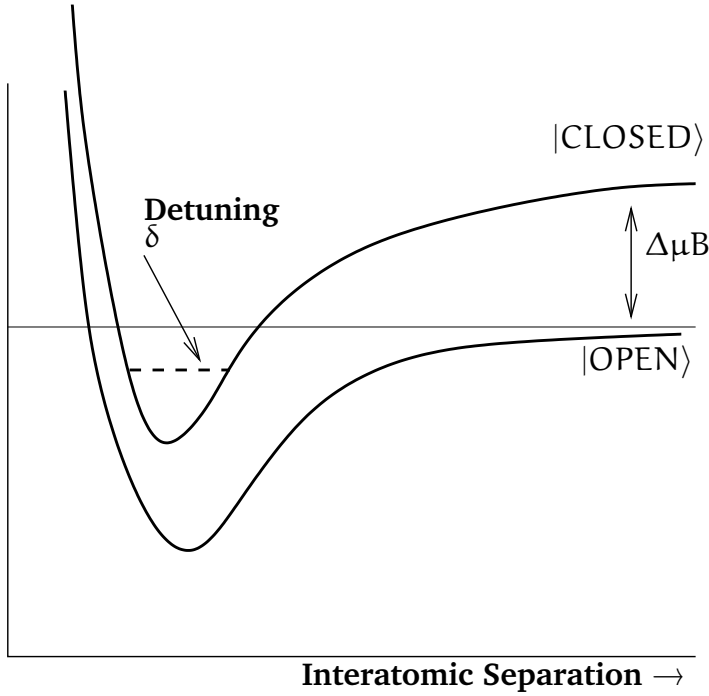
Figure 4.1: Illustration of the Feshbach resonance in a two-channel system. The two potential curves show the open and closed channel potential curves as a function of the interatomic separation.

that contains the closed channels. However, the experimentally most relevant case is when only a single bound-state with wave function $|\psi_m\rangle$ and energy E_m lies close to the energy E of the atoms in the open channel. In this limit, we ultimately obtain that [76, 41],

$$4\pi a \hbar^2/m = 4\pi a_{\text{bg}} \hbar^2/m - \frac{|\langle \psi_m|V_{\text{am}}|\psi_{\text{open}}\rangle|^2}{\delta}. \tag{4.12}$$

Note that the energy difference in the denominator of the above equation is simply the detuning δ. Moreover, we define

$$g = \begin{cases} \langle \psi_m|V_{\text{am}}|\psi_{\text{open}}\rangle/\sqrt{2} & \text{Bosons} \\ \langle \psi_m|V_{\text{am}}|\psi_{\text{open}}\rangle & \text{Fermions}, \text{Bose} - \text{Fermi} \ \ \text{mixtures} \end{cases}. \tag{4.13}$$

The additional factor of $1/\sqrt{2}$ for bosons in the above definition of g can diagramatically be understood because for identical bosons there are direct and exchange

contributions and we obtain an additional factor of two when we calculate the one-loop self-energy of the molecules.

Experimentally, the scattering length a is characterized by the width ΔB and the location B_0 of the resonance,

$$a(B) = a_{\text{bg}} \left(1 - \frac{\Delta B}{B - B_0} \right). \tag{4.14}$$

Here the first term describes the background interactions between the atoms and the second term is due to the coupling to the bound-state level in the closed channel. Moreover, the effective interactions between the atoms are still described by the T matrix, but now the scattering length is given by Eq. (4.14). Close to resonance the dominant contribution to the scattering length in Eq. (4.14) comes from the second term. If we neglect the background contribution to the scattering length and multiplying both the numerator and denominator with the difference in magnetic moments $\Delta\mu$, we find using Eq. (4.12) and Eq. (4.13) that the atom-molecule strength g obeys

$$g = \begin{cases} \hbar\sqrt{2\pi a_{\text{bg}}\Delta\mu\Delta B/m} & \text{Bosons} \\ \hbar\sqrt{4\pi a_{\text{bg}}\Delta\mu\Delta B/m} & \text{Fermions, Bose-Fermi Mixtures.} \end{cases} \tag{4.15}$$

4.3   A simple model

To illustrate the above we consider two colliding atoms with a coupling to a molecular state. The Hamiltonian for the coupled atom-molecule system is given by

$$H = H_{\text{a}} + H_{\text{m}} + V_{\text{am}}(\mathbf{r}_1 - \mathbf{r}_2). \tag{4.16}$$

Here the atomic part is described by

$$H_{\text{a}} = -\frac{\hbar^2\nabla_1^2}{2m} - \frac{\hbar^2\nabla_2^2}{2m}, \tag{4.17}$$

with V_{am} the atom-molecule coupling. The coupled system can be separated into center-of-mass and relative contributions and the time-independent Schrödinger equation for the relative coordinate of the coupled atom-molecule system is given by

$$\begin{pmatrix} H_0 & V_{\text{am}} \\ V_{\text{am}} & \delta \end{pmatrix} \begin{pmatrix} |\psi_{\text{a}}\rangle \\ |\psi_{\text{m}}\rangle \end{pmatrix} = E \begin{pmatrix} |\psi_{\text{a}}\rangle \\ |\psi_{\text{m}}\rangle \end{pmatrix}. \tag{4.18}$$

Here $H_0 = -\hbar^2\nabla_{\mathbf{r}}^2/m$ is the Hamiltonian for the relative coordinate system of the two atoms, $|\psi_{\text{a}}\rangle$ is the associated wave function, and δ_B the bare energy offset of the molecule with respect to the two-atom continuum. From the above equation

we obtain the following equation for the eigenenergy of the coupled atom-molecule system

$$E - \delta_B = \langle \psi_{\mathrm{m}} | V_{\mathrm{am}} \frac{1}{E - H_0} V_{\mathrm{am}} | \psi_{\mathrm{m}} \rangle. \tag{4.19}$$

The eigenstates $|\phi_{\mathbf{k}}\rangle$ of H_0 are plane waves with energies $E_{\mathbf{k}} = \hbar^2 \mathbf{k}^2/m$. Using these states Eq. (4.19) can be rewritten as

$$E - \delta_B = \int \frac{d^3\mathbf{k}}{(2\pi)^3} \frac{|\langle \psi_{\mathrm{m}} | \hat{V}_{\mathrm{am}} | \phi_k \rangle|^2}{E - \hbar^2\mathbf{k}^2/m}. \tag{4.20}$$

In the absence of the atom-molecule coupling the binding energy of the molecules is simply equal to the bare detuning. Due to the coupling the molecular binding energy is modified and the right-hand-side of Eq. (4.20) can be interpreted as the self-energy $\hbar\Sigma(E)$ of the molecules. The spatial extent of the molecular wave function is small and the matrix elements in Eq. (4.20) can therefore be approximated by the usual pseudopotential,

$$\langle \mathbf{r} | \hat{V}_{\mathrm{am}} | \phi_{\mathrm{m}} \rangle = \begin{cases} \sqrt{2} g \delta(\mathbf{r}) & \text{Bosons} \\ g \delta(\mathbf{r}) & \text{Fermions, Bose-Fermi mixtures} \end{cases} . \tag{4.21}$$

Here g is the atom-molecule coupling as given by Eq. (4.15).

Using this we evaluate the expression for the self-energy in the bosonic case and obtain,

$$
\begin{aligned}
\hbar\Sigma(E) &= \int \frac{d^3\mathbf{k}}{(2\pi)^3} \frac{|\langle \psi_{\mathrm{m}} | \hat{V}_{\mathrm{am}} | \phi_k \rangle|^2}{E - \hbar^2 k^2/m} \\
&= \lim_{\mathbf{r}\downarrow 0} \frac{4g^2}{(2\pi)^2} \int dk \; k^2 \frac{\phi_k^*(\mathbf{0})\phi_k(\mathbf{r})}{E - \hbar^2 k^2/m} \\
&= -i\frac{m^{3/2}g^2}{\hbar^3(2\pi)}\sqrt{E} + \lim_{\mathbf{r}\downarrow 0} 2g^2 \int \frac{d\mathbf{k}}{(2\pi)^3} \frac{m \, e^{i\mathbf{k}\cdot\mathbf{r}}}{\hbar^2 \mathbf{k}^2}.
\end{aligned} \tag{4.22}
$$

The divergent term in the self-energy in the above equation is energy independent and comes about because we have used an approximate delta-function potential instead of the actual interatomic potential. This term can be written as,

$$
\begin{aligned}
\lim_{\mathbf{r}\downarrow 0} 2g^2 \int \frac{d\mathbf{k}}{(2\pi)^3} \frac{m \, e^{i\mathbf{k}\cdot\mathbf{r}}}{\hbar^2 \mathbf{k}^2} &= \lim_{\mathbf{r}\downarrow 0} \frac{4\pi g^2 m}{(2\pi)^3 \hbar^2} \int dk \int d\theta \; \sin\theta \; e^{ikr\cos\theta} \\
&= \lim_{r\downarrow 0} \frac{mg^2}{\pi^2\hbar^2 r} \int dk \; \frac{\sin(kr)}{k} = \lim_{r\downarrow 0} \frac{mg^2}{2\pi\hbar^2 r}. \tag{4.23}
\end{aligned}
$$

To deal with this divergence we have to use the renormalized detuning instead of the bare detuning. The former is defined as $\delta = \delta_B - \lim_{r\downarrow 0} mg^2/2\pi\hbar^2 r$, where

$\delta = \Delta\mu(B - B_0)$ is determined by the experimental value of the magnetic field B_0 at resonance and $\Delta\mu$ is the difference in magnetic moments. For the case of fermions or a Bose-Fermi mixture the above expression for the self-energy is a factor of two smaller and in those cases the renormalized detuning is defined by $\delta = \delta_B - \lim_{r\downarrow 0} mg^2/4\pi\hbar^2 r$.

Chapter 5

Effective atom-molecule theory

—————— ABSTRACT

In this chapter we give a rigorous derivation of the effective action that describes ultracold atoms in an optical lattice near a Feshbach resonance. The effective theory takes the form of a generalized Hubbard model and in the following chapters we apply this theory to a Bose gas and a Bose-Fermi mixture near a Feshbach resonance.

5.1   Introduction

The reason for deriving an effective Hamiltonian for a resonantly-interacting atomic gas in an optical lattice is that in this manner we can make sure that a simple mean-field theory for the many-body physics of the gas automatically incorporates the relevant two-body physics exactly. As a result we start our derivation by considering first the Feshbach problem for two atoms on a single site. For a deep optical lattice a single site can be well approximated by a harmonic microtrap and the two-body Feshbach problem can then be solved exactly. This leads to the introduction of dressed molecular states on a site.

However, we are not primarily interested in the on-site two-body problem and actually want to describe the many-body physics of an atomic gas in an optical lattice. This implies that we must also allow for hopping, or tunneling, of the dressed molecular states from a site to a neighboring site. Since also single atoms can hop in this manner the effective theory becomes a theory describing a dilute gas of dressed molecules and atoms. It is now most important to realize that, in

contrast to the single-site problem, the interaction between the dressed molecules and the atoms is not equal to zero at long wavelengths. This follows, of course, from the mathematical derivation of the effective Hamiltonian as given below, but this can physically also be understood in the following two ways. First, if the dressed molecular energy band lies far above the atomic energy band the molecules can be integrated out, i.e., adiabatically eliminated, and we must obtain a Hubbard model for the atomic gas. It is precisely the dressed atom-molecule interaction that is needed to obtain the correct resonant interaction between the atoms in this Hubbard model. Second, the dressed atom-molecule interaction is needed to correctly describe important mean-field effects of an atomic and/or a molecular condensate, such as the Ramsey fringes or Josephson oscillations that have been observed without an optical lattice by Donley *et al.* [23]. It should be noted that the mean-field effects of an atomic condensate also occur in a many-body state that contains only empty sites or sites with precisely one atom or precisely one dressed molecule.

Applying our effective Hamiltonian to a particular problem has to be done with care, since it already incorporates the relevant two-body physics exactly. In general, if we apply a mean-field theory for the many-body physics to the effective Hamiltonian, we have to make sure that the mean-field theory does not incorporate the two-body physics again. Put differently, to derive the effective Hamiltonian we have already summed an infinite number of Feynman diagrams and we must take care that the desired mean-field theory does not sum these Feynman diagrams again. Two well-known examples where such a double counting in principle occurs are the Hartree-Fock-Bogoliubov theory for a Bose-Einstein condensed atomic Bose gas [69] and the Bardeen-Cooper-Schrieffer (BCS) theory for an atomic Fermi gas [70]. For the same reason exact Monte-Carlo simulations of atomic gases must make use of a nonlocal two-particle potential $V(\mathbf{r})$ that is constructed such that it reproduces exactly the scattering length a of the microscopic interatomic potential, instead of using the local interaction $(4\pi a\hbar^2/m)\delta(\mathbf{r})$ of the effective Hamiltonian [71].

Another, essentially equivalent but perhaps physically more appealing, way to look at the effective Hamiltonians used for ultracold atomic gases is from a renormalization group theory point of view. From this point of view the effective Hamiltonian is obtained by integrating out all high-energy (two-body) physics and can thus only be used to describe the low-energy (many-body) physics. In particular, this shows explicitly that the effective Hamiltonian can be used to account for the presence of a Bose-Einstein condensate in the gas, because this affects only the single-particle states with low energies. In the case of an atomic gas with a Feshbach resonance the microscopic theory can, also in an optical lattice, be formulated in terms of an interacting theory of atoms and molecules. Under the above mentioned renormalization procedure, both the molecules and the atom-molecule interaction get renormalized and consequently the effective theory takes

the form of an interacting theory of dressed molecules and atoms [76].

As mentioned previously, in the following chapters we consider an atomic Bose gas (Chapter 6) and an atomic Bose-Fermi mixture (Chapter 7) at low filling fractions of the optical lattice and near a Feshbach resonance. In particular, we have determined the critical point of the Ising and XY quantum phase transitions that respectively occur in these cases. To obtain the critical point of the Ising transition we can conveniently work in the phase in which the Bose gas contains a molecular condensate. For the XY transition we can even work in the normal state of the Bose-Fermi mixture. In both cases we are allowed to apply the relevant mean-field theory to our effective Hamiltonian, since possible double-counting problems are negligible for the low filling fractions of interest to us. Moreover, the effects of double-counting, which physically become important when many-body effects change the on-site wave function of the dressed molecules, can be systematically removed by including fluctuations around our mean-field theory.

5.2   Effective action

In a nutshell, the quantity of interest in a quantum-field theory is the generating functional Z of all the Green's functions. This functional determines all the possible correlation functions of the system. Specifically, let us consider the field theory for an atom-molecule gas that is described by the action $S[\psi_a^*, \psi_a, \psi_m^*, \psi_m]$, with ψ_a and ψ_m being the atomic and molecular fields, respectively. The generating functional in imaginary time is defined by

$$Z[J_a^*, J_a, J_m^*, J_m]$$
$$= \int d[\psi_a^*]\, d[\psi_a]\, d[\psi_m^*]\, d[\psi_m] \exp\left\{ -\frac{1}{\hbar} S[\psi_a^*, \psi_a, \psi_m^*, \psi_m] + S_J \right\}, \quad (5.1)$$

where the source currents couple to the fields according to,

$$S_J = \int d\tau \int d\mathbf{x}\, [\psi_a^*(\mathbf{x},\tau) J_a(\mathbf{x},\tau)\ + \psi_m^*(\mathbf{x},\tau) J_m(\mathbf{x},\tau)$$
$$+ J_a^*(\mathbf{x},\tau) \psi_a(\mathbf{x},\tau) + J_m^*(\mathbf{x},\tau) \psi_m(\mathbf{x},\tau)]\,.$$
$$(5.2)$$

By taking functional derivatives of Z with respect to the currents we can calculate all the correlation functions of the theory. Instead of working with Z we usually prefer to work with the generating functional W of all the connected Green's functions, which is related to Z through $Z = \exp\{W\}$. The functional derivatives of W with respect to the currents are the expectation values of the fields, i.e.,

$$\frac{\delta W}{\delta J_a} = \langle \psi_a^* \rangle \equiv \phi_a^* \qquad \frac{\delta W}{\delta J_m} = \langle \psi_m^* \rangle \equiv \phi_m^*. \qquad (5.3)$$

65

Similar equations hold for the expectation values of the conjugated fields ψ_a and ψ_m. Instead of using W, which only depends on the current sources, it is possible to define a functional Γ that depends explicitly on the fields ϕ_a and ϕ_m, and which is related to W by means of a Legendre transformation, i.e.,

$$\begin{aligned}
\Gamma[\phi_a^*, \phi_a, \phi_m^*, \phi_m] &= -W[J_a^*, J_a, J_m^*, J_m] \\
&+ \int d\tau \int d\mathbf{x} \; [\phi_a^*(\mathbf{x}, \tau)J_a(\mathbf{x}, \tau) \; + \phi_m^*(\mathbf{x}, \tau)J_m(\mathbf{x}, \tau) \\
&+ J_a^*(\mathbf{x}, \tau)\phi_a(\mathbf{x}, \tau) + J_m^*(\mathbf{x}, \tau)\phi_m(\mathbf{x}, \tau)] \,.
\end{aligned} \tag{5.4}$$

The reason for doing this is that Γ is related to the exact effective action of the system, through $S^{\mathrm{eff}} = -\hbar\Gamma$. Technically, Γ is the generating functional of all one-particle irreducible vertex functions. In our case, the exact effective action for the atom-molecule theory can be written as

$$\begin{aligned}
S^{\mathrm{eff}}[\phi_a^*, \phi_a, \phi_m^*, \phi_m] &= \mathrm{Tr}\left[-\phi_a^* \hbar G_a^{-1}\phi_a - \phi_m^* \hbar G_m^{-1}\phi_m \right. \\
&\left. + g\left(\phi_m^* \phi_a \phi_a + \phi_a^* \phi_a^* \phi_m\right) + \ldots \right],
\end{aligned} \tag{5.5}$$

where $G_{a,m}$ are the exact propagators of the atoms and molecules, respectively, and g is the exact three-point vertex. The dots denotes all possible other one-particle irreducible vertices, which turn out to be less relevant for our purposes.

5.3 Dressed molecules

Starting from the microscopic atom-molecule theory in an optical lattice we derive in this section the effective quantum field theory that contains the two-atom physics exactly. Without loss of generality we consider first bosonic atoms and we have in first instance for the total action

$$S = S_a + S_m + S_{am}, \tag{5.6}$$

where we have for the atoms

$$\begin{aligned}
S_a &= \int_0^{\hbar\beta} d\tau \int d\mathbf{x} \; \psi_a^*(\mathbf{x}, \tau)\left(\hbar\partial_\tau - \frac{\hbar^2\nabla^2}{2m} - \mu + V_0(\mathbf{x}) \right)\psi_a(\mathbf{x}, \tau) \\
&+ \frac{1}{2}\int_0^{\hbar\beta} d\tau \int d\mathbf{x} \; \frac{4\pi a_{\mathrm{bg}}\hbar^2}{m}\psi_a^*(\mathbf{x}, \tau)\psi_a^*(\mathbf{x}, \tau)\psi_a(\mathbf{x}, \tau)\psi_a(\mathbf{x}, \tau) \; . \tag{5.7}
\end{aligned}$$

and $V_0(\mathbf{x})$ is the external potential. In the following we are primarily interested in the effects of the resonant interactions between the atoms and molecules and as

a result we do not consider the effect of the background scattering on the atoms. The bare-molecular contribution to the action is given by

$$S_{\mathrm{m}} = \int_0^{\hbar\beta} d\tau \int d\mathbf{x} \ \psi_{\mathrm{m}}^*(\mathbf{x},\tau) \left(\hbar\partial_\tau - \frac{\hbar^2\nabla^2}{4m} + \delta_B - 2\mu + V_0(\mathbf{x}) \right) \psi_{\mathrm{m}}(\mathbf{x},\tau) \ .$$

(5.8)

The atom-molecule coupling that describes the formation of a molecule from two atoms and vice versa, is given by

$$S_{\mathrm{am}} = \int_0^{\hbar\beta} d\tau \int d\mathbf{x} \int d\mathbf{x}' \ g_{\uparrow\downarrow}(\mathbf{x} - \mathbf{x}') \left\{ \psi_{\mathrm{m}}^*((\mathbf{x} + \mathbf{x}')/2, \tau)\psi_{\mathrm{a}}(\mathbf{x}', \tau) \ \psi_{\mathrm{a}}(\mathbf{x}, \tau) \right.$$
$$\left. + \psi_{\mathrm{a}}^*(\mathbf{x}', \tau)\psi_{\mathrm{a}}^*(\mathbf{x}, \tau)\psi_{\mathrm{m}}((\mathbf{x} + \mathbf{x}')/2, \tau) \right\} .$$

(5.9)

Here the atom-molecule coupling is given by $g_{\uparrow\downarrow}(\mathbf{x}) = V_{\uparrow\downarrow}(\mathbf{x})\chi_{\mathrm{m}}(\mathbf{x})/\sqrt{2}$, where the properly normalized and symmetrized wave function χ_{m} obeys the Schrödinger equation in the closed channel. Next we want to include the effect of the resonant interactions on the molecules. We have,

$$S_{\mathrm{a}} + S_{\mathrm{am}} = \frac{1}{2} \int_0^{\hbar\beta} d\tau d\tau' \int d\mathbf{x} d\mathbf{x}' \ \left(\psi_{\mathrm{a}}^*(\mathbf{x},\tau) \ \ \psi_{\mathrm{a}}(\mathbf{x},\tau) \right) - \hbar\mathbf{G}_{\mathrm{a}}^{-1} \begin{pmatrix} \psi_{\mathrm{a}}(\mathbf{x}',\tau') \\ \psi_{\mathrm{a}}^*(\mathbf{x}',\tau') \end{pmatrix},$$

(5.10)

where the 2×2 (Nambu space) matrix Green's function obeys

$$\mathbf{G}_{\mathrm{a}}^{-1} = \mathbf{G}_{\mathrm{a},0}^{-1} - \mathbf{\Sigma} = \mathbf{G}_{\mathrm{a},0}^{-1} \left(1 - \mathbf{G}_{\mathrm{a},0}\mathbf{\Sigma} \right),$$

(5.11)

with

$$\mathbf{G}_{\mathrm{a},0}^{-1} = \begin{bmatrix} G_{\mathrm{a}}^{-1}(\mathbf{x},\tau;\mathbf{x}',\tau') & 0 \\ 0 & G_{\mathrm{a}}^{-1}(\mathbf{x}',\tau';\mathbf{x},\tau) \end{bmatrix}.$$

(5.12)

The self-energy matrix is given by,

$$\hbar\mathbf{\Sigma} = \begin{bmatrix} 0 & g(\mathbf{x} - \mathbf{x}')\psi_{\mathrm{m}}^*((\mathbf{x} + \mathbf{x}')/2, \tau) \\ g^*(\mathbf{x} - \mathbf{x}')\psi_{\mathrm{m}}((\mathbf{x} + \mathbf{x}')/2, \tau) & 0 \end{bmatrix} \delta(\tau - \tau').$$

(5.13)

With the above atom-molecule action we can calculate the grand-canonical partition function as a path integral

$$Z = \int d[\psi_{\mathrm{a}}^*]d[\psi_{\mathrm{a}}]d[\psi_{\mathrm{m}}^*]d[\psi_{\mathrm{m}}] \exp\left\{ -\frac{1}{\hbar}S[\psi_{\mathrm{a}}^*, \psi_{\mathrm{a}}, \psi_{\mathrm{m}}^*, \psi_{\mathrm{m}}] \right\}.$$

(5.14)

After integrating out the atoms the contribution to the molecular self-energy coming from the resonant interactions is given by

$$-\frac{1}{2}\mathrm{Tr}\left[\mathbf{G}_{\mathrm{a},0}\boldsymbol{\Sigma}\mathbf{G}_{\mathrm{a},0}\boldsymbol{\Sigma}\right]. \tag{5.15}$$

This term expresses that the molecule can break up into two atoms and recombine again. The space-time representation is not the most convenient one for our purposes, because the Green's functions are not diagonal in that representation. The zeroth-order Green's function for the atoms satisfies

$$\left\{\hbar\partial_\tau - \frac{\hbar^2\nabla^2}{2m} + V_0(\mathbf{x}) - \mu\right\}G_{\mathrm{a},0}(\mathbf{x},\tau;\mathbf{x}',\tau') = -\hbar\delta(\tau-\tau')\delta(\mathbf{x}-\mathbf{x}'). \tag{5.16}$$

Because this Green's function only depend on the difference between τ and τ', we can rewrite the above equation by performing a Fourier transform to Matsubara frequencies. We then find

$$\left\{-i\hbar\omega_n - \frac{\hbar^2\nabla^2}{2m} + V_0(\mathbf{x}) - \mu\right\}G_{\mathrm{a},0}(\mathbf{x};\mathbf{x}',i\omega_n) = -\hbar\delta(\mathbf{x}-\mathbf{x}'). \tag{5.17}$$

To proceed further we note that the solutions to the Schrödinger equation for a particle in a periodic potential are the Bloch wave functions. Specifically we have

$$\left[-\frac{\hbar^2\nabla^2}{2m} + V_0(\mathbf{x})\right]\chi_{\mathbf{k}}^{\mathrm{a}}(\mathbf{x}) = \epsilon_{\mathbf{k}}\chi_{\mathbf{k}}^{\mathrm{a}}(\mathbf{x}). \tag{5.18}$$

Here the wave functions satisfy $\chi_{\mathbf{k}}^{\mathrm{a}}(\mathbf{x}) = e^{i\mathbf{k}\cdot\mathbf{x}}u_{\mathbf{k}}(\mathbf{x})$ and the functions $u_{\mathbf{k}}(\mathbf{x})$ are invariant under translation by a multiple times the lattice spacing. The lattice momentum $\mathbf{k}$ is extended and runs from negative to positive infinity. These wave functions form a complete set and it is convenient to make a Fourier transform of the Green's function with respect to these functions. This gives

$$G_{\mathrm{a},0}(\mathbf{x},\mathbf{x}',i\omega_n) = \sum_{\mathbf{k},\mathbf{k}'}G_{\mathrm{a},0}(\mathbf{k},\mathbf{k}',i\omega_n)\chi_{\mathbf{k}}^{\mathrm{a}}(\mathbf{x})\chi_{\mathbf{k}'}^{\mathrm{a}*}(\mathbf{x}'). \tag{5.19}$$

Substituting this into Eq. (5.17) and representing the Dirac delta function in terms of the Bloch wave functions we obtain,

$$\left\{-i\hbar\omega_n - \frac{\hbar^2\nabla^2}{2m} + V_0(\mathbf{x}) - \mu\right\}\sum_{\mathbf{k},\mathbf{k}'}G_{\mathrm{a},0}(\mathbf{k},\mathbf{k}',i\omega_n)\chi_{\mathbf{k}}^{\mathrm{a}}(\mathbf{x})\chi_{\mathbf{k}'}^{\mathrm{a}*}(\mathbf{x}') =$$

$$\sum_{\mathbf{k},\mathbf{k}'}\left\{-i\hbar\omega_n + \epsilon_{\mathbf{k}} - \mu\right\}G_{\mathrm{a},0}(\mathbf{k},\mathbf{k}',i\omega_n)\chi_{\mathbf{k}}^{\mathrm{a}}(\mathbf{x})\chi_{\mathbf{k}'}^{\mathrm{a}*}(\mathbf{x}')$$

$$= -\hbar\sum_{\mathbf{k},\mathbf{k}'}\chi_{\mathbf{k}}^{\mathrm{a}}(\mathbf{x})\chi_{\mathbf{k}'}^{\mathrm{a}*}(\mathbf{x}')\delta_{\mathbf{k},\mathbf{k}'}.$$

$$\tag{5.20}$$

From this we immediately see that

$$G_{a,0}(\mathbf{k}, \mathbf{k}', i\omega_n) = \frac{-\hbar\delta_{\mathbf{k},\mathbf{k}'}}{-i\hbar\omega_n + \epsilon_{\mathbf{k}} - \mu} \equiv G_{a,0}(\mathbf{k}, i\omega_n)\delta_{\mathbf{k},\mathbf{k}'}. \tag{5.21}$$

The Green's function in Eq. (5.16) can thus be written as

$$G_{a,0}(\mathbf{x}, \tau; \mathbf{x}', \tau') = \frac{1}{\hbar\beta} \sum_{\mathbf{k},n} G_{a,0}(\mathbf{k}, i\omega_n)\chi_{\mathbf{k}}^{a}(\mathbf{x})\chi_{\mathbf{k}}^{a*}(\mathbf{x}')e^{-i\omega_n(\tau-\tau')}. \tag{5.22}$$

As before we use the Wannier functions introduced in Sec. 2.3, which implies

$$\psi_{m}^{\dagger}(\mathbf{x}, \tau) = \frac{1}{\sqrt{\hbar\beta}} \sum_{n} \sum_{\mathbf{p},i} b_{\mathbf{p},i}^{\dagger}(i\omega_n)w_{\mathbf{p}}^{*}(\mathbf{x} - \mathbf{x}_i)e^{i\omega_n\tau},$$

$$\psi_{m}(\mathbf{x}, \tau) = \frac{1}{\sqrt{\hbar\beta}} \sum_{n} \sum_{\mathbf{p},i} b_{\mathbf{p},i}(i\omega_n)w_{\mathbf{p}}(\mathbf{x} - \mathbf{x}_i)e^{-i\omega_n\tau}. \tag{5.23}$$

Here the operators $b_{n,i}^{\dagger}$ and $b_{n,i}$ create and annihilate a molecule in the n-th trap state of site i, respectively. Using this we find that the molecular part of the action in Eq. (5.8) is given by

$$
\begin{aligned}
S_{m} &= \int_{0}^{\hbar\beta} d\tau \int d\mathbf{x}\, \psi_{m}^{*}(\mathbf{x}, \tau) \left(\hbar\partial_\tau - \frac{\hbar^2\nabla^2}{4m} + \delta_B - 2\mu + V_0(\mathbf{x}) \right) \psi_{m}(\mathbf{x}, \tau) \\
&= \sum_{n} \sum_{i,j} \sum_{\mathbf{p},\mathbf{q}} b_{\mathbf{p},i}^{*}(i\omega_n)b_{\mathbf{q},j}(i\omega_n) \\
&\quad \times \int d\mathbf{x}\, w_{\mathbf{p}}^{*}(\mathbf{x} - \mathbf{x}_i) \left(-i\hbar\omega_n - \frac{\hbar^2\nabla^2}{4m} + V_0(\mathbf{x}) + \delta_B - 2\mu \right) w_{\mathbf{q}}(\mathbf{x} - \mathbf{x}_j).
\end{aligned}
\tag{5.24}
$$

From this we can read off the hopping term t_m and the on-site energy ϵ_m. As we will show later on the important case is when the molecules are in the lowest band. Specifically we then find for the hopping

$$t_{m} = - \int d\mathbf{x}\, w_0^{*}(\mathbf{x} - \mathbf{x}_i) \left[-\frac{\hbar^2\nabla^2}{4m} + V_0(\mathbf{x}) \right] w_0(\mathbf{x} - \mathbf{x}_j), \tag{5.25}$$

where i and j are nearest-neighbouring sites. The on-site energy ϵ_m is given by

$$\epsilon_{m} = \int d\mathbf{x}\, w_0^{*}(\mathbf{x} - \mathbf{x}_i) \left[-\frac{\hbar^2\nabla^2}{4m} + V_0(\mathbf{x}) \right] w_0(\mathbf{x} - \mathbf{x}_i). \tag{5.26}$$
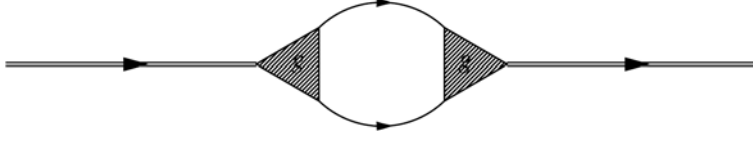
69

Figure 5.1: Diagramatic representation of the second-order term in Eq. (5.28).

The action in Eq. (5.24) can therefore be written as a lattice action

$$
\begin{aligned}
S_m \;=\; \sum_n \Bigg\{ & -t_{\mathrm{m}} \sum_{\langle i,j \rangle} b_i^*(i\omega_n) b_j(i\omega_n) \\
& + \sum_i \left(-i\hbar\omega_n + \epsilon_{\mathrm{m}} + \delta_B - 2\mu \right) b_i^*(i\omega_n) b_i(i\omega_n) \Bigg\},
\end{aligned}
$$
(5.27)

where $\langle i,j \rangle$ denotes the sum over nearest neighbours, and $\epsilon_{\mathrm{m}} = 3\hbar\omega/2$ in the tight-binding limit.

Next we consider the second-order contribution of Eq. (5.15) that introduces a self-energy for the molecules. We introduce center-of-mass $\mathbf{R} = (\mathbf{x}' + \mathbf{x}'')/2$, $\mathbf{R}' = (\mathbf{x} + \mathbf{x}''')/2$ and relative $\mathbf{r} = \mathbf{x}' - \mathbf{x}''$, $\mathbf{r}' = \mathbf{x}''' - \mathbf{x}$ coordinates. For the second-order term in Eq. (5.15) we thus obtain

$$
\begin{aligned}
\mathrm{Tr}\left[\mathbf{G}_{\mathrm{a},0}\boldsymbol{\Sigma}\mathbf{G}_{\mathrm{a},0}\boldsymbol{\Sigma}\right] = & \int_0^{\hbar\beta} d\tau \, d\tau' \int d\mathbf{R} \, d\mathbf{R}' \, d\mathbf{r} \, d\mathbf{r}' \; g(\mathbf{r})g(\mathbf{r}')\psi_{\mathrm{m}}^*(\mathbf{R},\tau)\psi_{\mathrm{m}}(\mathbf{R}',\tau') \\
& \times G_{\mathrm{a},0}(\mathbf{R}'+\mathbf{r}'/2,\tau;\mathbf{R}+\mathbf{r}/2,\tau')G_{\mathrm{a},0}(\mathbf{R}'-\mathbf{r}'/2,\tau;\mathbf{R}-\mathbf{r}/2,\tau').
\end{aligned}
$$
(5.28)

Diagramatically we have represented this term in Fig. 5.1. In the above expression we substitute the Wannier representation of the molecular fields and take the pseudopotential approximation $g(\mathbf{r}) = g\delta(\mathbf{r})$ to find

$$
\begin{aligned}
\mathrm{Tr}\left[\mathbf{G}_{\mathrm{a},0}\boldsymbol{\Sigma}\mathbf{G}_{\mathrm{a},0}\boldsymbol{\Sigma}\right] = & g^2 \frac{1}{\hbar\beta} \sum_{n,n'} \sum_{\mathbf{p},i} \sum_{\mathbf{q},j} \int_0^{\hbar\beta} d\tau \, d\tau' \int d\mathbf{R} \, d\mathbf{R}' \; b_{\mathbf{p},i}^*(i\omega_n) b_{\mathbf{q},j}(i\omega_{n'}) \\
& \times e^{i\omega_n \tau} e^{-i\omega_{n'}\tau'} w_{\mathbf{p}}^*(\mathbf{R}-\mathbf{x}_i) w_{\mathbf{q}}(\mathbf{R}'-\mathbf{x}_j) G_{\mathrm{a},0}(\mathbf{R}',\tau;\mathbf{R},\tau') G_{\mathrm{a},0}(\mathbf{R}',\tau;\mathbf{R},\tau').
\end{aligned}
$$
(5.29)

Taking also the Fourier transform of the Green's functions, i.e., using Eq. (5.22),

we obtain

$$
\text{Tr}\,[\mathbf{G}_{a,0}\mathbf{\Sigma}\mathbf{G}_{a,0}\mathbf{\Sigma}] = g^2 \frac{1}{(\hbar\beta)^3} \sum_{n,n'} \sum_{m,m'} \sum_{\mathbf{p},i} \sum_{\mathbf{q},j} \int_0^{\hbar\beta} d\tau \; d\tau' \int \; d\mathbf{R} \; d\mathbf{R}'
$$

$$
\times b_{\mathbf{p},i}^*(i\omega_n)b_{\mathbf{q},j}(i\omega_{n'})e^{i\omega_n\tau}e^{-i\omega_{n'}\tau'}e^{-i(\omega_m+\omega_{m'})(\tau-\tau')}w_{\mathbf{p}}^*(\mathbf{R}-\mathbf{x}_i)w_{\mathbf{q}}(\mathbf{R}'-\mathbf{x}_j)
$$

$$
\times \left[\sum_{\mathbf{k},\mathbf{k}'} G_{a,0}(\mathbf{k},i\omega_m)G_{a,0}(\mathbf{k}',i\omega_{m'})\chi_{\mathbf{k}}^{a}(\mathbf{R})\chi_{\mathbf{k}}^{a*}(\mathbf{R}')\chi_{\mathbf{k}'}^{a}(\mathbf{R})\chi_{\mathbf{k}'}^{a*}(\mathbf{R}') \right].
$$

(5.30)

The integrals over the imaginary time variables τ and τ' can now be performed and these give that $\omega_n = \omega_{n'} = \omega_m + \omega_{m'}$. We recall from section 2.3 that the single-particle wave functions that appear in the above equation are given by $\chi_{\mathbf{k}}^{a}(\mathbf{R}) = \sum_i e^{i\mathbf{k}\cdot\mathbf{x}_i}w_{\mathbf{n}}^{a}(\mathbf{R}-\mathbf{x}_i)$. In the tight-binding limit the Wannier functions are replaced by the tight-binding functions,

$$
w_{\mathbf{n}}(\mathbf{R}-\mathbf{x}_i) \quad \approx \quad \phi_{\mathbf{n}}(\mathbf{R}-\mathbf{x}_i). \tag{5.31}
$$

Here $\phi_{\mathbf{n}}(\mathbf{R}) = \phi_{n,\ell,m}(R,\theta,\phi)$ are the eigenstates of the atoms in the three-dimensional isotropic harmonic oscillator potential. In spherical coordinates they are given by

$$
\begin{aligned}
\phi_{\mathbf{n}}^{a}(\mathbf{R}) = \phi_{n,\ell,m}^{a}(\mathbf{R}) \quad &= \quad \sqrt{2/l^3}\left(\begin{array}{c} n+\ell+1/2 \\ n \end{array}\right)^{-1/2} \frac{1}{\sqrt{(\ell+1/2)!}} \\
&\times e^{-R^2/2l^2}L_n^{(1/2+\ell)}((R/l)^2)\;(R/l)^\ell\;Y_{\ell m}(\theta,\phi).
\end{aligned}
$$

(5.32)

Here $L_n^{(1/2+l)}(R)$ are the well-known generalized Laguerre polynomials, $Y_{\ell,m}(\theta,\phi)$ are again the spherical harmonic functions, and $l = \sqrt{\hbar/m\omega}$ is the harmonic oscillator length. In the extreme tight-binding limit the energies $\epsilon_{\mathbf{k}} = \epsilon_{\mathbf{n}} = (2n+\ell+3/2)\hbar\omega$ in Eq. (5.21) only depend on the radial and angular momentum quantum numbers n and l, respectively [44]. Explicitly, the states with zero angular momentum are given by

$$
\phi_{n,0,0}^{a}(\mathbf{R}) = \frac{1}{l^{3/2}\pi^{3/4}}e^{-R^2/2l^2}L_n^{(1/2)}((R/l)^2)/\sqrt{L_n^{(1/2)}(0)}. \tag{5.33}
$$

Note that for wave functions on different lattice sites the overlap is negligible. Therefore, we must have that $\mathbf{R}-\mathbf{x}_i$ and $\mathbf{R}-\mathbf{x}_j$ are on the same site and we assume that this is the case. As a result we can omit the $\mathbf{x}_i$ coordinate and simply write $\mathbf{R}$ and $\mathbf{R}'$.

Next, we evaluate the sum over Matsubara frequencies, keeping the external frequency $\omega_m + \omega_{m'} \equiv \omega_n$ of the molecules fixed. The product of Green's functions

71

can be rewritten as

$$G_{a,0}(\mathbf{n}, i\omega_m)G_{a,0}(\mathbf{n}', i\omega_{m'}) = -\hbar \frac{G_{a,0}(\mathbf{n}, i\omega_m) + G_{a,0}(\mathbf{n}', i\omega_{m'})}{-i\hbar(\omega_m + \omega_{m'}) + \epsilon_{\mathbf{n}} + \epsilon_{\mathbf{n}'} - 2\mu}. \tag{5.34}$$

We perform the sum and take the two-body limit, which amounts to taking the resulting occupation numbers equal to zero. We find

$$\mathrm{Tr}\left[\mathbf{G}_{a,0}\mathbf{\Sigma}\mathbf{G}_{a,0}\mathbf{\Sigma}\right] = g^2 \frac{1}{\hbar\beta} \sum_i \sum_{\mathbf{p},\mathbf{q}} \sum_{\mathbf{n},\mathbf{n}'} \sum_n \int \, d\mathbf{R} \, d\mathbf{R}' \, b^*_{\mathbf{p},i}(i\omega_n) b_{\mathbf{q},i}(i\omega_n)$$

$$\times \frac{\phi_{\mathbf{p}}^{\mathrm{m}*}(\mathbf{R})\phi_{\mathbf{q}}^{\mathrm{m}}(\mathbf{R}')\phi_{\mathbf{n}}^{\mathrm{a}}(\mathbf{R})\phi_{\mathbf{n}}^{\mathrm{a}*}(\mathbf{R}')\phi_{\mathbf{n}'}^{\mathrm{a}}(\mathbf{R})\phi_{\mathbf{n}'}^{\mathrm{a}*}(\mathbf{R}')}{-i\hbar\omega_n + \epsilon_{\mathbf{n}} + \epsilon_{\mathbf{n}'} - 2\mu}.$$

$$\tag{5.35}$$

For the systems of interest to us the molecules occupy only the lowest band, i.e., we take the band indices $\mathbf{p}$ and $\mathbf{q}$ of the molecular fields in the last expression equal to zero. In the following we then need the tight-binding function $\phi_{\mathbf{0}}^{\mathrm{m}}$ of the molecules, which is given by $\phi_{\mathbf{0}}^{\mathrm{m}}(\mathbf{R}) = \left(2/\pi l^2\right)^{3/4} e^{-(R/l)^2}$.

To proceed, we evaluate the integrals over the center-of-mass coordinates $\mathbf{R}$ and $\mathbf{R}'$, respectively. We have

$$\int d\mathbf{R}\phi_{\mathbf{0}}^{\mathrm{m}*}(\mathbf{R})\phi_{\mathbf{n}}^{\mathrm{a}}(\mathbf{R})\phi_{\mathbf{n}'}^{\mathrm{a}}(\mathbf{R}) = 2\left(2/\pi l^2\right)^{3/4}$$

$$\times \int dR \, d\theta \, d\phi \, R^{2+\ell+\ell'} \sin\theta \, e^{-2R^2} Y_{\ell m}(\theta, \phi) Y_{\ell' m'}(\theta, \phi)$$

$$\times \frac{L_n^{(1/2+\ell)}(R^2)}{\sqrt{(\ell+1/2)!}} \frac{L_{n'}^{(1/2+\ell')}(R^2)}{\sqrt{(\ell'+1/2)!}} \binom{n+\ell+1/2}{n}^{-1/2} \binom{n'+\ell'+1/2}{n'}^{-1/2}.$$

$$\tag{5.36}$$

In the right-hand side of the above equation the integral variable R is made dimensionless using the length l. The above integral looks formidable but the angular integrations can be directly evaluated using the orthonormality relations for the spherical harmonics. To evaluate the remaining integral over R we make use of the following relation [72]

$$\int dX \, e^{-2X^2} X^{2+2\ell} L_n^{(1/2+\ell)}(X^2) L_{n'}^{(1/2+\ell)}(X^2)$$

$$= \frac{1}{2} \int dy \, e^{-2y} y^{1/2+\ell} L_n^{(1/2+\ell)}(y) L_{n'}^{(1/2+\ell)}(y) = \frac{\Gamma(n+n'+\ell+3/2)}{2n!n'!} \frac{1}{2^{n+n'+\ell+3/2}}.$$

$$\tag{5.37}$$

Using this we find that Eq. (5.36) can be written as

$$\int d\mathbf{R}\phi_{\mathbf{0}}^{\mathrm{m}*}(\mathbf{R})\phi_{\mathbf{n}}^{\mathrm{a}}(\mathbf{R})\phi_{\mathbf{n}'}^{\mathrm{a}}(\mathbf{R}) = \delta_{m,-m'}\delta_{\ell,\ell'}\left(2/\pi l^2\right)^{3/4}\frac{\Gamma(n+n'+\ell+3/2)}{2n!n'!}$$

$$\times\frac{1}{2^{n+n'+\ell+3/2}}\frac{1}{(\ell+1/2)!}\binom{n+\ell+1/2}{n}^{-1/2}\binom{n'+\ell'+1/2}{n'}^{-1/2}.$$

$$(5.38)$$

The next step is now to evaluate the sums over the quantum numbers of the square of the above integral. Note that the energy denominator in Eq. (5.35) is determined by the sum of the two energies $\epsilon_{n,\ell}+\epsilon_{n',\ell}$. We then partially evaluate the resulting sum over the quantum numbers $\mathbf{n}$ and $\mathbf{n}'$ by summing out all the contributions that have the same energy $\epsilon_q \equiv \epsilon_{q,0} = \epsilon_{n+n',2\ell} - 3\hbar\omega/2$. Finally we then still have to perform the sum over q. Carrying out the partial sum gives

$$\sum_{\mathbf{n},\mathbf{n}'}\left[\int d\mathbf{R}\phi_{\mathbf{0}}^{\mathrm{m}*}(\mathbf{R})\phi_{\mathbf{n}}^{\mathrm{a}}(\mathbf{R})\phi_{\mathbf{n}'}^{\mathrm{a}}(\mathbf{R})\right]^2$$

$$= \sum_q \frac{1}{2\sqrt{2}}\,\phi_q^{\mathrm{a}*}(\mathbf{0})\phi_q^{\mathrm{a}}(\mathbf{0}),\qquad(5.39)$$

where $\phi_q^{\mathrm{a}}(\mathbf{R}) \equiv \phi_{q,0,0}^{\mathrm{a}}(\mathbf{R})$. The problem of two atoms in a three-dimensional harmonic oscillator can be separated into relative and center-of-mass problems. The wavefunctions with zero angular momentum for the relative coordinates are given by

$$\phi_n(\mathbf{r}) = \frac{1}{l^{3/2}(2\pi)^{3/4}}e^{-r^2/4l^2}L_n^{(1/2)}((r^2/2l^2))/\sqrt{L_n^{(1/2)}(0)}.\qquad(5.40)$$

In terms of these wavefunctions we have

$$\sum_{n,n'}\left[\int d\mathbf{R}\phi_{\mathbf{0}}^{\mathrm{m}*}(\mathbf{R})\phi_{\mathbf{n}}^{\mathrm{a}}(\mathbf{R})\phi_{\mathbf{n}'}^{\mathrm{a}}(\mathbf{R})\right]^2 = \sum_q \phi_q^*(\mathbf{0})\phi_q(\mathbf{0}).\qquad(5.41)$$

For the second order contribution to the self-energy we now obtain

$$\mathrm{Tr}\left[\mathbf{G}_{\mathrm{a},0}\mathbf{\Sigma}\mathbf{G}_{\mathrm{a},0}\mathbf{\Sigma}\right] = \frac{g^2}{\sqrt{2}\pi l^3}\frac{1}{\hbar\beta}\sum_{i,n}b_{\mathbf{0},i}^*(i\omega_n)b_{\mathbf{0},i}(i\omega_n)$$

$$\times\sum_q\frac{\phi_q^*(\mathbf{0})\phi_q(\mathbf{0})}{-i\hbar\omega_n + \epsilon_q + 3\hbar\omega/2 - 2\mu}.$$
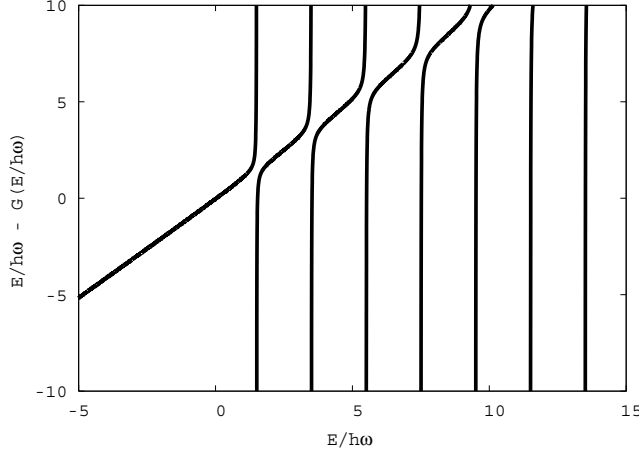
$$(5.42)$$

73

Figure 5.2: The function $E - G(E)$ as a function of the energy E.

We show in the next chapter that the resulting sum can be evaluated to give, after renormalisation of the bare detuning δ_B to the detuning δ, the following self-energy for the molecules,

$$\hbar\Sigma(i\hbar\omega_n) = g^2 \frac{G(i\hbar\omega_n - 3\hbar\omega/2 + 2\mu)}{\sqrt{2}\pi l^3 \hbar\omega}, \tag{5.43}$$

where $G(z)$ is the ratio of two gamma functions

$$G(z) = \Gamma(-z/2\hbar\omega + 3/4)/\Gamma(-z/2\hbar\omega + 1/4), \tag{5.44}$$

and ω is the angular frequency of the optical lattice sites. The propagator is therefore given by

$$D^{-1}(i\hbar\omega_n) = \left(-i\hbar\omega_n + 3\hbar\omega/2 - 2\mu + \delta + \hbar\Sigma(i\hbar\omega_n)\right)/\hbar. \tag{5.45}$$

We perform an analytic continuation $i\hbar\omega_n \to E + i\epsilon$ and the zeros of the above equation correspond now to the poles of the Green's function, which in turn correspond to the physical modes of the system. In Fig. 5.2 we have plotted the function $E - G(E)$. To study the modes we calculate the spectral weight function, which is given by

$$\rho(E) = -\frac{1}{\pi\hbar}\text{Im}\left[D^{(+)}(E)\right], \tag{5.46}$$

where $D^{(+)}(E)$ is the retarded Green's function of the system, i.e., $D^{(+)}(E) = D(E + i\epsilon)$. In the two-body limit the chemical potential is zero and because the

74

self-energy is real the spectral weight function now becomes a set of delta functions with strength Z_σ located at the solutions ϵ_σ of the equation

$$3\hbar\omega/2 + \delta = \epsilon_\sigma - g^2 \left[\frac{G(\epsilon_\sigma - 3\hbar\omega/2)}{\sqrt{2}\pi l^3 \hbar\omega} \right]. \tag{5.47}$$

Therefore, we can replace the bare molecular field b by the dressed fields b_σ with energy ϵ_σ. The coupling term between the bare atoms and bare molecules then has to be replaced by a coupling term between the bare atoms and the dressed molecules.

We now have all ingredients needed for the effective atom-molecule theory. The Hamiltonian representation of the effective action is then given by

$$
\begin{aligned}
H \;=\; & -t_a \sum_{\langle i,j \rangle} a_i^\dagger a_j - t_m \sum_\sigma \sum_{\langle i,j \rangle} b_{i,\sigma}^\dagger b_{j,\sigma} \\
& + \sum_\sigma \sum_i \left(\epsilon_\sigma - 2\mu \right) b_{i,\sigma}^\dagger b_{i,\sigma} + \sum_i (\epsilon_{\mathrm{a}} - \mu) a_i^\dagger a_i \\
& + \frac{U_{\mathrm{bg}}}{2} \sum_i a_i^\dagger a_i^\dagger a_i a_i + g' \sum_\sigma \sum_i \sqrt{Z_\sigma} \left(b_{i,\sigma}^\dagger a_i a_i + a_i^\dagger a_i^\dagger b_{i,\sigma} \right).
\end{aligned}
\tag{5.48}
$$

Here t_a and t_m are the tunneling amplitudes for the atoms and the molecules, respectively, and they are given by Eq. (2.22) and Eq. (5.25), respectively. Note that the similar looking Wannier functions in both expressions for the hopping energy refer to the Wannier functions of the atoms when we consider atoms and the Wannier function of the molecules when we consider molecules. The sum over $\langle i,j \rangle$ denotes a sum over nearest neighbours and the operators $a_i^\dagger$, a_i correspond to the creation and annihilation operators of a single atom at site i respectively. The operators $b_{i,\sigma}^\dagger$, $b_{i,\sigma}$ correspond to the creation and annihilation operators of the *dressed* molecules at site i, respectively. Also $\epsilon_{\mathrm{a}} = 3\hbar\omega/2$ is the on-site energy of a single atom. The background interaction energy U_{bg} is determined by Eq. (2.24) and the effective atom-molecule coupling in the optical lattice is given by

$$g' = g \int d\mathbf{x}\, [\phi_0^{\mathrm{m}*}(\mathbf{x})\phi_0^{\mathrm{a}}(\mathbf{x})\phi_0^{\mathrm{a}}(\mathbf{x})] = g \left[\int d\mathbf{x} |\phi_0^{\mathrm{a}}(\mathbf{x})|^4 \right]^{1/2}, \tag{5.49}$$

where g is the atom-molecule coupling in the absence of the optical lattice. Note that $(g')^2$ is proportional to $\int d\mathbf{x} |\phi_0^{\mathrm{a}}(\mathbf{x})|^4$ in exactly the same way as the background interaction term U_{bg}.

In summary, we have derived the effective atom-molecule theory in the tight-binding limit by calculating the generating functional $\Gamma[\phi_{\mathrm{a}}^*, \phi_{\mathrm{a}}, \phi_{\mathrm{m}}^*, \phi_{\mathrm{m}}]$ of *all* one-particle irreducible vertex functions in the approximation where we have summed over all two-body processes for the molecules. In this manner we have made sure
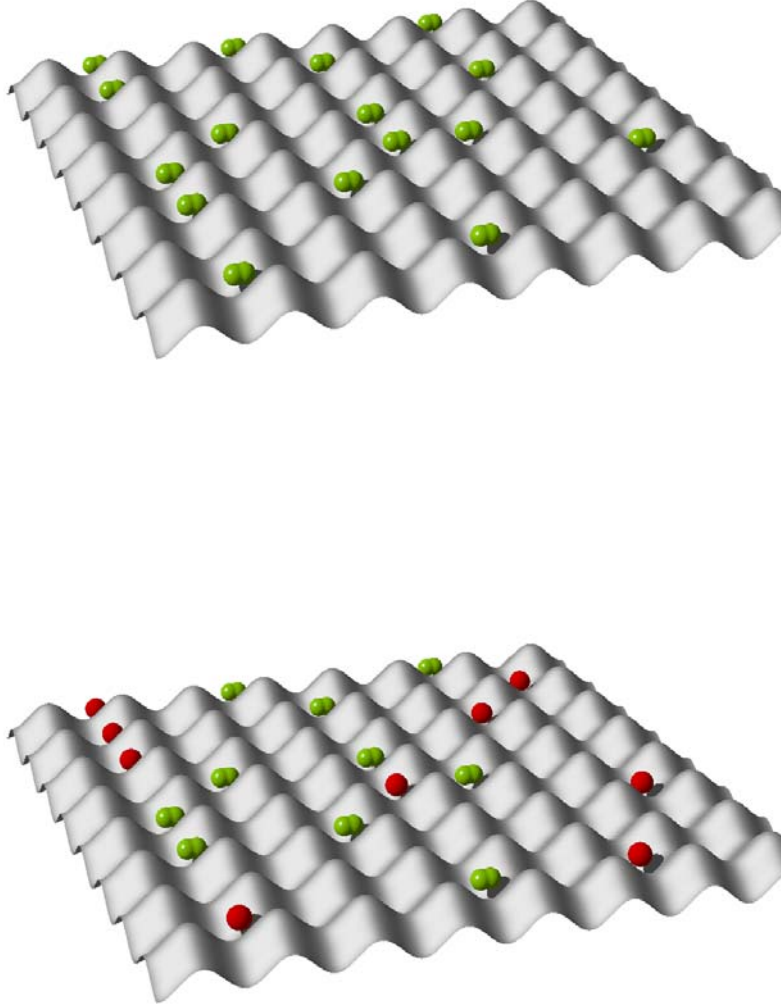
75

Figure 5.3: Illustration of the quantum Ising transition in a Bose gas near a Feshbach resonance.
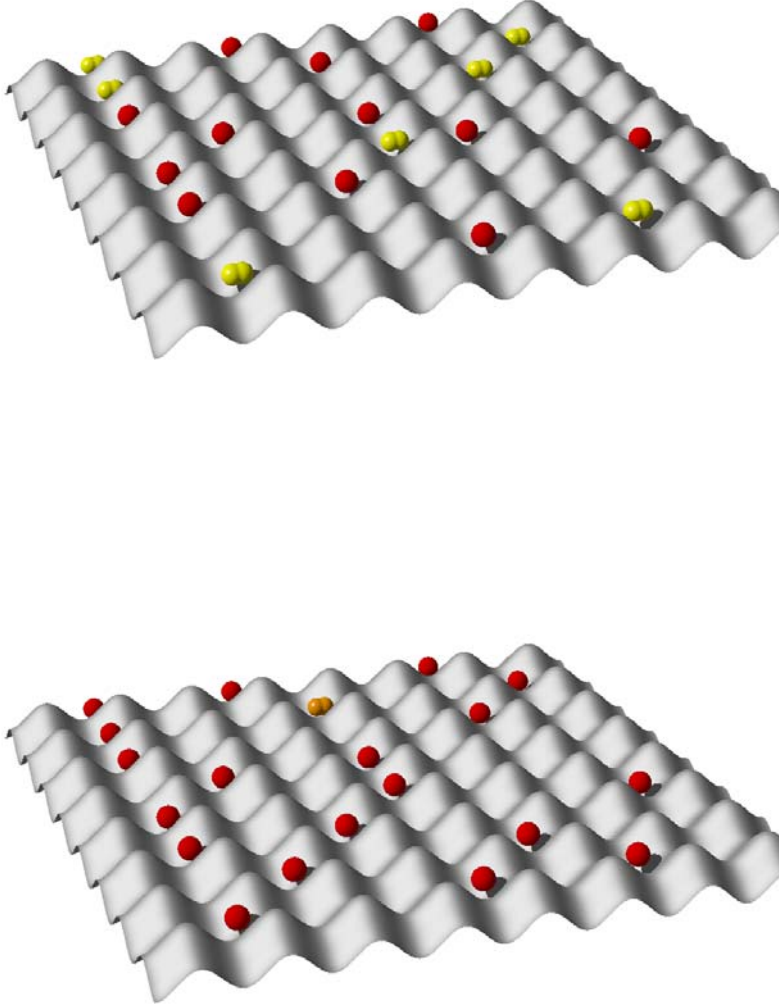
Figure 5.4: Illustration of the quantum Ising transition in a Bose gas near a Feshbach resonance.

that a simple mean-field theory for the many-body physics of the gas automatically incorporates the relevant two-body physics exactly. In the next chapter we derive the same result by considering first the Feshbach problem for two atoms on a single site. For a deep optical lattice a single site can be well approximated by a harmonic microtrap and the two-body Feshbach problem can then be solved exactly. This then leads to the introduction of the same dressed molecules. When we apply our theory to the Bose gas near a Feshbach resonance we obtain a picture for the quantum Ising transition that is sketched in Figs. 5.3 and 5.4. For negative detuning (Fig. 5.3 top picture) we have a Bose-Einstein condensate of dressed molecules which has a large amplitude in the bare-molecular channel. If we cross the quantum phase transition (Fig. 5.3 bottom picture) we also have an atomic Bose-Einstein condensate and the amplitude of the dressed molecules in the bare-molecular state becomes smaller. For even larger detunings (Fig. 5.4 top picture) the fraction of Bose-Einstein condensed atoms becomes larger and the remaining dressed molecules have a large amplitude in the open state (Fig. 5.4 bottom picture).

Chapter 6

Feshbach resonances in an optical lattice

————— ABSTRACT

We present the theory for ultracold atomic gases in an optical lattice near a Feshbach resonance. In the single-band approximation the theory describes atoms and molecules which can both tunnel through the lattice. Moreover, an avoided crossing between the two-atom and the molecular states occurs at every site. We determine the microscopic parameters of the generalized Hubbard model that describes this physics, using the experimentally known parameters of the Feshbach resonance in the absence of the optical lattice. As an application we also calculate the zero-temperature phase diagram of an atomic Bose gas in an optical lattice.

6.1   Introduction.

In the last few years there has been much excitement in the field of ultracold atomic gases. To a large extent this is due to two new experimental developments. The first is the use of so-called Feshbach resonances in the collision of two atoms, and the second is the use of an optical lattice. Both developments have led to an unprecedented controle over the physically relevant parameters of the atomic gas that can be used to explore new strongly-correlated regions of its phase diagram.

In this paper we propose to combine these two developments and study an atomic gas in an optical lattice near a Feshbach resonance.

A more specific motivation for studying Feshbach resonances in an optical lattice is that recently it has been shown that in an atomic Bose gas near a Feshbach resonance a quantum phase transition occurs between a phase with only a molecular condensate (MC) and a phase with both an atomic and a molecular condensate (AC+MC) [73, 74]. The experimental observation of this quantum Ising transition is, however, complicated by the fact that in a harmonic trap the fast vibrational relaxation of Feshbach molecules consisting of two bosonic atoms appears to prevent the creation of a molecular condensate in that case [75]. In an optical lattice with a low filling fraction molecule-molecule and atom-molecule collisions can essentially be neglected and we expect this problem to be much less severe.

Having this particular application in mind, we from now on focus on atomic Bose gases. However, our results can be immediately generalized to the case of a two-component Fermi gas or even an atomic Bose-Fermi mixture in an optical lattice. Moreover, we consider only such low filling fractions that it is justified to neglect the possibility of having three or more atoms per lattice site. The reason for this restriction is that in this case we have at most two atoms per site and the effect of the resonant interactions between the atoms can be incorporated into the theory exactly. The latter was shown previously to be very important for arriving at a quantitatively accurate description of a harmonically trapped atomic gas near a Feshbach resonance [76]. How this can be achieved also in an optical lattice is discussed next.

6.2 Generalized Hubbard model.

We consider the experimentally most interesting case of a deep optical lattice in which the on-site potential is, for low energies, well approximated by an isotropic harmonic potential with energy splitting $\hbar\omega$ and the tunneling energy t_a for atoms between sites obeys $t_a \ll \hbar\omega$. For two atoms on a single site the two-channel Feshbach problem in the relative coordinate, after splitting off the center-of-mass motion, is then given by the Schrödinger equation

$$\begin{pmatrix} H_0 + V_{aa} & V_{am} \\ V_{am} & \delta_B \end{pmatrix} \begin{pmatrix} |\psi_a\rangle \\ |\psi_m\rangle \end{pmatrix} = E \begin{pmatrix} |\psi_a\rangle \\ |\psi_m\rangle \end{pmatrix}. \tag{6.1}$$

Here the noninteracting atomic Hamiltonian is $H_0 = -\hbar^2\nabla_{\mathbf{r}}^2/m + m\omega^2\mathbf{r}^2/4$. The bare detuning is denoted by δ_B, $\mathbf{r}$ is the relative coordinate between the atoms and m is the atomic mass. The nonresonant or background atom-atom interaction is V_{aa} and the atom-molecule coupling is denoted by V_{am}. In first instance only the relative part is relevant, since only this part is affected by the interactions between the atoms. The center-of-mass part determines the tunneling. From Eq. (6.1) we

obtain the following equation for the molecules

$$\langle\psi_{\rm m}|V_{\rm am}\frac{1}{E - H_0 - V_{\rm aa}}V_{\rm am}|\psi_{\rm m}\rangle \quad = \quad E - \delta_{\rm B}, \tag{6.2}$$

where $|\psi_{\rm m}\rangle$ is the bare molecular wavefunction. Note that in the above we have implicitly taken the extent of this wavefunction to be so small that its energy is not affected by the optical lattice, which is well justified in practice. Because for most atoms we also have that $|V_{\rm aa}| \ll \hbar\omega$, we can neglect in the atomic propagator $V_{\rm aa}$ compared to H_0. Moreover, the eigenstates $|\phi_n\rangle$ of H_0 with energy $E_n = (2n + 3/2)\hbar\omega$ that are relevant for an s-wave Feshbach resonance, can be written in terms of the generalized Laguerre polynomials as $\langle\mathbf{r}|\phi_n\rangle = e^{-\mathbf{r}^2/4l^2}L_n^{1/2}(\mathbf{r}^2/2l^2)/(2\pi l^2)^{3/4}[L_n^{1/2}(0)]^{1/2}$. Here $l = \sqrt{\hbar/m\omega}$ is the harmonic oscillator length. Using these states Eq. (6.2) can be rewritten as

$$\sum_n \frac{|\langle\psi_{\rm m}|V_{\rm am}|\phi_n\rangle|^2}{E - E_{\rm n}} = E - \delta_{\rm B}. \tag{6.3}$$

Using also the usual pseudopotential approximation, we have that $\langle\mathbf{r}|V_{\rm am}|\psi_{\rm m}\rangle = \sqrt{2}g\delta(\mathbf{r})$, where the atom-molecule coupling $g = \hbar\sqrt{2\pi a_{\rm bg}\Delta B\Delta\mu/m}$ depends on the background scattering length $a_{\rm bg}$, the width of the resonance ΔB, and the difference in magnetic moments $\Delta\mu$ of the relevant Feshbach resonance [76]. From this we then find that the energy of the molecules obeys

$$\begin{aligned} E - \delta_B &= 2g^2\sum_m \frac{\phi_m^*(0)\phi_m(0)}{E - E_m} \\ &= g^2\left[\frac{G(E)}{\sqrt{2}\pi l^3\hbar\omega} - \lim_{r\to 0}\frac{m}{2\pi\hbar^2 r}\right]. \end{aligned} \tag{6.4}$$

The function $G(E)$ is the ratio of two gamma functions $G(E) = \Gamma(-E/2\hbar\omega + 3/4)/\Gamma(-E/2\hbar\omega + 1/4)$. The divergence in Eq. (6.4), which was first obtained by Busch *et al.* in the context of a single-channel problem [47], can be dealt with by using the following renormalisation procedure. The right-hand side of Eq. (6.4) can be interpreted as the selfenergy of the molecules $\hbar\Sigma_{\rm m}(E)$. The divergence in the selfenergy is energy-independent and is related to an ultraviolet divergence that comes about because we have used pseudopotentials. To deal with this divergence we have to use the renormalized detuning instead of the bare detuning. The former is defined as $\delta = \delta_B - \lim_{r\downarrow 0}mg^2/2\pi\hbar^2 r$, where $\delta = \Delta\mu(B - B_0)$ is determined by the experimental value of the magnetic field B_0 at resonance. Note that, as expected, the required subtraction is exactly equal to the one needed in the absence of the optical lattice. In the latter case we have to subtract $2g^2\int d\mathbf{k}\, m/\hbar^2\mathbf{k}^2(2\pi)^3$ [76, 77], which can be interpreted as $\delta = \delta_{\rm B} - \lim_{\mathbf{r}\downarrow 0}2g^2\int d\mathbf{k}\, e^{i\mathbf{k}\cdot\mathbf{r}}m/\hbar^2\mathbf{k}^2(2\pi)^3$.
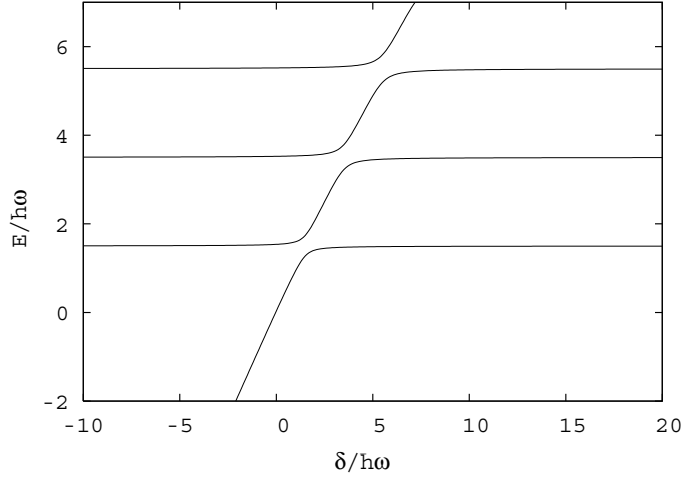
Figure 6.1: The relative energy levels of the atom-molecule system as a function of the detuning δ. This figure was calculated for $g^2/\sqrt{2}\pi l^3(\hbar\omega)^2 = 0.1$

In this manner we obtain the relative energy levels of the dressed molecules as a function of the experimental detuning that is shown in Fig. 6.1.

From this figure we see that for very negative detuning the molecular state lies below the ground-state of the on-site microtrap and the bound-state energy is well approximated by the detuning. As it approaches the ground-state level of the trap there is an avoided crossing and as a result the lowest trap state is shifted upward. If the avoided crossings between the molecular level and subsequent trap states do not strongly overlap, the system can be well described by considering only the lowest trap state. The overlap between the avoided crossings is determined by the strength of the atom-molecule coupling and can be neglected if $g^2/\sqrt{2}\pi l^3(\hbar\omega)^2 \ll 1$. In this paper we restrict ourselves to a single-band approximation, although the generalization to the multi-band situation is straightforward. This means that we only take into account the wavefunctions of the molecular state and the ground state of the on-site microtrap. In that case only two energy levels are of importance when there are two atoms on a lattice site. We denote these levels by $\epsilon_\uparrow$ and $\epsilon_\downarrow$ and their behaviour as a function of detuning is shown in Fig. 6.2.

The effective atom-molecule coupling in the optical lattice is given by $g' = g(\int d\mathbf{x}|\psi_0(\mathbf{x})|^4)^{1/2} = g/(2\pi l^2)^{3/4}$, where $\psi_0(\mathbf{x})$ is the Wannier function in the lowest band of the optical lattice. The effective atom-atom interaction is now given by $U_{\text{eff}} = U_{\text{bg}} - 2(g')^2/(\delta - 3\hbar\omega/2)$, where the background on-site interaction strength $U_{\text{bg}} = \left(4\pi a_{\text{bg}}\hbar^2/m\right)\int d\mathbf{x}|\psi_0(\mathbf{x})|^4 = \sqrt{2/\pi}\hbar\omega\,(a_{\text{bg}}/l)$. It is interesting to note that in order for the single-band approximation to be valid we do not need

82

to have that $U_{\text{eff}} \ll \hbar\omega$ because the on-site two-atom problem has been solved exactly. In Fig. 6.2 we also show a close-up of the avoided crossing and the wavefunction renormalisation factors Z_σ that give the amplitude of the closed channel part of the molecules in the state $|\psi_\sigma\rangle$. Explicitely, we thus have in the single-band approximation that

$$|\psi_\uparrow\rangle = \sqrt{Z_\uparrow}|\psi_{\text{m}}\rangle - \sqrt{1 - Z_\uparrow}|\psi_0\psi_0\rangle$$
$$|\psi_\downarrow\rangle = \sqrt{Z_\downarrow}|\psi_{\text{m}}\rangle + \sqrt{1 - Z_\downarrow}|\psi_0\psi_0\rangle. \qquad (6.5)$$

The probability Z_σ is determined by the selfenergy of the molecules through the relation $Z_\sigma = 1/(1 - \partial\hbar\Sigma_{\text{m}}(E)/\partial E)$ [74]. Note that in Fig. 6.2 the probability $Z_\uparrow$ already shows the effect of the avoided crossing at a detuning of about $3\hbar\omega$. As long as the single-band approximation is valid this will, however, not affect any of the results because the two-atom state that is involved in this avoided crossing will not be populated.

Combining the above we thus find a generalized Hubbard Hamiltonian that is given by

$$\begin{aligned}
H &= -t_a \sum_{\langle i,j \rangle} a_i^\dagger a_j - t_m \sum_\sigma \sum_{\langle i,j \rangle} b_{i,\sigma}^\dagger b_{j,\sigma} \\
&\quad + \sum_\sigma \sum_i (\epsilon_\sigma - 2\mu)\, b_{i,\sigma}^\dagger b_{i,\sigma} + \sum_i (\epsilon_{\text{a}} - \mu) a_i^\dagger a_i \\
&\quad + \frac{U_{\text{bg}}}{2} \sum_i a_i^\dagger a_i^\dagger a_i a_i + g' \sum_\sigma \sum_i \sqrt{Z_\sigma} \left(b_{i,\sigma}^\dagger a_i a_i + a_i^\dagger a_i^\dagger b_{i,\sigma} \right). \qquad (6.6)
\end{aligned}$$

Here t_a and t_m are the tunneling amplitudes for the atoms and the molecules, respectively, and $\langle i,j \rangle$ denotes a sum over nearest neighbours. The operators $a_i^\dagger$, a_i correspond to the creation and annihilation operators of a single atom at site i respectively. The operators $b_{i,\sigma}^\dagger$, $b_{i,\sigma}$ correspond to the creation and annihilation operators of the dressed molecules at site i respectively. Also $\epsilon_{\text{a}} = 3\hbar\omega/2$ is the on-site energy of a single atom. In the tight-binding limit the hopping amplitudes can be conveniently expressed in terms of the lattice parameters as [78]

$$t_{\text{a,m}} = \frac{\hbar\omega}{2} \left[1 - \left(\frac{2}{\pi}\right)^2 \right] \left(\frac{\lambda}{4l_{\text{a,m}}} \right)^2 e^{-(\lambda/4l_{\text{a,m}})^2}. \qquad (6.7)$$

Here λ is the wavelength of the light used to create the optical lattice and $l_{\text{m}}\sqrt{2} = l_{\text{a}} = l$. Note that, as expected, we have that $t_{\text{m}} \propto t_{\text{a}}^2/\hbar\omega \ll t_{\text{a}}$. Note also that our harmonic approximation to the on-site potential in principle slightly underestimates the hopping parameter. A more accurate determination of these parameters would involve the calculation of the appropriate Wannier functions. The chemical potential μ is added because we perform our next calculations in the grand-canonical ensemble.
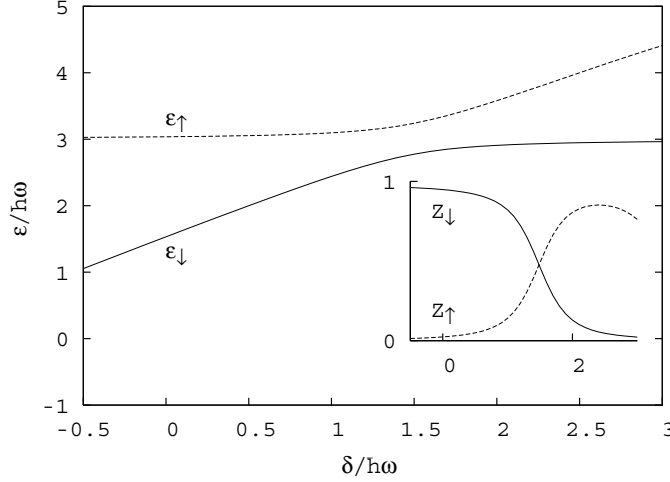
Figure 6.2: Details of the physical content of our theory. We show the avoided crossing between the molecular level and the lowest two-atom trap state. The inset shows the probability Z_σ as a function of the detuning δ. This figure was calculated for $g^2/\sqrt{2}\pi l^3(\hbar\omega)^2 = 0.1$ Note that the center of mass contribution to the energy has been taken into account here.

6.3   Phase diagram.

To find the mean-field phase diagram of a Bose gas in an optical lattice, we consider at sufficiently negative detuning the phase with only a Bose-Einstein condensate of molecules and perform a quadratic expansion of the Hamiltonian in the fluctuations of the molecular annihilation operator $b_{\mathbf{k},\sigma}$ around the nonzero expectation value $\langle b_{\mathbf{k},\sigma}\rangle = \sqrt{n_{\mathrm{mc}}}\delta_{\mathbf{k},\mathbf{0}}\delta_{\sigma,\downarrow}$. The effective Hamiltonian is then diagonalized by a Bogoliubov transformation and from the result we determine the equation of state of the gas as a function of the detuning δ and the temperature $T \equiv 1/k_B\beta$. For the equation of state for the total filling fraction we find (cf. Ref. [74]) $n = n_{\mathrm{a}} + 2\sum_\sigma n_{\mathrm{m}}^\sigma$ with the molecular filling fractions obeying

$$
\begin{aligned}
n_{\mathrm{m}}^\downarrow &= n_{\mathrm{mc}} + \frac{1}{N_s}\sum_{\mathbf{k}\neq\mathbf{0}}\frac{1}{e^{\beta\hbar\omega_{\mathbf{k},\downarrow}}-1},\\
n_{\mathrm{m}}^\uparrow &= \frac{1}{N_s}\sum_{\mathbf{k}}\frac{1}{e^{\beta\hbar\omega_{\mathbf{k},\uparrow}}-1},
\end{aligned}
\tag{6.8}
$$

84

and the atomic filling fraction

$$n_{\mathrm{a}} = \frac{1}{N_s} \sum_{\mathbf{k}} \left\{ \frac{2\epsilon_{\mathbf{k}}^{\mathrm{a}} - \epsilon_{\mathrm{m}}}{2\hbar\omega_{\mathbf{k}}} \frac{1}{e^{\beta\hbar\omega_{\mathbf{k}}} - 1} \right.$$
$$\left. + \frac{2\epsilon_{\mathbf{k}}^{\mathrm{a}} - \epsilon_{\mathrm{m}} - 2\hbar\omega_{\mathbf{k}}}{4\hbar\omega_{\mathbf{k}}} \right\} . \tag{6.9}$$

Moreover, we have that N_s is the total number of sites in the lattice, $\epsilon_{\mathbf{k}}^{\mathrm{a}} = -2t_{\mathrm{a}} \sum_{j=1}^{3} \cos\left(k_j \lambda/2\right) + \epsilon_{\mathrm{a}}$, $\epsilon_{\mathbf{k},\sigma}^{\mathrm{m}} = -2t_{\mathrm{m}} \sum_{j=1}^{3} \cos\left(k_j \lambda/2\right) + \epsilon_{\sigma}$, and $\hbar\omega_{\mathbf{k},\sigma} = \epsilon_{\mathbf{k},\sigma}^{\mathrm{m}} + \epsilon_{\mathrm{m}}$ is the molecular dispersion. Likewise we find that $\hbar\omega_{\mathbf{k}} = [(\epsilon_{\mathbf{k}}^{\mathrm{a}} - \epsilon_{\mathrm{m}}/2)^2 - 4g'^2 Z_{\downarrow} n_{\mathrm{mc}}]^{1/2}$ is the atomic Bogoliubov dispersion with $\epsilon_{\mathrm{m}} = \epsilon_{\downarrow} - zt_{\mathrm{m}}$ equal to twice the chemical potential and z is the number of nearest neighbours.

The critical temperature for the Bose-Einstein condensation of the molecules follows from the condition $n_{\mathrm{mc}} = 0$. The location of the Ising quantum phase transitions follows from the zero-momentum instability in the atomic Bogoliubov dispersion when the detuning $\epsilon_{\mathrm{m}} = -4g'\sqrt{Z_{\downarrow}}\sqrt{n_{\mathrm{mc}}} + 2\epsilon_{\mathrm{a}} - 2zt_{\mathrm{a}}$. In Fig. 6.3a we show the results for this condition as a function of the total filling fraction and detuning. Note that in the limit of vanishing density the quantum critical point is determined by the ideal gas condition for Bose-Einstein condensation, i.e., $\mu = \epsilon_{\mathrm{m}}/2 = \epsilon_{\mathrm{a}} - zt_{\mathrm{a}}$. From this condition it follows that for low enough filling fractions the location of the quantum phase transition shifts to higher detuning with increasing strength of the atom-molecule coupling. On the other hand at large negative detuning a larger value of the atom-molecule coupling implies a larger quantum depletion and hence a smaller molecular condensate fraction. This effect shifts the Ising transition to lower detuning.

For completeness we would like to point out that at $n = 1$ the phase diagram can also contain a Mott-insulator phase [80]. This phase can occur at sufficiently large positive detuning such that $U_{\mathrm{eff}}/zt_{\mathrm{a}} \geq 3 + 2\sqrt{2}$ [78, 79]. In contrast to the quantum Ising transition, this transition has already been observed experimentally by Greiner *et al.* [10] after the theoretical prediction by Jaksch *et al.* [81]. Its existence does not rely on the presence of the Feshbach resonance and we, therefore, have not included it in the phase diagram in Fig. 6.3. It is important to realize that this Mott insulator can only exist for repulsive interactions between the atoms, which requires U_{bg} to be positive.

6.4   Conclusions and discussion.

In summary, we have shown how to determine the microscopic parameters of the generalized Hubbard model in Eq.(6.6) that describes the physics of resonantly-interacting atoms in an optical lattice, using the experimentally known parameters of the Feshbach resonance in the absence of the optical lattice. As an application
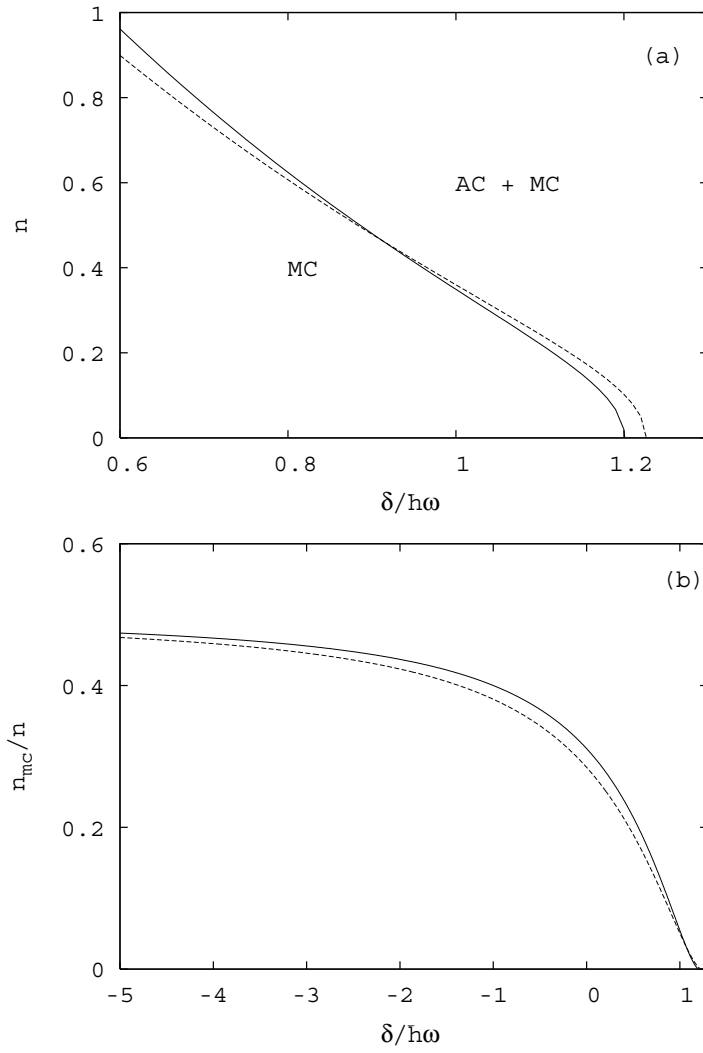
Figure 6.3: Zero temperature phase diagram as a function of the filling fraction per site and the detuning δ in units of $\hbar\omega$. The different curves that separate the MC and the AC+MC phases correspond to values of $g'/\hbar\omega = 0.10$ (full curve) and $g'/\hbar\omega = 0.12$ (dashed curve) respectively. In both cases we have taken ω to be 10^4 rad/s.

we also calculated the zero-temperature phase diagram of an atomic Bose gas in an optical lattice in the single-band approximation. By using an optical lattice one can suppress three-body recombination processes that lead to a fast decay of the molecular condensate.

For the single-band approximation to be valid the atom-molecule coupling constant g has to be small enough such that the avoided crossings between subsequent bands do not overlap with each other. In some cases, however, this coupling constant can be too large for realistic conditions and the single-band approximation will not hold anymore. In those cases we have to include higher-lying two-atom states. To avoid this complication the atom-molecule coupling g can be made smaller by using a more narrow Feshbach resonance or by using two-photon Raman transitions to convert atoms into molecules [82]. Inclusion of higher-lying two-atom states is, however, easily achieved in our theory by adding more atomic and molecular states into the generalized Hubbard model. In principle, we have to add several dressed molecular states $|\psi_\sigma\rangle$ for each additional atomic band that is required for a sufficiently accurate description of the atomic gas in the optical lattice. More precisely, for M atomic bands we need to include $M^2 + 1$ dressed molecular states into the theory.

Chapter 7

Quantum phases in a resonantly-interacting Bose-Fermi mixture

ABSTRACT

We consider a resonantly-interacting Bose-Fermi mixture of ^{40}K and ^{87}Rb atoms in an optical lattice. We show that by using a red-detuned optical lattice the mixture can be accurately described by a generalized Hubbard model for ^{40}K and ^{87}Rb atoms, and ^{40}K-^{87}Rb molecules. The microscopic parameters of this model are fully determined by the details of the optical lattice and the interspecies Feshbach resonance in the absence of the lattice. We predict a quantum phase transition to occur in this system already at low atomic filling fraction, and present the phase diagram as a function of the temperature and the applied magnetic field.

7.1 Introduction.

In the last few years experiments have shown that it is possible to realize a quantum degenerate gas of fermionic atoms [4]. Combining such a degenerate Fermi gas with a Bose-Einstein condensate of atoms, it is also possible to obtain a quantum degenerate Bose-Fermi mixture [83], thus creating a dilute analog of the liquid

^{3}He-^{4}He mixture. The recent observation of interspecies Feshbach resonances in a Bose-Fermi mixture [38, 39] opens up even richer physics, as this couples the fermionic and bosonic atoms to a third species, namely the fermionic heteronuclear molecules. An interesting aspect of the resonantly-interacting mixture that we address in much more detail in the following, is the possibility to reversibly destroy a Bose-Einstein condensate of atoms, by associating the bosonic atoms into fermionic molecules and thus creating a degenerate Fermi gas of dipolar particles. Moreover, the Bose-Einstein condensed phase is very interesting by itself because it contains a macroscopic quantum coherence between the fermionic atoms and molecules. However, in experiments with magnetic or optical traps the molecules quickly decay due to inelastic atom-molecule and molecule-molecule collisions [75]. By loading the degenerate Bose-Fermi mixture into an optical lattice with a total filling factor less then unity, these collisions can be prevented and the lifetime of the molecules is expected to be dramatically enhanced.

Bose-Fermi mixtures in an optical lattice, but in the absence of an interspecies Feshbach resonance, have been the subject of active theoretical investigation lately. In particular, domain boundaries due to a trapping potential [84], lattice symmetry breaking [85], the existence of quantum phases that involve the pairing of fermions with bosons [86], and also unconventional fermion pairing [87, 88] have been predicted. It is the main objective of this Letter to generalize these studies to the case of a resonantly-interacting Bose-Fermi mixture. Although our theoretical methods are very general, we consider as a concrete example a mixture of fermionic ^{40}K atoms and the bosonic ^{87}Rb atoms, as this system is now becoming available experimentally [89, 90]. A gas consisting of these two atoms is especially promising as their wavelength is relatively close and readily accessible using Ti:Sapphire lasers. Furthermore, the mass of ^{40}K is much larger than the mass of the other experimentally available fermionic atom ^{6}Li, which makes it much easier to trap this species in an optical lattice.

In order to analyze the properties of a resonantly-interacting Bose-Fermi mixture most easily, it is convenient to assume that all the species in the optical lattice, i.e., the fermionic atoms, the bosonic atoms, and the fermionic molecules, experience the same on-site trapping frequency. Because the potassium atoms are lighter than the rubidium atoms, the potential for the former should thus be less deep than that for the latter. Moreover, as is shown in the inset of Fig. 7.1, both the D1 and D2 lines of potassium are blue compared to the D1 and D2 lines of rubidium. As a result equal on-site trapping frequencies can only be achieved in an optical lattice that is red detuned with respect to all these four transitions. Making use of the fact that the hyperfine structure of the atoms is no longer resolved for the detunings used in optical lattice experiments [40], we have calculated the ratio of the two on-site trapping frequencies as a function of the wavelength of the lattice laser. As can be seen from Fig. 7.1, using a wavelength of 806 nm, ensures that the trapping frequencies for both atomic species are the same. In princi-

ple the polarizability of the molecule is not known. However, recent experiments have shown that for homonuclear molecules, the resulting trap frequency for the molecules is almost the same as that of the atoms [82]. In the following, we make the reasonable assumption that this also holds for the vibrationally highly excited heteronuclear ^{40}K-^{87}Rb molecules of interest to us.

For the particular detuning given above, the on-site trapping frequency is related to the Rabi frequency Ω of the lattice laser by $\omega \equiv \omega_F = \omega_B = 2.1 \cdot 10^{-5}\,\Omega$. Having to use a red-detuned optical lattice has the disadvantage that the atoms are trapped in the light and not in the dark, which in principle results in a larger decay due to spontaneous emission. We have therefore also calculated this emission rate and find that $\Gamma/\Omega^2 = 1.9 \cdot 10^{-21}$ s for the optimal wavelength. The lifetime is always longer than one second for Rabi frequencies less than 4 GHz $(8\pi \cdot 10^9$ rad/s) and spontaneous emission can then be safely neglected.
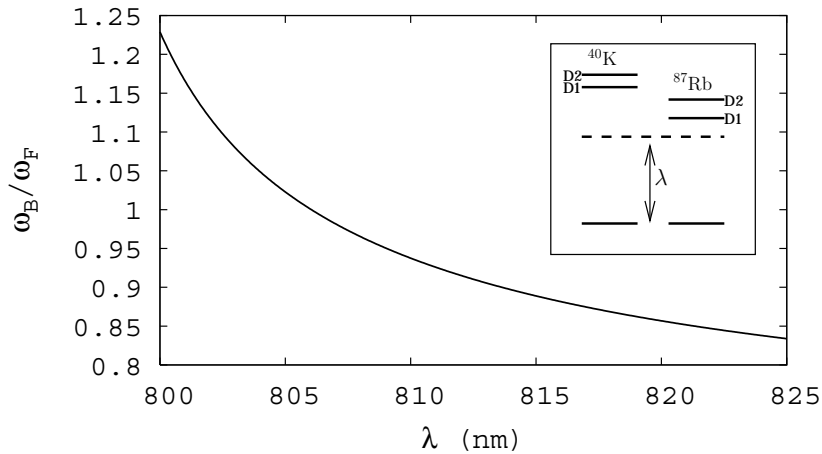

Figure 7.1: Ratio of the on-site trap frequencies of the boson ^{87}Rb and the fermion ^{40}K, as a function of the lattice laser wavelength. The inset shows the fine-structure levels of the two atomic species.

7.2 Generalized Hubbard model.

We now consider the many-body aspects of the Bose-Fermi mixture near a Feshbach resonance. We consider a mixture of ^{40}K and ^{87}Rb that is loaded into a three-dimensional and cubic optical lattice that is sufficiently deep, so that we are allowed to use a tight-binding approximation for the band structure of the single-particle states. Experimentally this requires the Rabi frequency of the lattice laser to be larger than about 1 GHz. For the reasons mentioned above, we consider only

low filling fractions, which limits the maximum number of atoms on a single site. As a result, we can neglect atom-molecule and molecule-molecule interactions. Furthermore, for low filling fractions there is also no problem of phase separation of the atomic Bose-Fermi mixture [91] and it is justified to neglect possible Mott physics in the mixture [80, 92].

Under these conditions we have recently derived the theory for resonantly-interacting ultracold atomic gases in an optical lattice [93]. Within this theory the two-body Feshbach problem at a single site is solved exactly, which physically leads to a dressing of the molecules and to various avoided crossings in the on-site energy levels of two atoms $\epsilon_\sigma(B)$ as the magnetic field B is swept through the Feshbach resonance. After having solved the on-site problem, the various hopping parameters can be calculated in the tight-binding approximation. In this manner the microscopic parameters of the generalized Hubbard model that describes the Bose-Fermi mixture near the Feshbach resonance are completely determined by the details of the optical lattice potential and the experimentally known parameters of the Feshbach resonance in the absence of the optical lattice. Ultimately, the mixture is described by the following effective Hamiltonian,

$$
\begin{aligned}
H = & -t_{\mathrm{F}} \sum_{\langle i,j \rangle} c_i^\dagger c_j - t_{\mathrm{B}} \sum_{\langle i,j \rangle} a_i^\dagger a_j - t_{\mathrm{m}} \sum_\sigma \sum_{\langle i,j \rangle} b_{i,\sigma}^\dagger b_{j,\sigma} \\
& + \sum_i \left(\epsilon_{\mathrm{a}} - \mu_{\mathrm{F}} \right) c_i^\dagger c_i + \sum_i \left(\epsilon_{\mathrm{a}} - \mu_{\mathrm{B}} \right) a_i^\dagger a_i \\
& + \sum_\sigma \sum_i \left(\epsilon_\sigma - \mu_{\mathrm{F}} - \mu_{\mathrm{B}} \right) b_{i,\sigma}^\dagger b_{i,\sigma} + \frac{U^{\mathrm{BB}}}{2} \sum_i a_i^\dagger a_i^\dagger a_i a_i \\
& + U_{\mathrm{bg}}^{\mathrm{BF}} \sum_i a_i^\dagger c_i^\dagger c_i a_i + g' \sum_\sigma \sum_i \sqrt{Z_\sigma} \left(b_{i,\sigma}^\dagger c_i a_i + a_i^\dagger c_i^\dagger b_{i,\sigma} \right).
\end{aligned}
$$

$$(7.1)$$

Here t_{F}, t_{B} and t_m are the tunneling or hopping amplitudes for the fermionic atoms, the bosonic atoms, and the fermionic molecules, respectively. The symbol $\langle i,j \rangle$ denotes a sum over nearest neighbors. The operators $c_i^\dagger$, c_i and $a_i^\dagger$, a_i correspond to the creation and annihilation operators of a single fermionic and bosonic atom at site i, respectively. The operators $b_{i,\sigma}^\dagger$, and $b_{i,\sigma}$ correspond to the creation and annihilation operators of the various dressed molecules at site i that are enumerated by the index σ. Also $\epsilon_{\mathrm{a}} = 3\hbar\omega/2$ is the on-site energy of a single atom. The on-site interaction between two bosons is given by U^{BB}, and $U_{\mathrm{bg}}^{\mathrm{BF}}$ denotes the on-site background interaction between the bosons and the fermions. In the tight-binding limit the hopping amplitudes are for our purposes sufficiently

accurately determined in terms of the lattice parameters by [78]

$$t_\nu = \frac{\hbar\omega}{2}\left(1 - \left(\frac{2}{\pi}\right)^2\right)\left(\frac{\lambda}{4l_\nu}\right)^2 e^{-(\lambda/4l_\nu)^2}. \tag{7.2}$$

Here ν distinguishes the different species in the mixture, i.e., $\nu = $ F for the fermionic atoms, $\nu = $ B for the bosonic atoms, and $\nu = $ m for the molecules. Moreover, λ is the wavelength of the light used to create the optical lattice, and the harmonic oscillator lengths obey $l_\nu = \sqrt{\hbar/m_\nu\omega}$, where m_F, m_B, and $m_m = m_F + m_B$ are the masses of the fermions, bosons, and molecules, respectively. Note that because of the higher mass of the molecules and the desired validity of the tight-binding approximation, we have in general that $t_m \ll t_{F,B} \ll \hbar\omega$. We have also introduced a chemical potential for each atomic species, since it is experimentally possible to control both the filling fraction of the fermions as well as the bosons in the mixture.

Sufficiently close to resonance we can always neglect the on-site interactions U^{BB} and U^{BF}_{bg} compared to the resonant atom-molecule interaction. The strength of the atom-molecule coupling in the lattice is given by $g' = g/(\pi(l_B^2 + l_F^2))^{3/4}$, where $g = \hbar\sqrt{4\pi a_{bg}\Delta\mu\Delta B/m_r}$ is the bare atom-molecule coupling without the lattice and $m_r = m_F m_B/(m_F + m_B)$ is the reduced mass. For the ^{40}K-^{87}Rb mixture with potassium in the hyperfine state $|9/2, -9/2\rangle$ and rubidium in the hyperfine state $|1, 1\rangle$ there occurs a Feshbach resonance at $B_0 = 510$ Gauss for which the parameters that determine g are given by the background scattering length $a_{bg} = 150\ a_0$ and the width of the resonance $\Delta B = 1$ Gauss [38, 94]. The difference in magnetic moments $\Delta\mu$ is equal to $29/22$ Bohr magneton in that case. In Fig. 7.2 we show a close-up of the avoided crossing and the wavefunction renormalisation factors Z_σ that give the probability for the dressed molecules to be in the bare molecular state of this Feshbach resonance. The probability Z_σ is determined by the self-energy of the molecules $\hbar\Sigma_m(E) = (g^2/\pi l_r^3\hbar\omega) \cdot \Gamma(-E/2\hbar\omega + 3/4)/\Gamma(-E/2\hbar\omega + 1/4)$, with $\Gamma(z)$ the gamma function, through the relation $Z_\sigma = 1/(1 - \partial\hbar\Sigma_m(E)/\partial E)$ [93]. Note that in Fig. 7.2 the sum of the probabilities $Z_\downarrow + Z_\uparrow$ does not add up to one. This means that for this relatively broad interspecies Feshbach resonance a single-band approximation is not valid to determine the dressed molecular wavefunctions. However, a single-band approximation in terms of dressed molecules is always possible for the low filling fractions of interest to us, because the higher-lying on-site dressed molecular states will not be populated as we show now.

7.3   Phase diagram.

With the above formalism we next determine the phase diagram for the ^{40}K and ^{87}Rb mixture. For simplicity we consider only equal densities for both atomic
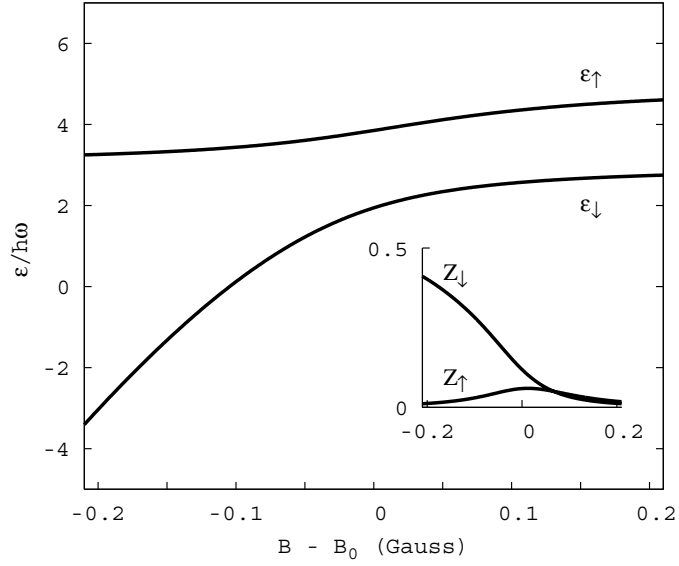
Figure 7.2: Details of the physical content of our theory. We show the avoided crossing between the bare molecular level and the lowest two-atom trap state, which results in two dressed molecular states denoted by $|\downarrow\rangle$ and $|\uparrow\rangle$. The inset shows the probability Z_σ as a function of the magnetic field. This figure was calculated for the ^{40}K - ^{87}Rb mixture with $\lambda = 806$ nm and $\Omega/2\pi = 1$ GHz.

94

species, although the generalization is immediate. We mentioned already that we consider a deep optical lattice for which the hopping strengths of the atoms are small with respect to the level splitting in the on-site microtrap realized by the optical lattice. The hopping strength of the molecules can be completely neglected in this limit and consequently the band-structure for the molecules is essentially flat. At zero temperature the energy $\epsilon_\downarrow$ of the lowest molecular state can, depending on the magnetic field, be either smaller or larger than the sum of the lowest atomic energy levels. As a result, the ground state is either a Fermi sea of ^{40}K - ^{87}Rb molecules, or a Fermi sea of ^{40}K atoms and a Bose-Einstein condensate of ^{87}Rb atoms. Because of the different symmetries of these ground states there exists a quantum phase transition between these two states that breaks a $U(1)$ symmetry and is in the same universality class as the XY model with dynamical exponent $z = 2$. In the following, we calculate the phase diagram as a function of total filling fraction and temperature by performing a mean-field analysis of the normal state of the Hamiltonian in Eq. (7.1).

For the equation of state for the total filling fraction we find always that $n = n_{\mathrm{F}} + n_{\mathrm{B}} + 2\sum_\sigma n_{\mathrm{m},\sigma}$. In the normal state no condensate exists and the molecular and atomic filling fractions obey $n_{\mathrm{m},\sigma} = (1/N_s)\sum_{\mathbf{k}}(e^{\beta\hbar\omega_{\mathbf{k},\sigma}} + 1)^{-1}$, and $n_{\mathrm{F,B}} = (1/N_s)\sum_{\mathbf{k}}(e^{\beta\hbar\omega_{\mathbf{k},\mathrm{F,B}}} \pm 1)^{-1}$, where $\hbar\omega_{\mathbf{k},\sigma} = \epsilon_{\mathbf{k},\sigma} - (\mu_{\mathrm{F}} + \mu_{\mathrm{B}})$ is the molecular dispersion. The dispersion relations for the fermionic and bosonic atoms are given by $\hbar\omega_{\mathbf{k},\mathrm{F}} = \epsilon_{\mathbf{k},\mathrm{F}} - \mu_{\mathrm{F}}$ and $\hbar\omega_{\mathbf{k},\mathrm{B}} = \epsilon_{\mathbf{k},\mathrm{B}} - \mu_{\mathrm{B}}$, respectively. Here $\epsilon_{\mathbf{k},\mathrm{F,B}} = -2t_{\mathrm{F,B}}\sum_{j=1}^{3}\cos{(k_j\lambda/2)} + \epsilon_{\mathrm{a}}$ for the atoms and $\epsilon_{\mathbf{k},\sigma} = \epsilon_\sigma$ for the molecules. The number of sites on the lattice is N_s. We have seen that at zero temperature there is a quantum phase transition between a phase where the ^{87}Rb atoms are Bose-Einstein condensed and a phase with only a Fermi sea of molecules. The quantum critical point is determined by the ideal gas condition for Bose-Einstein condensation, i.e., $\epsilon_\downarrow = 2\epsilon_{\mathrm{a}} - 6(t_{\mathrm{B}} + t_{\mathrm{F}})$. In the approximation that we can neglect the hopping of the molecules, their band structure is flat and the quantum critical point is independent of the filling fraction of the molecules. Including the molecular band structure would lead to a critical magnetic field that slowly shifts to lower magnetic fields as the density increases. At nonzero temperatures we can also determine the critical temperature as a function of the detuning and the total filling fraction from the equation of state. The critical surface in Fig. 7.3 shows how at constant total atomic filling fraction the critical temperature depends on the magnetic field. For large enough magnetic fields there are no molecules and the critical temperature is determined for low densities by the critical temperature of an ideal gas, which is proportional to $n^{2/3}$. Note that the critical temperature always obeys $T_c \ll \hbar\omega/k_B$, which *a posteriori* shows that a single-band approximation for the dressed molecules is indeed consistent.
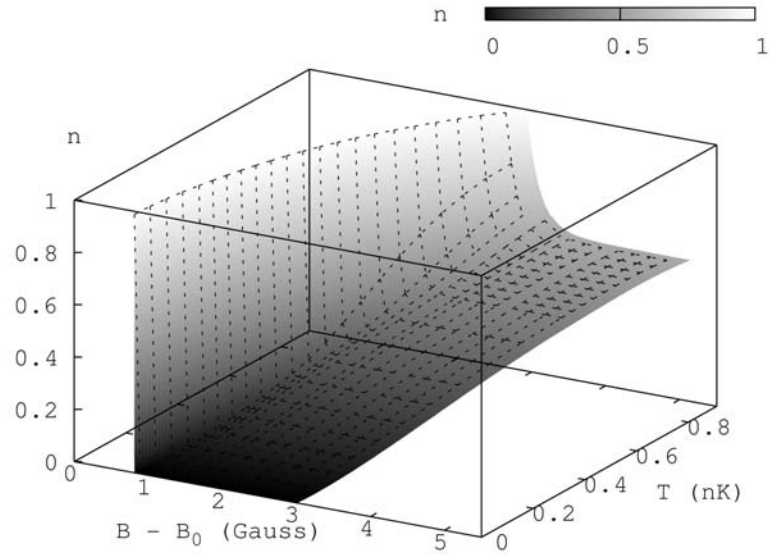
Figure 7.3: Critical surface of the ^{40}K and ^{87}Rb mixture as a function of the total filling fraction, magnetic field and temperature. This figure was calculated for the ^{40}K - ^{87}Rb mixture with $\lambda = 806$ nm and $\Omega/2\pi = 1$ GHz.

7.4 Conclusions and Discussion.

In summary we have shown that by using a red-detuned optical lattice with a wavelength of 806 nm the Bose-Fermi mixture of ^{40}K and ^{87}Rb atoms can be accurately described by a generalized Hubbard model. Moreover, we have shown that the model contains a quantum phase transition associated with the Bose-Einstein condensation of rubidium. To facilitate the quantitative analysis we have considered the case of equal trapping frequencies for both atomic species. However, the quantum phase transition exists independently of this assumption. Interestingly, the presence of a Bose-Einstein condensate induces also a macroscopic coherence between the fermionic atoms and molecules, because of the specific form of the atom-molecule coupling near a Feshbach resonance. What is especially interesting is that such a coherence cannot be obtained by solely making use of lasers in this case because it involves a quantum coherence between two different species. It would, therefore, be very exciting to observe Rabi oscillations between fermionic atoms and molecules by an appropriate manipulation of the atomic Bose-Einstein condensate density.

Using the known atomic physics of the Feshbach resonance to determine the parameters in the generalized Hubbard Hamiltonian we have calculated the phase diagram for low filling fractions as a function of the applied magnetic field and temperature. Our analysis of the quantum phases of a resonantly-interacting Bose-Fermi mixture has been based on mean-field theory. In particular, this implies that we have not considered the attractive finite-range interaction between the fermionic atoms that can be mediated by density fluctuations in the Bose-Einstein condensate [95, 96]. In principle this mechanism can lead to a BCS pairing between the fermionic atoms. However, for the spin-polarized mixture discussed here this pairing must take place in a p-wave channel, which is expected to have a very small critical temperature at small filling fractions. We, therefore, do not consider this interesting possibility in detail here and leave that to future investigations.

Chapter 8

Feshbach molecules in a one-dimensional Fermi gas

—————— ABSTRACT

We consider the binding energy and the wave function of Feshbach molecules confined in a one-dimensional matter waveguide. We compare the binding energy with the experiment of Moritz *et al.* [97] and find excellent agreement for the full magnetic field range explored experimentally.

8.1   Introduction

In a beautiful experiment Moritz *et al.* recently reported the observation of two-particle bound states of ^{40}K confined in a one-dimensional matter waveguide [97]. In the experiment an array of equivalent one-dimensional quantum systems is realized by trapping a mixture of two hyperfine states of ^{40}K atoms in a two-dimensional optical lattice. The atoms are trapped at the intensity maxima and the radial confinement is only a fraction of the lattice period. At a given value of the magnetic field the binding energy E_B of the bound states is probed by radio-frequency spectroscopy.

Although Moritz *et al.* realized its limitations, the description of the experiment makes use of a single-channel model of radially confined atoms interacting with a pseudopotential [47, 98]. Within this model the bound-state energy E_B is

related to the s-wave scattering length a of the atoms by

$$\frac{a}{a_\perp} = -\frac{\sqrt{2}}{\zeta(1/2, 1/2 - E_B/2\hbar\omega_\perp)}, \tag{8.1}$$

where $a_\perp = \sqrt{\hbar/m\omega_\perp}$, m is the atomic mass, and $\omega_\perp$ is the radial trapping frequency. To vary the scattering length, however, the experiment makes use of a Feshbach resonance at a magnetic field of $B_0 = 202.1$ Gauss. For such a Feshbach resonance a two-channel approach is physically more realistic.

For the Feshbach problem the molecular binding energy E_B always satisfies the equation [76],

$$E_B - \delta(B) = \hbar\Sigma(E_B). \tag{8.2}$$

Here the detuning $\delta(B) = \Delta\mu(B-B_0)$ varies as a function of the magnetic field and depends on the difference in magnetic moments $\Delta\mu$ between the open and closed channels in the Feshbach problem. The resonance is located at the magnetic field strength B_0. For the homogeneous Fermi gas the molecular self-energy is given by [76]

$$\hbar\Sigma(E) = -\left(\frac{g^2 m^{3/2}}{4\pi\hbar^3}\right)\frac{i\sqrt{E}}{1 - i|a_{\text{bg}}|\sqrt{mE/\hbar^2}}, \tag{8.3}$$

which leads to corrections to the single-channel result $-\hbar^2/ma^2$.

Here $g = \hbar\sqrt{4\pi a_{\text{bg}}\Delta B\Delta\mu/m}$ is the atom-molecule coupling, ΔB is the width of the Feshbach resonance, $\Delta\mu$ is the difference in magnetic moments, and a_{bg} is the background scattering length. In Fig. 8.1 we show for this three-dimensional case the molecular binding energy for both the single and two-channel approaches, respectively. Whereas the single-channel results deviate significantly from the experimental data, there is an excellent agreement with the two-channel theory. It is therefore *a priori* not clear that in the one-dimensional case the single-channel theory as given by Eq. (8.1) is sufficiently accurate for the full range of magnetic fields explored by the experiment. In the following we derive the self-energy for the confined case and make a comparison with the experimental data.

8.2 Theory

Two atoms in a waveguide near a Feshbach resonance are described by the following Hamiltonian,

$$H = H_{\text{a}} + H_{\text{m}} + V_{\text{am}}. \tag{8.4}$$

Here H_{a} represents the atomic contribution, H_{m} describes the bare molecules, and V_{am} is the atom-molecule coupling. Explicitly we have for the atoms,

$$H_{\text{a}} = \sum_{i=1,2}\left\{K_i + \frac{m\omega_\perp^2}{2}(x_i^2 + y_i^2)\right\} + V_{\text{aa}}\delta(\mathbf{r}), \tag{8.5}$$

with $K_i = -\hbar^2 \nabla_i^2 / 2m$ the kinetic energy of atom i, V_{aa} the strength of the nonres-
onant atom-atom interaction, and $\mathbf{r}$ the relative coordinate of the two atoms. The
atoms are coupled to a molecular channel with a coupling V_{am}. We show in Fig.
8.2 that near the resonance we have that $V_{\mathrm{aa}} \ll V_{\mathrm{am}}$, which allows us to neglect the
nonresonant atom-atom interaction in that case. Note that outside the magnetic
field range considered in Figs. 8.1 and 8.2 there are in principle corrections to
the molecular binding energy coming from the background atom-atom scattering.
For two atoms in the waveguide the two-channel Feshbach problem in the relative
coordinate, after splitting off the center-of-mass motion, is then given by,

$$\begin{pmatrix} H_0 & V_{\mathrm{am}} \\ V_{\mathrm{am}} & \delta_B \end{pmatrix} \begin{pmatrix} |\psi_{\mathrm{a}}\rangle \\ |\psi_{\mathrm{m}}\rangle \end{pmatrix} = E \begin{pmatrix} |\psi_{\mathrm{a}}\rangle \\ |\psi_{\mathrm{m}}\rangle \end{pmatrix}. \tag{8.6}$$

Here the atomic Hamiltonian is $H_0 = -\hbar^2 \nabla_{\mathbf{r}}^2 / m + m\omega_\perp^2 \mathbf{r}_\perp^2 / 4$, where $\nabla_{\mathbf{r}}^2 = \partial_\perp^2 + \partial_z^2$
and $\mathbf{r}_\perp$ is the radial component of $\mathbf{r}$. Only the relative part is relevant here, since
only this part contains the interaction between the atoms. The bare detuning is
denoted by δ_B. The eigenstates $|\psi_{n,k_z}\rangle$ of H_0 that are relevant for an s-wave Fesh-
bach resonance are a product state of a two-dimensional harmonic oscillator wave
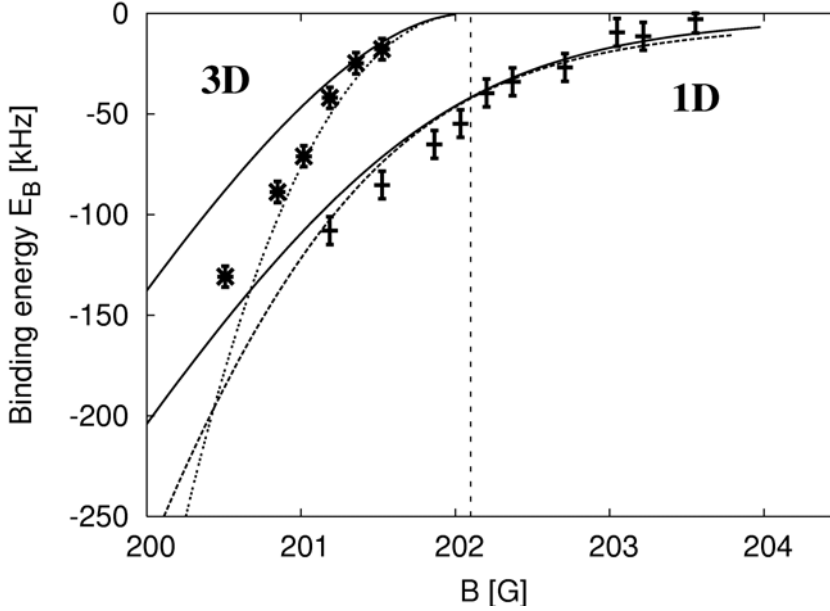

Figure 8.1: Binding energies for 1D and 3D molecules as a function of the magnetic
field. The solid lines correspond to the single-channel result. The dashed lines are
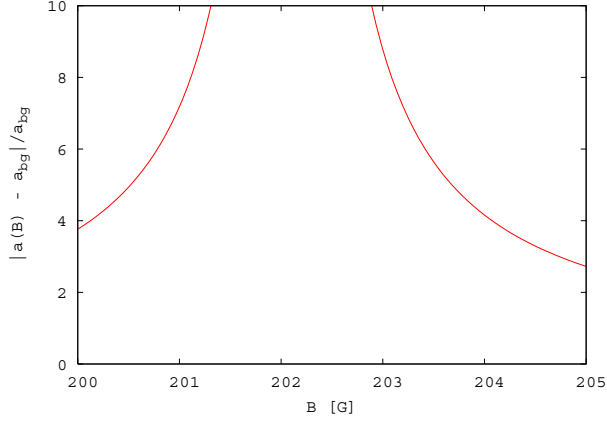calculated within the two-channel theory.

Figure 8.2: The ratio of the resonant part of the *s*-wave scattering length and the background scattering length a_{bg}.

function in the radial direction and a plane wave along the axial direction. The associated energies are given by $E_{n,k_z} = (2n+1)\hbar\omega_\perp + \hbar^2 k_z^2/m$. The eigenstates of the two-dimensional harmonic oscillator that are relevant for s-wave scattering can be written as $\psi_n(r_\perp,\phi) = \left(2\pi a_\perp^2\right)^{-1/2} e^{-r_\perp^2/4a_\perp^2} L_n^{(0)}(r_\perp^2/2a_\perp^2)$, where $L_n^{(0)}(x)$ is the generalized Laguerre polynomial and $\hbar\omega_\perp = \hbar^2/ma_\perp^2$. From Eq. (8.6) we obtain the following equation determining the binding energy of the molecules:

$$\langle\psi_{\mathrm{m}}|V_{\mathrm{am}}\frac{1}{E-H_0}V_{\mathrm{am}}|\psi_{\mathrm{m}}\rangle = E - \delta_B. \tag{8.7}$$

Using the above mentioned eigenstates of H_0, Eq. (8.7) can be written as

$$\sum_{n=0}^{\infty}\int \frac{dk_z}{2\pi}\,\frac{|\langle\psi_{\mathrm{m}}|V_{\mathrm{am}}|\psi_{n,k_z}\rangle|^2}{E - E_{n,k_z}} = E - \delta_B. \tag{8.8}$$

Using also the usual pseudopotential approximation for the atom-molecule coupling, we have that $\langle\mathbf{r}|V_{\mathrm{am}}|\psi_{\mathrm{m}}\rangle = g\delta(\mathbf{r})$. Substituting this and performing the k_z integration we obtain

$$
\begin{aligned}
E - \delta_B &= \lim_{r_\perp\downarrow 0}\frac{-g^2 m}{\sqrt{2}(4\pi a_\perp\hbar^2)} \\
&\quad\times \sum_{n=0}^{\infty}\frac{e^{-r_\perp^2/4a_\perp^2}\,L_n^{(0)}(r_\perp^2/2a_\perp^2)}{\sqrt{n+1/2-E/2\hbar\omega_\perp}}.
\end{aligned}
\tag{8.9}
$$

The inverse square root $1/\sqrt{n+1/2-E/2\hbar\omega_\perp}$ in the summand can be represented by the integral $(2/\sqrt{\pi})\int_0^\infty dt\, e^{-(n+1/2-E/2\hbar\omega_\perp)\,t^2}$. To evaluate the sum

102

over n we substitute the above integral representation. The dependence on n of the summand appears now in the exponent and in the degree of the Laguerre polynomial. As a result the sum can be directly evaluated by making use of the generating functions of the Laguerre polynomials,

$$\sum_{n=0}^{\infty} L_n^{(0)}(x) \, z^n = (1-z)^{-1} \exp\left(\frac{xz}{z-1}\right). \qquad (8.10)$$

In our case we have $z = e^{-t^2}$. Using this result and making the transformation $y = t^2$ we arrive at

$$
\begin{aligned}
E - \delta_B &= \lim_{r_\perp \downarrow 0} \frac{-g^2 m}{\sqrt{2\pi}(4\pi a_\perp \hbar^2)} \int_0^\infty \exp\left(\frac{r_\perp^2}{2a_\perp^2} \frac{e^{-y}}{e^{-y}-1}\right) \\
&\times \quad \frac{\exp\{-(1/2 - E/2\hbar\omega_\perp)\, y\}}{\sqrt{y}\,(1 - e^{-y})} \, dy
\end{aligned}
\qquad (8.11)
$$

For small values of y the integrand in the above equation behaves as $y^{-3/2} e^{-r^2/2y}$. Note that we have

$$\frac{1}{\sqrt{\pi}} \int_0^\infty dy \, y^{-3/2} e^{-r^2/2y} = \sqrt{2}/r. \qquad (8.12)$$

We add and subtract this integral from Eq. (8.11) and in doing so we explicitly split off the $1/r$ divergence from the sum. The divergence in the self-energy is energy independent and is related to the ultraviolet divergence that comes about because we have used pseudopotentials. To deal with this divergence we have to use the renormalized detuning instead of the bare detuning. The former is defined as $\delta = \delta_B - \lim_{r\downarrow 0} mg^2/4\pi\hbar^2 r$, where $\delta = \Delta\mu(B - B_0)$ is determined by the experimental value of the magnetic field B_0 at resonance and the magnetic moment difference $\Delta\mu = 16/9$ Bohr magneton for the ^{40}K atoms of interest. Note that, as expected, the required subtraction is exactly equal to the one needed in the absence of the optical lattice. In the latter case we have to subtract $g^2 \int d\mathbf{k} \, m/\hbar^2 \mathbf{k}^2 (2\pi)^3$ [76, 77], which can be interpreted as $\delta = \delta_B - \lim_{\mathbf{r}\downarrow 0} g^2 \int d\mathbf{k} \, e^{i\mathbf{k}\cdot\mathbf{r}} m/\hbar^2 \mathbf{k}^2 (2\pi)^3$. Using the renormalized detuning we find that the binding energy of the dressed molecules satisfies the desired equation

$$E_B - \delta(B) = \hbar\Sigma(E_B), \qquad (8.13)$$

where the molecular self-energy for the harmonically confined one-dimensional system is given by

$$\hbar\Sigma(E) = -\frac{mg^2}{\sqrt{2}\,(4\pi a_\perp \hbar^2)} \, \zeta(1/2, 1/2 - E/2\hbar\omega_\perp). \qquad (8.14)$$

103

8.3 Results and discussion

Using the self-energy for the confined gas we can now solve for the binding energy in Eq. (8.13). The result is also shown in Fig. 8.1. We find an improved description of the experiment, although the differences with the single-channel prediction are small near resonance and only become large for larger detunings. This presents one way in which to experimentally probe these differences. Alternatively, it is also possible to directly measure the bare molecule fraction Z of the dressed molecules [32], which is always equal to zero in the single-channel model. To be concrete we have for the dressed molecular wave function

$$|\psi_{\text{dressed}}\rangle = \sqrt{Z}|\psi_{\text{closed}}\rangle + \sqrt{1-Z}|\psi_{\text{open}}\rangle, \qquad (8.15)$$

where $|\psi_{\text{closed}}\rangle$ is the wave function of the bare molecules and $|\psi_{\text{open}}\rangle$ denotes the wave function of the atom pair in the open channel of the Feshbach resonance. With this application in mind we have plotted in Fig. 8.3 also the probability Z, which is determined from the above self-energy by $Z = 1/(1 - \partial\hbar\Sigma(E_B)/\partial E_B)$.
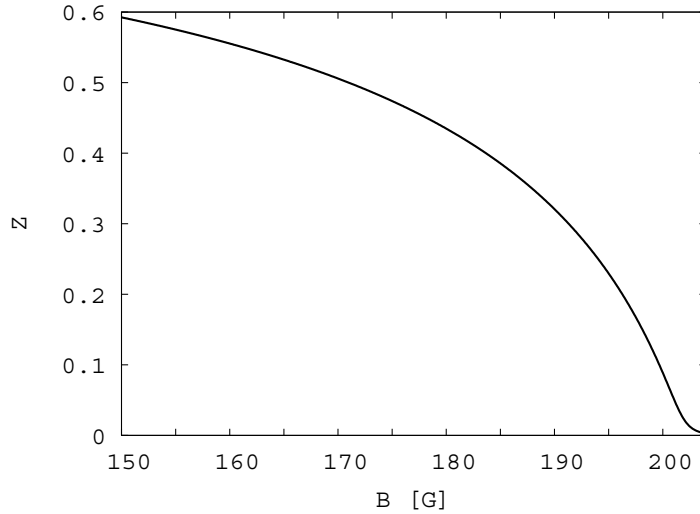

Figure 8.3: The bare molecule fraction Z as a function of the magnetic field.

Bibliography

[1] M. H. Anderson, J. R. Ensher, M. R. Matthews, C. E. Wieman, and E. A. Cornell, Science **269**, 198 (1995).

[2] C. C. Bradley, C. A. Sackett, J. J. Tollett, and R. G. Hulet, Phys. Rev. Lett. **75**, (1995); C. C. Bradley, C. A. Sackett, and R. G. Hulet, Phys. Rev. Lett. **78**, 985 (1997).

[3] K. B. Davis, M.-O. Mewes, M. R. Andrews, N. J. van Druten, D. S. Durfee, D. M. Kurn and W. Ketterle, Phys. Rev. Lett. **75**, 3969 (1995).

[4] B. DeMarco and D. S. Jin, Science **285**, 1703 (1999).

[5] F. Schreck, L. Khaykovich, K. L. Corwin, G. Ferrari, T. Bourdel, J. Cubizolles, and C. Salomon, Phys. Rev. Lett. **87**, 080403 (2001).

[6] A. Görlitz, J. M. Vogels, A. E. Leanhardt, C. Raman, T. L. Gustavson, J. R. Abo-Shaeer, A. P. Chikkatur, S. Gupta, S. Inouye, T. Rosenband, and W. Ketterle, Phys. Rev. Lett. **87**, 130402 (2001).

[7] Markus Greiner, Immanuel Bloch, Olaf Mandel, Theodor W. Hänsch, and Tilman Esslinger, Phys. Rev. Lett. **87**, 160405 (2001).

[8] For a review see, P.S. Jessen and I.H. Deutsch, Adv. At. Mol. Opt. Phys. **37**, 95 (1996).

[9] M. P. A. Fisher, P. B. Weichman, G. Grinstein, and D. S. Fisher, Phys. Rev. B **40**, 546 (1989).

[10] M. Greiner, O. Mandel, T. Esslinger, T. W. Hänsch, and I. Bloch, Nature **415**, 39 (2002).

[11] For a review see, J. J. Garcia-Ripoll, P. Zoller, J. I. Cirac, J. Phys. B: At. Mol. Opt. Phys. **38**, 567 (2005) and references therein.

[12] O. Mandel, M. Greiner, A. Widera, T. Rom, T. W. Hänsch, and I. Bloch, Phys. Rev. Lett. **91**, 10407 (2003).

[13] G. K. Brennen, C. M. Caves, P. S. Jessen, and I. H. Deutsch, Phys. Rev. Lett. **82**, 1060 (1999).

[14] D. Jaksch, H.-J. Briegel, J. I. Cirac, C. W. Gardiner, and P. Zoller, Phys. Rev. Lett. **82**, 1975 (1999).

[15] O. Mandel, M. Greiner, A. Widera, T. Rom, T. W. Hänsch, I. Bloch, Nature **425**, 937 (2003).

[16] W. C. Stwally, Phys. Rev. Lett. **37**, 1628 (1976).

[17] E. Tiesinga, B. J. Verhaar, and H. T. C. Stoof, Phys. Rev. A **47**, 4114 (1993).

[18] S. Inouye, M. R. Andrews, J. Stenger, H. -J. Miesner, D. M. Stamper-Kurn, and W. Ketterle, Nature **392**, 151 (1998).

[19] C. C. Bradley, C. A. Sackett, J. J. Tollett, and R. G. Hulet, Phys. Rev. Lett. **75**, 1687 (1995); C. C. Bradley, C. A. Sackett, and R. G. Hulet, Phys. Rev. Lett. **78**, 985 (1997).

[20] J. L. Roberts, N. R. Claussen, S. L. Cornish, E. A. Donley, E. A. Cornell, and C. E. Wieman, Phys. Rev. Lett. **86**, 4211 (2001).

[21] E. A. Donley, N. R. Claussen, S. L. Cornish, J. L. Roberts, E. A. Cornell, and C. E. Wieman, Nature **412**, 295 (2001).

[22] K. S. Strecker, G. B. Partridge, A. G. Truscott, and R. G. Hulet, Nature **417**, 150 (2002).

[23] E. A. Donley, N. R. Claussen, S. T. Thompson, and C. E. Wieman, Nature **417**, 529 (2002).

[24] J. Herbig, T. Kraemer, M. Mark, T. Weber, C. Chin, H. -C. Nägerl, and R. Grimm, Science **301**, 1510 (2003).

[25] K. Xu, T. Mukaiyama, J. R. Abo-Shaeer, J. K. Chin, D. E. Miller, and W. Ketterle, Phys. Rev. Lett. **91**, 210402 (2003).

[26] S. Dürr, T. Volz, A. Marte, and G. Rempe, Phys. Rev. Lett. **92**, 020406 (2004)

[27] M. Greiner, C. A. Regal, and D. S. Jin, Nature **426**, 537 (2003)

[28] M. W. Zwierlein, C. A. Stan, C. H. Schunck, S. M. F. Raupach, S. Gupta, Z. Hadzibabic, and W. Ketterle, Phys. Rev. Lett. **91**, 250401 (2003).

[29] T. Bourdel, L. Khaykovich, J. Cubizolles, J. Zhang, F. Chevy, M. Teichmann, L. Tarruell, S. J. J. M. F. Kokkelmans, and C. Salomon, Phys. Rev. Lett. **93**, 050401 (2004).

[30] J. Kinast, S. L. Hemmer, M. E. Gehm, A. Turlapov, and J. E. Thomas, Phys. Rev. Lett. **92** 150402 (2004); J. Kinast, A. Turlapov, J. E. Thomas, Q. Chen, J. Stajic, and K. Levin, Science **307**, 1296 (2005).

[31] M. Bartenstein, A. Altmeyer, S. Riedl, S. Jochim, C. Chin, J. Hecker Denschlag, and R. Grimm, Phys. Rev. Lett. **92** 203201 (2004).

[32] G. B. Partridge, K. E. Strecker, R. I. Kamar, M. W. Jack, and R. G. Hulet, Phys. Rev. Lett. **95**, 020404 (2005).

[33] M. Köhl, H. Moritz, T. Stöferle, K. Günter, and T. Esslinger, Phys. Rev. Lett. **94**, 080403 (2005).

[34] S. Sachdev, "Quantum Phase Transitions", (Cambridge University Press, New York, 2001).

[35] N. Bogoliubov, J. Phys. (U. S. S. R.), **11**, 23 (1947).

[36] V. N. Popov, "Functional Integrals in Quantum Field Theory and Statistical Physics", (Reidel, Dordrecht, 1983) and references therein.

[37] H. T. C. Stoof and M. Bijlsma, Phys. Rev. E. **47**, 939 (1993).

[38] S. Inouye, J. Goldwin, M. L. Olsen, C. Ticknor, J. L. Bohn, and D. S. Jin, Phys. Rev. Lett. **93**, 183201 (2004).

[39] C. A. Stan, M. W. Zwierlein, C. H. Schunck, S. M. F. Raupach, and W. Ketterle, Phys. Rev. Lett. **93**, 143001 (2004).

[40] R. Grimm, M. Weidemüller, and Y. B. Ovchinnikov, Adv. At. Mol. Opt. Phys. **42**, 95 (2000).

[41] C. J. Pethick and H. Smith, "Bose-Einstein condensation in dilute gases", (Cambridge University Press, Cambridge, 2002).

[42] P. S. Jessen, C. Gerz, P. D. Lett, W. D. Phillips, S. L. Rolston, R. J. C. Spreeuw, and C. I. Westbrook, Phys. Rev. Lett. **69**, 49 (1992).

[43] H. J. Metcalf, and P. van der Straten, "Laser Cooling and Trapping", (Springer-Verlag, New York, 1999).

[44] B. H. Bransden, and C. J. Joachain, "Physics of atoms and molecules", (Longman, Harlow, 1996).

[45] J. M. Ziman, "Theory of Solids", (Cambridge University Press, Cambridge, 1972).

[46] N. W. Ashcroft, and N. D. Mermin, "Solid State Physics", (Saunders College Publishing, Orlando, 1976).

[47] T. Busch, B.-G. Englert, K. Rzazewski, and M. Wilkens, Found. Phys., **28**, 549 (1998).

[48] D. van Oosten, "Quantum gases in optical lattices: the atomic Mott insulator", (PhD thesis, Utrecht University, Utrecht, 2004).

[49] K.Sheshadri, H. R. Krishnamurthy, R. Pandit, and T. V. Ramakrishnan, Europhys. Lett. **22**, 257 (1993).

[50] D. van Oosten, P. van der Straten, and H. T. C. Stoof, Phys. Rev. A **67**, 033606 (2003).

[51] R. Roth, K. Burnett, Phys. Rev. A **67**, 031602 (2003).

[52] W. Zwerger, J. of Opt. B 5, s9-s16 (2003).

[53] G. Kotliar, and A. E. Ruckenstein, Phys. Rev. Lett. **57**, 1362 (1986).

[54] K. Ziegler, Europhys. Lett. **23**, 463 (1993).

[55] R. Frésard, e-print cond-mat/9405053 (1994).

[56] J. W. Negele, and H. Orland, "Quantum Many-Particle Systems", (Westview Press, Boulder, 1998).

[57] H. T. C. Stoof, in "Coherent Atomic Matter Waves", edited by R. Kaiser and F. David (Springer, Berlin, 2001), p. 219.

[58] A remedy for this discrepancy may be envisioned in allowing the right-hand side of Eq. (3.34) to deviate sligthly from 1. We do not explore this possibility here.

[59] We have also studied the case where the $(n^3 - n^2)$-term is included with n^3 put equal to 0. This leads to the undesirable feature that $T_c \to 0$ for $U \to 0$. Including this term, that is associated with processes involving triply occupied sites, probably is inconsistent with allowing a maximum occupancy of two.

[60] For instance, at $U = 0$, the 3-slave-boson approach can only result in $n^0 = n^1 = n^2 = 1/3$, whereas the exact solution for 4 bosons on a 4-site lattice gives $n^0 = 0.35, n^1 = 0.38, n^2 = 0.20, n^3 = 0.059$, and $n^4 = 0.008$ at $\beta = 1$ [62].

[61] In particular, for $\bar{U} = 4$ we find at T_c that $n^0 = 0.125, n^1 = 0.751, n^2 = 0.122$, and $n^3 = 0.0018$, whereas the 3-slave-boson result is $n^0 = 0.111, n^1 = 0.778$, and $n^2 = 0.111$.

[62] G. G. Batrouni, and R. T. Scalettar, Phys. Rev. B **46**, 9051 (1992).

[63] For a detailed account one can consult Refs. [76] and [64].

[64] E. Timmermans, P. Tommasini, M. Hussein, and A. Kernan, Phys. Rep. **315**, 199 (1999).

[65] J. J. Sakurai,"Modern Quantum Mechanics", (Addison-Wesley, New-York, 1994).

[66] H. T. C. Stoof, M. Bijlsma, and M. Houbiers, J. Res. Natl. Inst. Stand. Technol. **101**, 443 (1996).

[67] H. Feshbach, Ann. Phys. **19**, 287 (1962).

[68] D. Jaksch and P. Zoller, Ann. Phys. **315**, 52 (2005).

[69] N. P. Proukakis, K. Burnett, and H. T. C. Stoof, Phys. Rev. A **57**, 1230 (1998).

[70] M. Houbiers, R. Ferwerda, H. T. C. Stoof, W. I. McAlexander, C. A. Sackett, and R. G. Hulet, Phys. Rev. A **56**, 4864 (1997).

[71] G. E. Astrakharchik and S. Giorgini, Phys. Rev. A **66**, 053614 (2002).

[72] I. S. Gradhsteyn, I. M. Ryzhik, "Table of integrals, series, and products", (Academic Press, London, 1963).

[73] L. Radzihovsky, J. Park, and P. B. Weichman, Phys. Rev. Lett. **92**, 160402 (2004).

[74] M. W. J. Romans, R. A. Duine, S. Sachdev, and H. T. C. Stoof, Phys. Rev. Lett. **93**, 020405 (2004).

[75] K. Xu, T. Mukaiyama, J. R. Abo-Shaeer, J. K. Chin, D. E. Miller, and W. Ketterle, Phys. Rev. Lett. **91**, 210402 (2003).

[76] R. A. Duine and H. T. C. Stoof, Phys. Rep. **396**, 115 (2004).

[77] S. J. J. M. F. Kokkelmans and M. J. Holland, Phys. Rev. Lett. **89**, 180401 (2002).

[78] D. van Oosten, P. van der Straten, and H. T. C. Stoof, Phys. Rev. A **63**, 053601 (2001).

[79] D. B. M. Dickerscheid, D. van Oosten, P. J. H. Denteneer,and H. T. C. Stoof, Phys. Rev. A **68**, 043623 (2003).

[80] K. Sengupta and N. Dupuis, Europhys. Lett. **70**, 586 (2005).

109

[81] D. Jaksch, C. Bruder, J. I. Cirac, C. W. Gardiner, and P. Zoller, Phys. Rev. Lett. **81**, 3108 (1998).

[82] T. Rom, T. Best, O. Mandel, A. Widera, M. Greiner, T. W. Hänsch, and I. Bloch, Phys. Rev. Lett. **93**, 073002 (2004).

[83] A. G. Truscott, K. E. Strecker, W. I. McAlexander, G. B. Partridge, and R. G. Hulet, Science **291**, 2570 (2001).

[84] M. Cramer, J. Eisert, and F. Illuminati, Phys. Rev. Lett. **93**, 190405 (2004).

[85] A. Albus, F. Illuminati, and J. Eisert, Phys. Rev. A **68**, 023606 (2003).

[86] M. Lewenstein, L. Santos, M.A. Baranov and H. Fehrmann, Phys. Rev. Lett. **92**, 050401 (2004).

[87] W. Hofstetter, J. I. Cirac, P. Zoller, E. Demler, and M. D. Lukin, Phys. Rev. Lett. **89**, 220407 (2002).

[88] D.-W. Wang, M. D. Lukin and E. Demler, cond-mat/0410494.

[89] G. Modugno, F. Ferlaino, R. Heidemann, G. Roati, and M. Inguscio, Phys. Rev. A **68**, 011601(R) (2003).

[90] C. Schori, T. Stöferle, H. Moritz, M. Köhl, and T. Esslinger, Phys. Rev. Lett. **93**, 240402 (2004).

[91] H. P. Büchler and G. Blatter, Phys. Rev. A **69**, 063603 (2004).

[92] L. D. Carr and M. J. Holland, cond-mat/0501156.

[93] D. B. M. Dickerscheid, U. Al Khawaja, D. van Oosten, and H. T. C. Stoof, Phys. Rev. A **71**, 043604 (2005).

[94] S. Inouye and C. Thicknor, private communication.

[95] M. J. Bijlsma, B. A. Heringa, H. T. C. Stoof, Phys. Rev. A **61**, 053601 (2000).

[96] H. Heiselberg, C. J. Pethick, H. Smith, and L. Viverit, Phys. Rev. Lett. **85**, 2418 (2000).

[97] H. Moritz, T. Stöferle, K. Günter, M. Köhl, and T. Esslinger, Phys. Rev. Lett. **94**, 210401 (2005).

[98] T. Bergeman, M. G. Moore, and M. Olshanii, Phys. Rev. Lett. **91**, 163201 (2003).

Samenvatting

ABSTRACT

In dit hoofdstuk wordt een samenvatting in het Nederlands gegeven van de inhoud van dit proefschrift. Centraal in dit proefschrift staan ultrakoude atomaire gassen die gevangen zijn in een zogenaamd optisch rooster. Deze systemen blijken zeer flexibel en een ideale speeldoos te zijn om experimenteel sterk-gecorreleerde systemen uit de vaste-stof-fysica en gecondenseerde-materie na te bootsen. Door naast het optisch rooster ook nog gebruik te maken van een magneetveld is het mogelijk om ook de interacties tussen de atomen in te stellen en nog meer controle over het systeem te krijgen.

Koude gassen

Dit proefschrift richt zich op het deelgebied van de natuurkunde dat zich bezig houdt met de bestudering van ultrakoude atomaire gassen. Door een enorme technologische progressie in de laatste tien jaar is het nu mogelijk om deze gassen te vangen met behulp van magneetvelden en lasers en af te koelen tot temperaturen die zeer dicht bij het absolute nulpunt liggen. Specifiek hebben deze gassen dichtheden van zo'n $10^{12} - 10^{14}$ deeltjes per kubieke centimeter bij temperaturen van enkele nano-Kelvins. De indrukwekkende controle die men in het laboratorium heeft, maakt dat we precies de onderliggende microscopische details van deze systemen kennen en hierdoor is een preciese quantitative analyse mogelijk. Voor de theoretische beschrijving van deze systemen volstaat de Newtoniaanse mechanica niet meer en moeten we gebruik maken van de quantum mechanica. Zo blijkt dat bij de lage temperaturen die we beschouwen de deeltjes zich op twee fundamenteel verschillende wijzen gedragen, en beschreven worden door óf de Fermi-Dirac statistiek óf de Bose-Einstein statistiek. De bosonische atomen die aan de laatstgenoemde statistiek voldoen kunnen bij voldoende lage temperaturen collectief de laagste één-deeltjes energietoestand bezetten. De realisatie in 1995 van deze reeds lang voorspelde nieuwe toestand der materie leidde tot een stormvloed aan

111

experimenteel en theoretisch onderzoek in dit vakgebied.

Optische roosters en Feshbach resonanties

Een belangrijke nieuwe ontwikkeling op het gebied van de ultrakoude atomaire gassen is de bestudering van de eigenschappen van een dergelijk gas in een optisch rooster, dat wil zeggen in een periodieke potentiaal die veroorzaakt wordt door het interferentiepatroon van een aantal laserbundels. Een reden voor deze belangstelling is dat op deze wijze de effecten van de interatomaire interacties in het gas enorm versterkt kunnen worden. De hoge mate van controleerbaarheid van de optische roosters maakt dat deze systemen bijzonder geschikt zijn als simulatie systemen voor roostermodellen, welke van fundamenteel belang zijn binnen de vaste-stof en gecondenseerde-materie fysica. Een van de centrale thema's in deze vakgebieden is de bestudering van zogenaamde quantumfaseovergangen. Een quantumfaseovergang vindt plaats bij het absolute nulpunt van temperatuur tussen twee verschillende toestanden van materie en wordt gedreven door de variatie van een externe parameter.

In het bijzonder is twee jaar geleden experimenteel aangetoond dat in een optisch rooster een zogenaamde quantumfaseovergang van een Bose-Einstein-condensaat naar een Mott-isolator tot stand gebracht kan worden. Diep in de Mott-isolator-toestand heeft het gas precies één atoom op elke roosterpositie, wat deze toestand bij uitstek geschikt maakt voor toepassingen op het gebied van quantumcomputatie en quantuminformatieverwerking. In dit proefschrift hebben we de hierboven genoemde quantumfaseovergang bestudeerd en met onze theorie hebben we het fasediagram als functie van temperatuur en de interactiesterkte kunnen bepalen.

Een tweede experimentele techniek die voor veel opschudding heeft gezorgd binnen het vakgebied is het gebruik van zogenaamde Feshbach resonanties. Een dergelijke resonantie treed op wanneer twee atomen tijdens een botsing voor enige tijd een molecuul vormen. Het cruciale punt van een Feshbach-resonantie is echter dat dit molecuul een magnetisch moment heeft dat niet gelijk is aan twee keer het magnetisch moment van het atoom. Ten gevolge van het Zeeman-effect kan dus met behulp van een extern magneetveld het energieverschil tussen het molecuul en de twee atomen beïnvloed worden, en daarmee ook rechtstreeks de interacties tussen de atomen. Het combineren van zowel het optische rooster als het gebruik van Feshbach resonanties is zeer wenselijk want het zorgt voor nog meer vrijheidsgraden waar we gebruik van kunnen maken. In dit proefschrift leiden we de theorie voor Feshbach resonanties in optische roosters af en passen dit toe op een Bose gas in de buurt van een Feshbach resonantie. In het bijzonder hebben we laten zien dat in een Bose-Einstein-condensaat in een optisch rooster ook een nieuwe quantumfaseovergang tussen twee superfluide fasen kan optreden. In meer detail betreft dat laatste een atomair Bose-Einstein-condensaat in de buurt van

een Feshbach-resonantie.

Is dit energieverschil voldoende negatief dan bestaat het gas uit een Bose-Einstein-condensaat van moleculen. Maken we het energieverschil minder negatief dan treedt op een gegeven moment een quantumfaseovergang op naar een fase bestaande uit een Bose-Einstein-condensaat van moleculen en een Bose-Einstein-condensaat van atomen. Atomaire Bose gassen bieden hierdoor de mogelijkheid om in detail allerlei theoretische voorspellingen voor de statische en dynamische eigenschappen van deze zogenaamde quantum-Ising-overgang te confronteren met experiment, hetgeen in gecondenseerde-materie-systemen nog niet eerder gelukt is. Een andere toepassing van onze theorie betreft een mengsel van bosonische en fermionische atomen met een Feshbach resonantie. Ook hier kan een nieuwe quantumfaseovergang optreden. Het bijzondere hier is dat het mogelijk is om op een omkeerbare manier een Bose-Einstein condensaat van atomen te vernietigen door deze met behulp van de fermionische atomen om te zetten in fermionische moleculen.

Hoewel bovengenoemde systemen nog niet zijn gerealiseerd is men er inmiddels al wel in geslaagd om Feshbach resonanties en optische roosters te combineren. In de groep van T. Esslinger is men erin geslaagd om in een twee-dimensionaal optisch rooster met behulp van Feshbach resonanties moleculen van fermionische atomen te creeren. Met behulp van onze theorie hebben we ook een quantitatieve analyse van dit systeem gegeven.

Curriculum vitae

Ik ben geboren op 3 augustus 1978 te 's-Gravenhage. Van 1989 tot en met 1996 doorliep ik het Voortgezet Wetenschappelijk Onderwijs aan het Erasmuscollege te Zoetermeer. In september 1996 begon ik aan de studies natuurkunde en wiskunde aan de Universiteit Utrecht. Mijn afstudeeronderzoek in de theoretische natuurkunde betrof het model van spinloze fermionen in een statisch en random magneetveld en werd verricht onder de begeleiding van prof. dr. P. Stamp. Hierna begon ik in januari 2002 aan het promotieonderzoek dat geleid heeft tot dit proefschrift. Gedurende mijn promotie heb ik diverse conferenties bezocht in binnen en buitenland. Ik heb deelgenomen aan zomerscholen en voordrachten gegeven op nationale en internationale conferenties en workshops. Bij verscheidene werkcolleges in Utrecht en Leiden heb ik studenten begeleid.

In mijn vrije tijd bezondigde ik me zeker aan het begin van mijn promotie nog regelmatig aan het spelen van het door mij geliefde snookerspel en ook vervulde ik enkele jaren een bestuursfunctie binnen de Haagse Snooker Club. Om mijn conditie op pijl te houden fiets, ren, voetbal, drum en zwem ik af en toe. Na mijn promotie zal ik nog enkele maanden aan het Instituut voor Theoretische Fysica te Utrecht verbonden blijven en gaan schrijven aan een tekstboek over de statistische veldentheorie.

List of publications

- "Ultracold atoms in optical lattices", D. B. M. Dickerscheid, D. van Oosten, P. J. H. Denteneer, and H. T. C. Stoof, Phys. Rev. A **68**, 043623 (2003).

- "Inelastic light scattering from a Mott insulator", D. van Oosten, D. B. M. Dickerscheid, B. Farid, P. van der Straten, and H. T. C. Stoof, Phys. Rev. A **71**, 021601(R) (2005).

- "Feshbach resonances in an optical lattice ", D. B. M. Dickerscheid, U. Al Khawaja, D. van Oosten, and H. T. C. Stoof, Phys. Rev. A **71**, 043604 (2005) .

- "Quantum phases in a resonantly-interacting Bose-Fermi mixture", D. B. M. Dickerscheid, D. van Oosten, E. J. Tillema, and H. T. C. Stoof, Phys. Rev. Lett. **94**, 230404 (2005).

- "Feshbach molecules in a one-dimensional Fermi gas", D. B. M. Dickerscheid and H. T. C. Stoof, Phys. Rev. A **72**, 053625 (2005).

- "Reply to "Comment on 'Feshbach resonances in an optical lattice' " ", D. B. M. Dickerscheid and H. T. C. Stoof, accepted for publication in Phys. Rev. A.

Dankwoord

Bij het onderzoek in de afgelopen vier jaar dat geleid heeft tot dit proefschrift heb ik regelmatig gebruik mogen maken van de hulp en kennis van anderen. Het dankwoord is bovendien een van de weinige delen van een proefschrift dat door iedereen gelezen wordt en ik wil graag hen bedanken die een positieve bijdrage hebben geleverd aan de tot stand koming van dit proefschrift.

Als eerste wil ik mijn promotor Henk Stoof bedanken. Zonder jouw betrokkenheid bij mijn onderzoek zou dit proefschrift niet tot stand zijn gekomen. Je hebt me zeer veel fysica bijgebracht in de afgelopen jaren. Ik heb onze samenwerking altijd als zeer prettig ervaren en ben blij dat we daar nog een tijdje mee door kunnen gaan na mijn promotie.

Naast mijn promotor ben ik mijn co-promotor Peter Denteneer dank verschuldigd.Met name aan het begin van mijn promotie werkten we veel samen en bood je altijd een luisterend oor.

Ten slotte is er nog een lijstje van mensen die ik graag expliciet zou willen bedanken;

Rembert Duine, Bas Zoetekouw, Mathijs Romans, Miguel Cazalilla (thanks for inviting me to San Sebastian), Nick Proukakis, Jasper Reijnders, Jani Martikainen ("Olemmeko täällä ryyppäämässä vai puhumassa paskaa?"), Vladimir Cvetkovic ("Zdravo, vlasteline"), Vladimir Juricic (" hajde bre! "), Henk Vocks ("Fokkie!"), Dries van Oosten ("He pik!"), Danielle, Geerten & Saskia (dank voor jullie enorme gastvrijheid), Tim Out, mijn ouders, and finally a big thank you to all my collegues in Utrecht (and Leiden during my time there) for creating a pleasant atmosphere in the institute(s) .